

Study on Development of Ecological and Highly
Efficient Combustion Technology for Upgraded
Brown Coal (UBC)

AKIYAMA Katsuya

Study on Development of Ecological and Highly Efficient Combustion Technology for Upgraded Brown Coal (UBC)

(改質褐炭を利用した環境調和型高効率燃焼技術に関する研究)

AKIYAMA Katsuya

DEPARTMENT OF MECHANICAL SCIENCE AND
ENGINEERING
NAGOYA UNIVERSITY
NAGOYA, JAPAN

JULY 2011

Contents

1	Introduction	1
1.1	Background of the Research	1
1.2	Upgraded Brown Coal (UBC) Process	5
1.3	Review of Previous Studies	11
1.3.1	Characteristics of Coal Combustion	11
1.3.2	Technologies for Controlling Gaseous Emissions	13
1.3.3	Studies on Ash Deposition Phenomena	14
1.3.4	Upgrading Technologies for Low-Rank Coal	21
1.3.4.1	Coal Blending	21
1.3.4.2	Coal Briquetting	21
1.3.4.3	Drying of Coals	22
1.3.4.4	Chemical Upgrading of Low-Grade Coals	23
1.4	Purpose of this Study	25
1.5	Outline of the Thesis	26
2	Combustion and Emission Characteristics of UBC	35
2.1	Introduction	35
2.2	Experimental Section	36
2.3	Results and Discussion	41
2.3.1	Basic Combustion Behavior	41
2.3.2	Burnout Characteristics under Single-stage Combustion	45
2.3.3	NO _x and SO _x Emission Characteristics under Single-stage Combustion	48
2.3.4	Effect of Two-Stage Combustion on Burnout and NO _x Emission Characteristics	52
2.4	Conclusions	54
3	Elucidation of Ash Deposition Behavior of UBC, Bituminous Coal and their Blended Coal	57
3.1	Introduction	57

3.2	Experimental Section	58
3.3	Results and Discussion	62
3.3.1	Ash Deposition Behavior	62
3.3.2	Chemical Equilibrium Calculations	68
3.4	Conclusions	73
4	Elucidation of Mechanisms of the Reduction of Ash Deposition Using Additive	75
4.1	Introduction	75
4.2	Chemical Equilibrium Calculations	76
4.3	Experimental Section	79
4.4	Results and Discussion	82
4.4.1	Fraction of Molten Slag with and without MgO Addition Obtained by Chemical Equilibrium Calculations	82
4.4.2	Ash Deposition Behavior during Coal Combustion	87
4.4.3	Mechanisms for the Reduction of Ash Deposition	91
4.5	Conclusions	95
5	Demonstration of UBC Combustion in 145 MW Practical Coal Combustion Boiler	97
5.1	Introduction	97
5.2	Coal Samples	98
5.3	Chemical Equilibrium Calculations	101
5.4	Experimental Section	102
5.5	Results and Discussion	107
5.5.1	Fraction of Molten Slag Obtained by Chemical Equilibrium Calculations	107
5.5.2	Ash Deposition Behavior in the Boiler	111
5.5.3	Combustion and Emission Characteristics	118
5.6	Conclusions	120
6	Conclusions	123
	Acknowledgments	127

Chapter 1

Introduction

1.1 Background of the Research

Coal has primarily been used as a solid fuel to produce electricity and heat through combustion. World coal consumption was about 6.74 billion tons in 2006, and is expected to increase up to 9.98 billion tons by 2030 [1,2]. When coal is used for electricity generation, it is usually pulverized and then burnt in a furnace with a boiler. The combustion heat converts boiler water to steam, which is then used to spin turbines to generate electricity. At least 40 % of the world's electricity comes from coal, and in 2008 approximately 27 % of Japanese electricity came from coal [3].

Coal is usually categorized into several types according to its properties. It can also be divided into two major types of high-rank and low-rank coal. Generally speaking, bituminous coals, which are categorized as high-rank coals, are most commonly consumed in industrial sectors. In contrast, demand for low-rank coals such as sub-bituminous coal, lignite and brown coal is limited because of their lower heating value and/or higher moisture content, compared with bituminous coal. Therefore, the low-rank coal is usually utilized as fuel only in some specific local regions around its mine. Recently, efficient technologies to utilize low-rank coals have drawn attention, because there are limited reserves of the high-rank coals as shown in

Figure 1–1. Additionally, the price of high rank coal is increasing due to the high consumption in newly developing countries as shown in Figure 1–2.

Some Indonesian low–rank coals have high moisture content, so that their heating values are relatively lower than those of the high–rank coals. However, the ash, nitrogen and sulfur contents in the Indonesian low–rank coals are lower than those of the high–rank coals. If effective drying or dewatering technologies for those coals could be developed, then, it would be possible to use them as new fossil fuel resources. Kobe Steel, Ltd. has developed an UBC process, based on a slurry dewatering technology [4–6]. The UBC stands for Upgraded Brown Coal. Although extensive knowledge can be obtained from large background of studies on coal combustion, it is difficult to quantify the combustion and ash deposition characteristics of UBC in the practical coal combustion boiler. The major concerns can be emphasized as below:

- The UBC contains large volatile matter and possess the high heating value. This may influence the NO_x and SO_x generation and char burnout characteristics.
- The ash melting points of Indonesian low–rank coals are relatively lower than those of the high–rank coals. Therefore, slagging and fouling problems may occur in pulverized coal combustion boilers. Ash deposits on heat exchanger tubes reduce the overall heat transfer coefficient because of the low thermal conductivity with the deposits. Consequently, it is difficult to use those low–rank coals alone in pulverized coal combustion boilers.

The combustion characteristics of coal are known to be influenced by coal properties (moisture content, volatile matter content, fixed carbon content, ash content, chemical composition of combustible material, particle size distribution of coal, etc.), stoichiometric combustion air ratio, residence time and so on. Ash deposition phenomena are also influenced by factors such as the type of coal (ash compositions, melting temperature and distribution of

mineral matter), reaction atmosphere, particle temperature, surface temperature of heat exchanger tubes, tube materials and flow dynamics. Several reviews relating to the combustion and ash deposition characteristics have already been reported. Even from those researches, however, quantitative knowledge of the combustion and ash deposition characteristics of the UBC has not been elucidated yet.

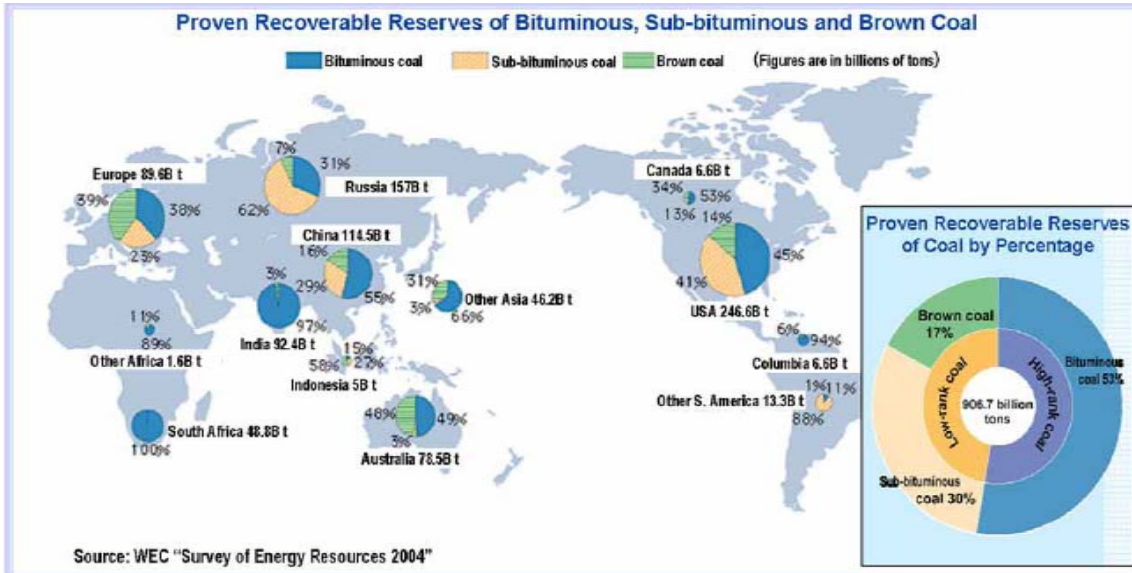


Figure 1-1: Proven recoverable reserves of coal in the world.

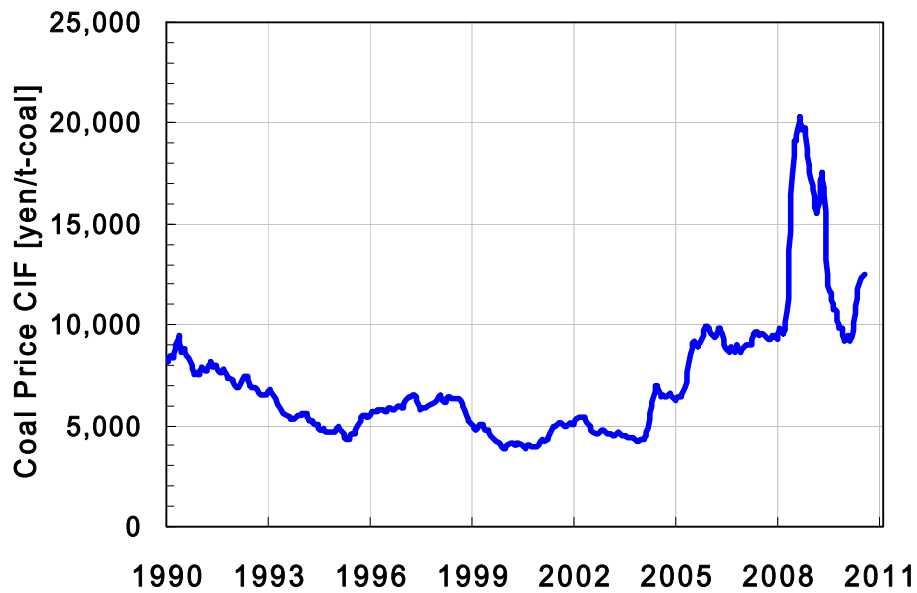


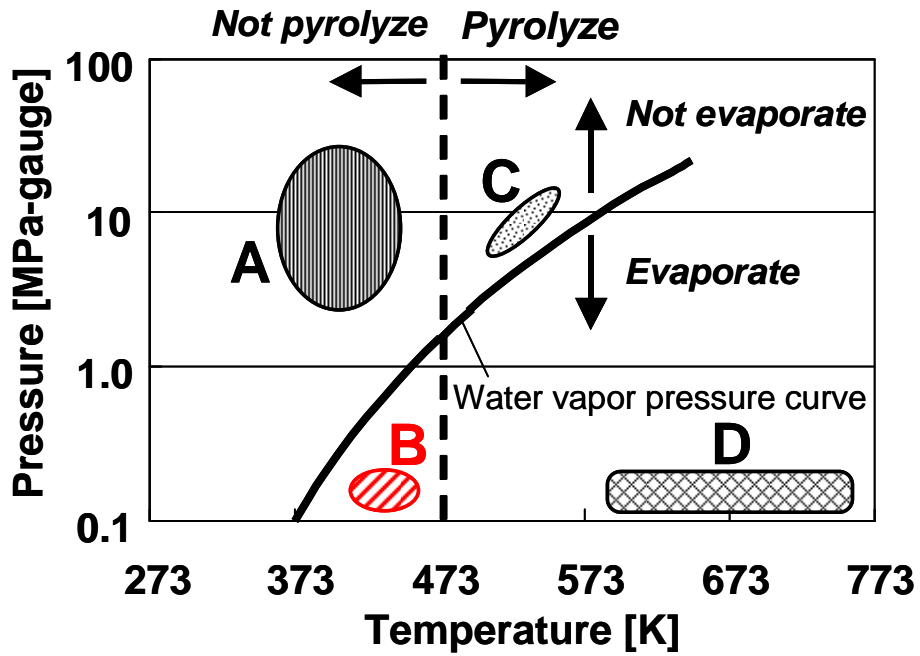
Figure 1-2: Price of steam coal in Japan. (Ref.: British Petroleum report 2010)

1.2 Upgraded Brown Coal (UBC) Process

There are actually several methods for upgrading low-rank coal as fuel [4]. Those methods are categorized into four major groups, based on the processing conditions of temperature and pressure as shown in Figure 1–3. Most of the proposed processes shown in this figure have not been commercialized yet due to mainly economical reasons. The UBC process belongs to Group B and its processing temperature and pressure are 415 K and 0.3 MPa–gauge, respectively. Under the condition of Group B, the water is evaporated but the pyrolysis doesn't occur easily. Therefore, the processes belong to the group B are the most advantageous to minimize the processing cost.

Figure 1–4 shows a schematic diagram of the UBC process. The UBC process [5–7] developed by Kobe Steel can increase the quality of low-rank coal by means of a slurry dewatering technique at low temperature and pressure without chemical reactions. The technology produces binderless briquettes in a double-roll press from low-rank coals predried in a light oil slurry. Kobe steel started developing this UBC process for Australian brown coal in 1993. The 3 ton/day pilot plant for Indonesian UBC has been operated successfully since 2001. Recently, the 600 ton /day demonstration plant has been operated in Satui, South Kalimantan as shown in Figure 1–5. In the UBC process, the low-rank coal is first crushed and then is mixed with oil and a small amount of asphalt to produce the slurry. This coal–oil slurry is heated in order to be dewatered. The energy for evaporating the coal moisture is recovered by vapor recompression. The UBC produced adsorbs very little moisture since the asphalt can deactivate the active sites effectively. After the coal is separated from the oil, it is dried and pressed to make transportable briquettes as shown in Figure 1–6. Figure 1–7 shows the dewatering mechanism in the UBC process. The particle of low-rank coal is normally porous and it contains water on the surface and in the pores. During the slurry dewatering, water is taken off and the heavy oil such as asphalt, which is added with a very small amount of

typically 0.5 wt% on coal, is effectively absorbed by the micro pores of the coal. As a result, the surface of UBC becomes hydrophobic. The asphalt seems to suppress spontaneous combustion of the UBC owing to less reactivity with oxygen. As mentioned above, the UBC process can effectively remove the moisture in low-rank coal and can increase its heating value without changing its other properties. Therefore, the UBC produced from Indonesian low-rank coal has useful properties, such as low nitrogen, sulfur and ash contents. However, this process can not change the melting point of UBC ash at all.



Group	Example of Process
A	Press Dewatering
B	<u>Upgraded Brown Coal (UBC)</u> Steam Tube Dryer (STD) Steam Fluidized Bed Dryer (SFBD)
C	Fleissner Hot Water Dewatering (HWD) KFUEL+
D	ENCOAL SYNCOAL KFUEL

Figure 1-3: Methods of the upgrading for low rank coal.

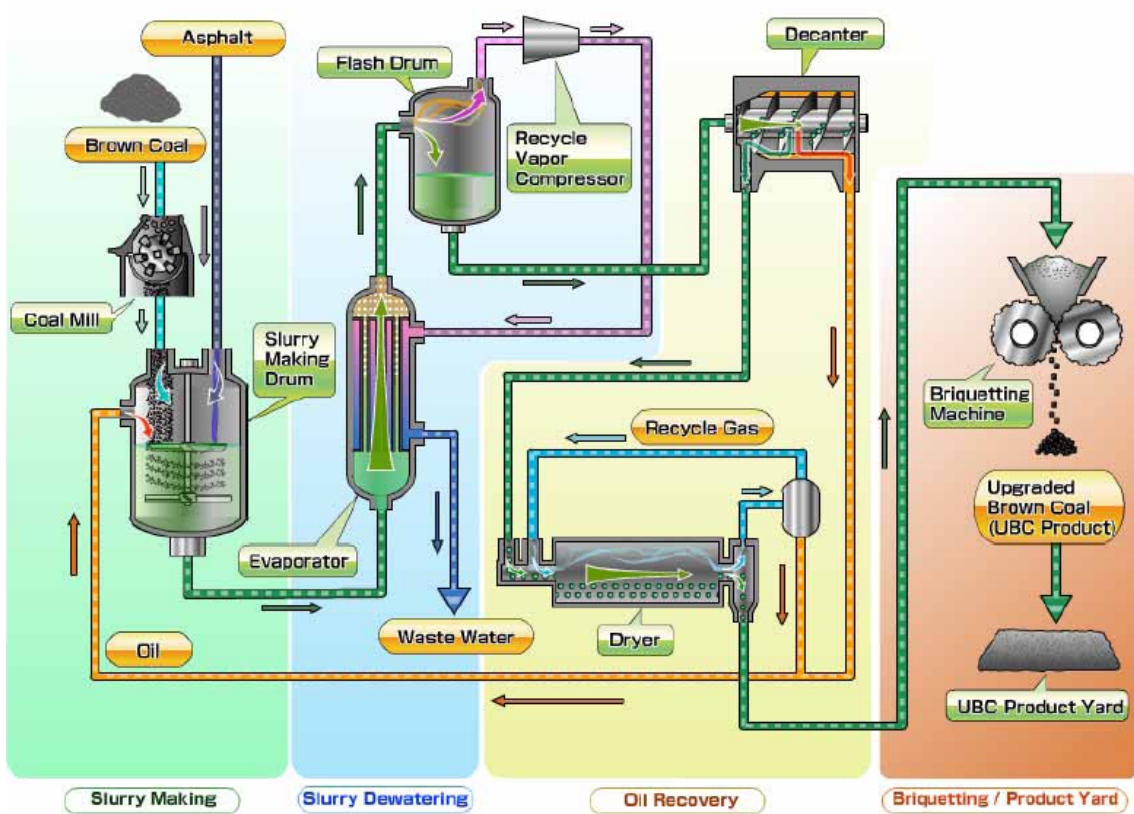


Figure 1-4: Schematic diagram of UBC process.

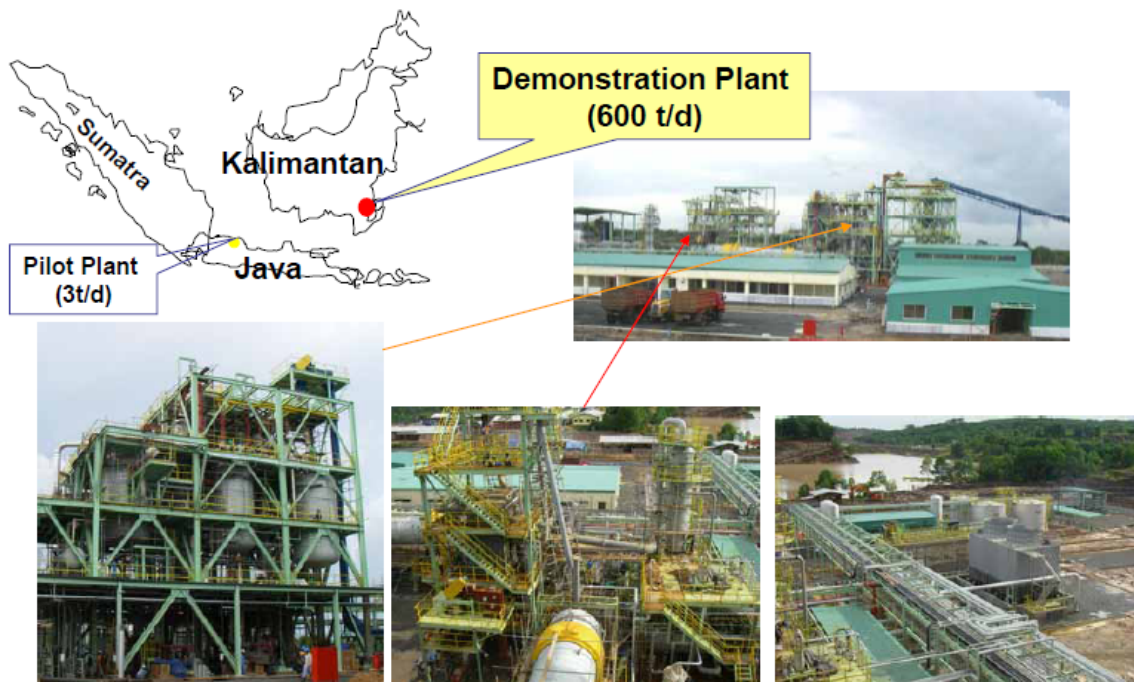


Figure 1-5: Photos of the UBC demonstration plant (DP).



Figure 1-6: Photo of the UBC briquettes.

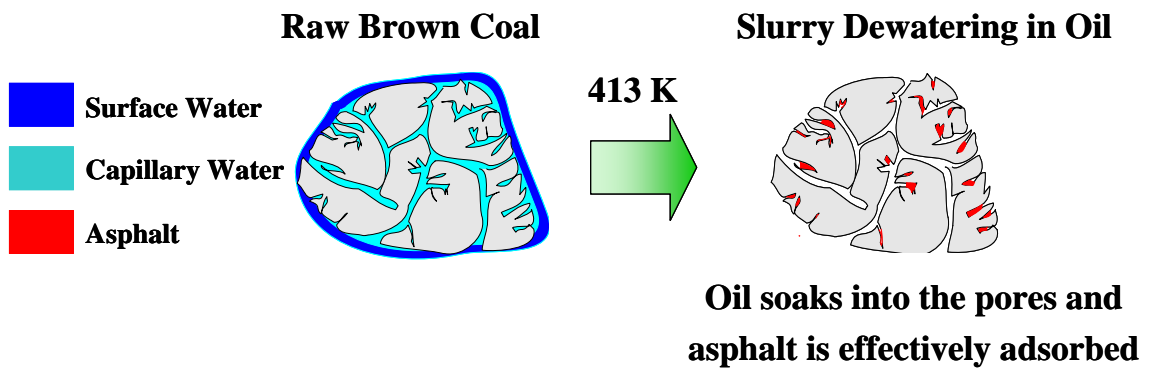


Figure 1-7: Dewatering mechanism in the UBC process.

1.3 Review of Previous Studies

Here, I review the previous studies relating to the coal combustion characterization, the technologies for controlling gaseous emissions and ash deposition phenomena and low-rank coal upgrading.

1.3.1 Characteristics of Coal Combustion

The combustion of individual coal particles comprises the following sequence of processes, which are partly overlapping, and all dependent on both physical conditions and coal properties:

- Heating of the particles;
- Release of volatile matter;
- Combustion of volatile matter;
- Combustion of the char.

The heating of the particles and the release of volatile matter occur very quickly, but these vary with coal quality and particle size. The initial gases released ignite and burn momentarily, consuming the oxygen in the air surrounding the particle. The volatile matter burns independently of the char particle at this stage. The rate of char combustion is dependent upon several factors:

- Initial coal structure;
- Diffusion of reactants;
- Reaction by various species (O_2 , H_2O , CO_2 , H_2);
- Particle size effects;

- Pore diffusion;
- Mineral content in char (catalysis);
- Changes in surface area as the reaction proceeds;
- Char fracturing;
- Variations with temperature and pressure.

There are extensive amounts of literature, which review the work carried out in the field of coal combustion [8–14]. For instance, Jenkins *et al.* [15] used a thermo–gravimetric analyzer to study oxidation of over twenty different chars in air at 773 K. They found that char reactivity increased with decreasing rank. Snow *et al.* [16] had already shown that higher hydrogen contents in carbon blacks resulted in higher reactivities. Thus, Jenkins *et al.* concluded that the enhanced reactivity of the chars derived from low–rank coals is at least partly due to higher hydrogen content. Dutta and Wen [17] studied the oxidation of several chars in air at temperature of 697–849 K. They concluded that reactivity of a given char in oxygen depended on the changes in pore structure during oxidation. However, they did not observe a direct relationship between reactivity and surface area. Tseng and Edgar [18] studied oxidation of a lignite char at temperatures of 698–1173 K, and found that char reactivity strongly depended on pyrolysis conditions. The physical structure of the chars also depended on pyrolysis condition. The conclusions of these studies were that low–temperature oxidation rates for various char differ widely [19], and that much of the variation in observed reactivity is due to the influence of the porous structure of the char. The presence of ash also affected observed reaction rates of chars at low temperatures. Jenkins *et al.* [15] used demineralized chars in an attempt to understand the role of ash during low–temperature combustion. They demonstrated that ash had a catalytic effect on char oxidation. Hengel and Walker [20] showed that calcium was a particularly active catalyst. Tong *et al.* [21] used oxygen chemisorption to determine the active

surface area (ASA) of pyrolytic carbon, and found good correlation with observed oxidation rate. Radovic *et al.* [22] applied this technique to several chars. They found that reactivity was proportional to ASA. They also found that increasing severity of pyrolysis conditions reduced the ASA.

1.3.2 Technologies for Controlling Gaseous Emissions

Nitrogen oxides (NO_x) and sulfur oxides (SO_x) are acid rain precursors and relate to the generation of photochemical smog through ozone production. Thus, the reduction of NO_x and SO_x emissions from coal-fired power plants is currently a major environmental issue and posed one of the greatest challenges in the field of environmental protection. With increasing public demand for pollution reduction, many countries have lowered their NO_x and SO_x emission limits.

The formation of NO_x mainly depends on oxygen partial pressure, temperature and coal properties such as the content of nitrogen and volatile matter. The level of NO_x produced by pulverized coal combustion can be reduced by the methods of staged combustion, low- NO_x burners, low-excess air operation and flue gas recirculation [23]. Among those methods, the staged combustion has been proven as an effective primary method to reduce the NO_x emissions in the suspension combustion system [24–38]. Coda *et al.* [32] carried out experiments in an electrically heated entrained-flow reactor using four bituminous coals. They concluded that the NO_x abatement efficiency of air staging related to volatile nitrogen release from the coal. NO level in the gas phase had a major impact on the conversion of char nitrogen to NO under oxidizing conditions. Spliethoff *et al.* [33] conducted an investigation on air staging in an electrically heated tube reactor, evaluating the effects of stoichiometry and residence time in the primary (fuel-rich) zone and the effects of temperature for air staging with different coals.

They concluded that an increase in residence time in the primary zone reduced NO_x emissions, reaching an optimum in air-lean conditions. Li *et al.* [34] investigated NO_x emissions of air-staged combustion in a 1 MW tangentially fired furnace. The results suggested that NO_x reduction efficiency monotonically increased with increasing OFA nozzle location along the furnace height. The degree of NO_x reduction by two-stage combustion and the optimal stoichiometry of the fuel-rich zone considerably depended upon the type of fuels. However, it was reported that the unburned carbon content in the fly ash increased when the operations to reduce the emission of NO_x were performed in pulverized coal-fired boilers [35–38]. Even from those references, however, the influence of two-stage combustion on the NO_x emissions and unburned carbon in fly ash for the UBC has not been elucidated yet.

On the other hand, since sulfur emissions are proportional to the sulfur content of the fuel, an effective means of reducing SO_x emissions is to burn low-sulfur coal. The sulfur in coal consists of the organic and the inorganic sulfurs of pyritic or mineral sulfate form, respectively. The formation of SO_x during combustion mainly depends on the swirl of the combustion air, stoichiometric ratio and coal type [39,40]. Zaugg *et al.* [40] concluded that the increasing the stoichiometric ratio increased sulfur conversion and SO_2 levels, and decreased H_2S , COS , and CS_2 levels. Even from those references, however, quantitative knowledge of the combustion characteristics of UBC, which has features such as high volatile matter and low sulfur content, has not been elucidated yet.

1.3.3 Studies on Ash Deposition Phenomena

Ash deposition is one of the most important operational problems associated with the efficient utilization of coal [41,42]. The occurrence of extensive ash deposits can create the following problems in a boiler:

- Reducing heat transfer – due to a reduction in boiler surface absorptivity and thermal resistance of the deposit;
- Impedance of gas flow – due to partial blockage of the gas path in the convective section of the boiler;
- Physical damage to pressure parts – due to excessive load of the structures and/or impact damage when pieces of the deposit break off and fall down through the furnace;
- Corrosion of pressure parts – due to chemical attack of metal surfaces by constituents of ash;
- Erosion of pressure parts – resulting from abrasive components of fly ash.

Deposit problems within a boiler are classified as either slagging or fouling. Slagging refers to deposits within the furnace and on widely spaced pendant superheaters in those areas of the unit, which are directly exposed to flame radiation. Fouling refers to deposits on the more closely spaced convection tubes in those areas of the unit not directly exposed to flame radiation. The coal ash deposition process involves numerous aspects of coal combustion and mineral matter transformations/reactions. Figure 1–8 summarizes the mechanisms for fly ash formation [42–45]. During combustion, the inorganics can undergo fusion, agglomeration, separation, fragmentation, vaporization and condensation. Those processes may be sequential or simultaneous, and are determined by spatial relationships and the time temperature cycle seen by particles together with their chemical environment. The process of disintegration and subsequent coalescence of ash from the burning char greatly influences the particle size distribution of the fly ash formed. This directly affects the surface area available for alkali–ash reactions and the condensation of vapours on the surface and thus affects the deposition of fly ash on the boiler tubes. If the char retains its integrity, and burns as a shrinking sphere, the ash will tend to emerge as a single coalesced particle. Conversely at high heating rates, the char

may be released into the furnace gases. There may also be a very large number of submicron particles arising from the vaporization and subsequent condensation of volatile components [44]. At various stages, this condensation mechanism involves the formation of aerosols and submicron size droplets, which may stick to other particles, or to tube surfaces, before solidifying or reacting.

Benson *et al.* [46] summarized the mechanisms of ash deposit and growth as shown in Figure 1–9. A clean surface collects only sticky particles, and as long as the deposit is thin, these solidify. As the deposit thickens, its surface temperature increases, and some particles may remain sticky, thus holding on to dry incident particles. Some of the deposited particles will be removed by erosion, and in many situations, the build–up is controlled by regular sootblowing. Wibberley [4] explained the four requirements for deposit formation as follows:

- The vapours and fly ash penetrate the boundary layer of the tube or wall surface, and touch the cold metal;
- The material adheres to the surface;
- There is sufficient cohesion to prevent the material from detaching as a result of local turbulence, vibration, sootblowing or temperature cycling;
- The thermal and chemical compatibility of the steel surface and depositing material.

Based on these observations above, a lot of researches relating to ash behaviors are conducted. As for the fusibility of ash, Huffman *et al.* [47] and Gibson *et al.* [48] investigated the high–temperature behavior of ash in reducing and oxidizing atmospheric conditions. Wall *et al.* [49] used thermo–mechanical analysis to characterize the fusibility of laboratory ash, and Winegartner *et al.* [50] and Seggiani *et al.* [51] related ash fusion temperature to chemical composition and mineral matter, thereby establishing fairly detailed relationships, both statistical and empirical. Studies on the fusibility of laboratory ash were recently undertaken

with aid of computer thermodynamic modeling of phase equilibria [52–54]. However, to our knowledge, little work has been published regarding the fusibility of slag. Additionally, the flow properties of ash and slag have been widely investigated. For example, Sage and Mcilroy [55] applied ash to predict the liquid slag behavior in the furnace and concluded that the chemical composition of ash related the viscosity of ash. Schobert *et al.* [56] discussed flow properties of ash from low-rank coals in a reducing atmosphere. Wall *et al.* [57,58] measured the viscosity of ash and quantified the flux additions necessary for slag flow in slagging gasifier using the thermo-mechanical analysis. Patterson and Hurst [59] presented data on slag viscosity versus temperature for several New South Wales and Queensland coal deposits. Oh *et al.* [60] discussed the effect of crystalline phase formation on the viscosity of slag.

On the other hand, as for ash deposition characteristics, several reviews have already been reported. For instance, Raask [61] elucidated the deposit initiation, and Walsh *et al.* [62] and Baxter [63] studied the deposition characteristics and growth. Beer *et al.* [64] attempted to develop theories of ash behavior, while Benson *et al.* [65] summarized the behavior of ash formation and deposition during coal combustion. Naruse *et al.* [66] evaluated the ash-deposition characteristics under high-temperature conditions, Vuthaluru *et al.* [67] evaluated the ash formation of brown coal, and Li *et al.* [68] investigated the coal char-slag transition under oxidation conditions. Bai *et al.* [69] characterized low-temperature coal ash at high temperatures under a reducing atmosphere. Abbott *et al.* [70] and Naganuma *et al.* [71] investigated the adhesion force between slag and oxidized steel, while Harb *et al.* [54] predicted ash behavior using a chemical equilibrium calculation, and Hansen *et al.* [72] quantified ash fusibility using differential scanning calorimetry. Ichikawa *et al.* [73] measured the liquid-phase ratio of ash using differential thermal analysis, and Song *et al.* [74] investigated the effect of coal ash composition on ash fusion temperatures. Rushdi *et al.* [75] studied the effect of the coal blending on ash deposition during combustion, and concluded that the

behavior of the blends was not additive in nature. Even in those references, however, the precise, quantitative knowledge of the deposition of coal ash with a low melting temperature during coal combustion is insufficient. In particular, the ash deposition behavior under the coal blending condition has not been elucidated yet.

Also, several papers relating to Mg-based fuel additives for boilers have already been reported. Pohl *et al.* [76] investigated the effect of the injection of Mg(OH)₂ slurry on the reduction of slagging in a coal-fired boiler, while Libutti *et al.* [77], Williams *et al.* [78], and Sinha [79] studied the effect of the injection of MgO additives on the reduction of fireside corrosion in an oil-fired boiler. Ninomiya *et al.* [80] evaluated the addition of a Mg-based additive to coal on the emission/reduction of particulate matter (PM) during coal combustion. Even in those references, however, the mechanisms by which MgO addition to the coal affects the reduction of ash deposition have not been elucidated.

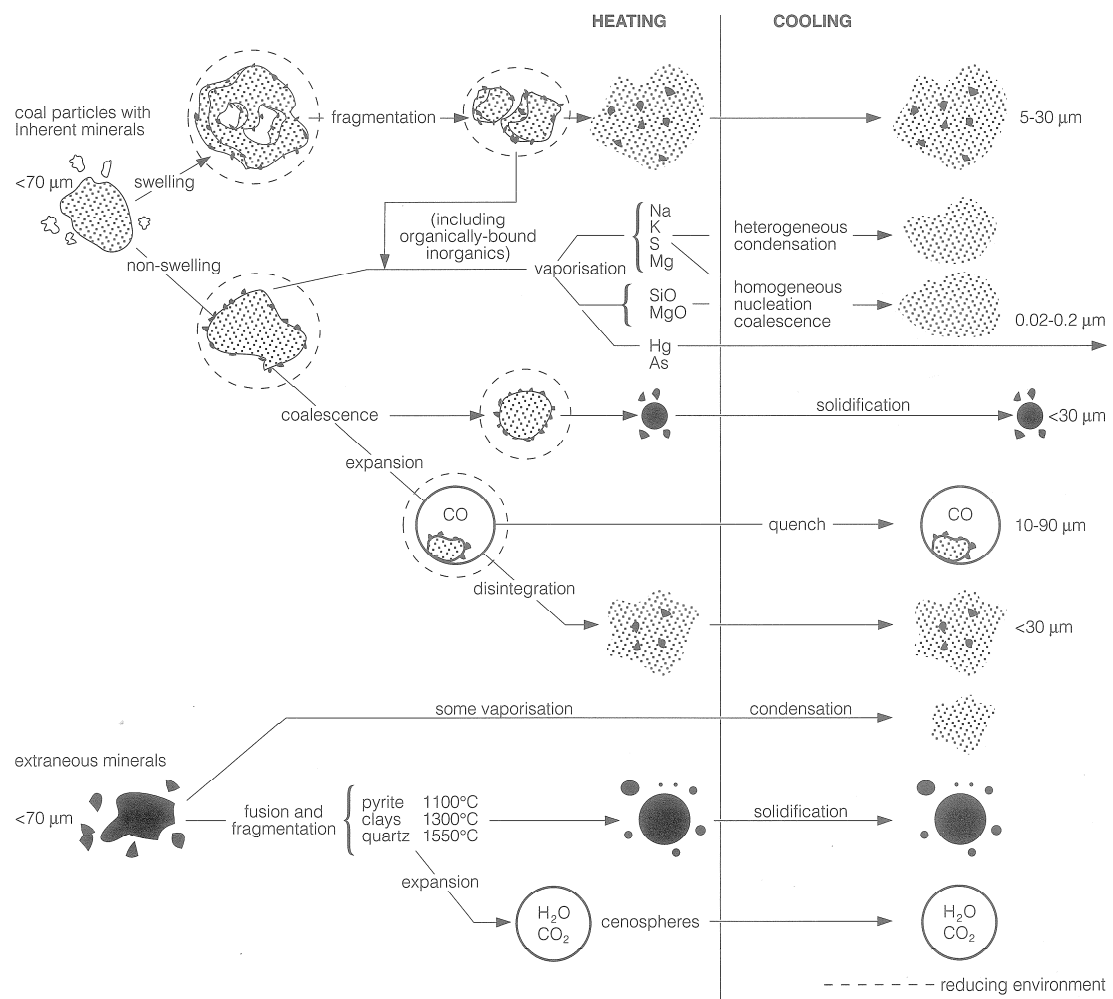


Figure 1-8: Mechanisms for fly ash formation during coal combustion [42-45].

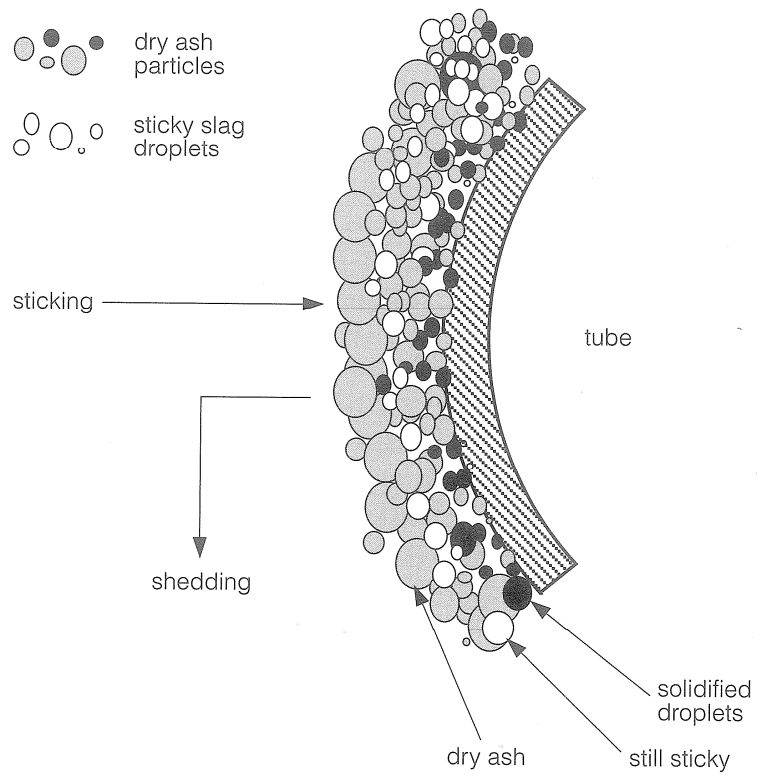


Figure 1-9: Processes contributing to ash deposit growth and removal [46].

1.3.4 Upgrading Technologies for Low–Rank Coal

Low–rank coals are generally categorized into low–grade coals because of very high moisture contents and low heating values and these coals need specific technologies for their application to power generation. The approach toward the upgrading of low–grade coal has been very diverse, but the techniques all aim at removing excess moisture and the unwanted organic and inorganic matter from the coal. Major techniques to upgrade the coals have been (i) blending, (ii) briquetting, (iii) drying, and (iv) chemical upgrading [81]. The UBC process [5–7] developed by Kobe Steel has processes of both drying and briquetting.

1.3.4.1 Coal Blending

Coal blends have been an attractive fuel for pulverized fuel power stations. One of the principal reasons for blending of low–grade coals commercially is to meet specifications by blending inferior and superior coal to maximize the volume of saleable coal under a contract. This blending can be to control ash content or other key properties, such as sodium, sulfur, nitrogen, etc., any of which may cause problems in the use of a particular coal. Generally, blending provides a way of minimizing costs by making use of several low–grade coals to achieve desired properties. Specific advantages of blending include (a) reducing fuel costs, (b) controlling emission limits, (c) enhancing fuel flexibility and extending the range of acceptable coals, (d) providing a uniform product from coal of varying quality, and (e) solving existing problems, such as poor carbon burnout, slagging, and fouling, and improving boiler performance.

1.3.4.2 Coal Briquetting

Coal briquetting has been researched worldwide since the beginning of this century to

produce briquettes from coal of various types and with different characteristics for particular uses. There are several reasons for the wide extent of this research. First, all coals are not alike, and often research has been aimed at developing an improved briquetting process for a particular coal. Second, briquetting can be performed with or without a binder to help in agglomerating and giving cohesive strength to the briquette. Much research has gone into suitable binders and processes to briquette without a binder. Third, some research has been directed at improving the properties of the briquettes, such as maintaining ignitability while keeping volatile matter low or reducing smoke and sulfur emissions during combustion. Therefore, through briquetting, low-grade coal can be upgraded and used [82–86].

1.3.4.3 Drying of Coals

Drying of coal involves removing the moisture from the coal, and this can be achieved through (i) evaporative drying or (ii) non-evaporative drying (dewatering).

As for the evaporative drying, drying techniques in which the moisture is transformed into the gaseous phase in the course of drying are referred to as evaporative drying and, in most cases, involve steam. Generally, in evaporative drying, low-rank coals are dried by evaporating interstitial water in a superheated steam flow countercurrently passed through a sealed rotary cylindrical vessel. A composite steam discharged from the vessel is partially condensed to remove an amount of water substantially equal to the amount of water removed from the coal, with a resultant flow of residual steam reheated and returned to the cylindrical vessel for further drying of coal. Some of the specific techniques that are used in evaporative drying are steam drying and steam fluidized bed drying [87–89].

As for non-evaporative drying, the earliest non-evaporative thermal dewatering process was developed in Austria in the 1920s and is known as Fleissner drying, after the inventor. Another technology is K-Fuel, formerly known as KF_x. In recent years, new technologies

working on the same principals have been explored, mainly because of the fact that the latent heat of vaporization in these processes is saved, thus leading to efficiency improvement and reduction in greenhouse gas emission. In addition, beneficial removal of some cations, principally Na, present in the lignite occurs. However, the perceived advantage of non-evaporative dewatering, saving the latent heat of evaporation, is no longer limited to dewatering. It can now also be achieved with evaporative drying, as in the Steam Fluidized Bed Drying (SFBD), with energy recovery or vapor recompression.

1.3.4.4 Chemical Upgrading of Low-Grade Coals

Recently, there are two main types of chemical upgrading of coals: (i) one aiming to produce the so-called “ultra-clean coal”, which is supposed to contain less than 0.1 % mineral matter and (ii) the other producing the so-called “hyper coal”, which basically is an ash free coal.

As for Ultra-clean Coal (UCC), the demand for UCC is predicted to increase because UCC presents solutions to some of the problems arising from the use of coal. Steel and Patrick [90] investigated the production of UCC by chemical demineralization by performing leaching experiments on a U.K. bituminous coal with ash of 7.9 % by treating it with aqueous HF followed by aqueous HNO₃. The residence time and temperature for both treatments were 3 hours and 338 K, respectively. It was found that the ash content reduced to approximately 0.6 %.

As for Hyper Coal, the preceding section on UCC has shown that, despite efforts to remove the minerals from coal by chemical leaching, there has always been some ash remaining. Yoshida *et al.* [91] reports that the amount of ash left behind in the UCCs is between 0.1 and 0.7 %. Therefore, they tried to produce an ash free coal, whose ash content will be less than 200 ppm, and decided against the use of hydrogen sources as solvent because CO₂ cannot be avoided during the hydrogen production process. Solvent extraction was carried out at 473–653

K using various organic solvents under nitrogen, and the effect of coal and solvent types and extraction temperatures on the extraction yield was studied. Of the nine coal types used in their study [92], the team succeeded to produce ash free coal with less than 0.1 % in ash content in seven types of the coals.

1.4 Purpose of this Study

The purpose of this study is to develop the ecological and highly efficient combustion technology, which enables Indonesian Upgraded Brown Coal (UBC) to be utilized in the practical coal combustion boiler. First, the NO_x and SO_x emission and the burnout characteristics are evaluated quantitatively. Second, the method to control ash deposition using both coal blending and MgO additives into coal is built up after the relationship between ash deposition characteristics and ash melting characteristics is clarified. Additionally, the mechanisms of ash deposition decreasing are elucidated. Finally, the practical combustion tests in a 145 MW coal combustion boiler are performed to evaluate both the combustion characteristics such as NO_x and SO_x emission and the burnout, and the ash deposition behavior such as slagging for the blended coal of UBC with bituminous coal.

1.5 Outline of the Thesis

The contents of this thesis consist of six chapters as outlined below.

Chapter 1 is the present introduction, which describes the background of the research and the review of previous studies and the purpose of this study.

In Chapter 2, the purpose here is to evaluate the combustion characteristics of Indonesian UBC, compared to the bituminous coal. The volatilization and char combustion characteristics are analyzed, using thermo-gravimetric analysis (TG-DTA). Moreover, the combustion tests are conducted using a refractory furnace with the parameters of the two-stage combustion ratio. The combustion characteristics of UBC and bituminous coal, their NO_X and SO_X emissions and the burnout characteristics are studied quantitatively.

In Chapter 3, the relationship between ash deposition characteristics and ash melting characteristics is elucidated. Indonesian UBC and two types of bituminous coal with different melting temperatures and ash compositions are used for the combustion tests. It is proved that the molten slag fraction in ash obtained by the chemical equilibrium calculation correlates with the deposition fraction of ash obtained in experiments even under mixing conditions of UBC to bituminous coal, and that the molten slag fraction in ash obtained by the chemical equilibrium calculations is one of useful indices to predict the blending method with UBC to reduce the deposition fraction of ash.

In Chapter 4, the objectives are to evaluate the effect of MgO addition to the coal on the reduction of ash deposition for UBC and to understand the mechanisms of this reduction of ash deposition. It is elucidated that the MgO addition plays a role in decreasing the molten slag fraction, and that the amount of ash deposition for UBC with MgO is relatively diminished. From the observations of deposited ash, the reduction mechanism of ash deposition using MgO addition to the coal is elucidated.

In Chapter 5, the objectives are to evaluate both the combustion characteristics such as

NO_x and SO_x emissions and the burnout, and the ash deposition behavior such as slagging for the blended coal with UBC in a 145 MW practical coal combustion boiler. The combustion tests operated for 8 days are conducted on blended coal consisting of 20 wt% of UBC and 80 wt% of bituminous coal. The coal blending condition is decided by the method described at Chapter 3. It is demonstrated that an appropriate blending of UBC with bituminous coal enables UBC with a low ash melting point to be used without any ash deposition problems in a practical boiler.

Finally, Chapter 6 summarizes the conclusions drawn from each of the previous chapters.

References

- [1] World coal consumption 1980–2006 October 2008 EIA statistics
- [2] EIA, World Energy Projections Plus (2009)
- [3] IEA World Energy Outlook 2009
- [4] G. R. Couch, Lignite Upgrading, IEACR/23, ISBN 92–9029–176–1, (1990) p.25.
- [5] S. Sugita, T. Deguchi, T. Shigehisa, S. Katsushima, Demonstration of UBC process in Indonesia, ICCS&T, Okinawa, Japan, (2005) Oct.
- [6] S. Sugita, T. Deguchi, T. Shigehisa, Demonstration of a UBC (Upgrading of Brown Coal) Process in Indonesia, Kobe Steel Engineering Reports, 56 (2) (2006) pp.23–26.
- [7] S. Yamamoto, S. Sugita, Y. Mito, T. Deguchi, T. Shigehisa, Y. Otaka, Development of Upgraded Brown Coal Process, The Institute for Briquetting and Agglomeration (IBA), Savannah, GA, (2007) Oct.
- [8] Morrison GF, Understanding pulverized coal combustion, ICTIS/TR34, London, UK, IEA Coal Research, (1986) p.46.
- [9] Laurendau NM, Heterogeneous kinetics of coal char gasification and combustion, Progress in Energy and Combustion Science, 4 (4), (1978), pp.221–270.
- [10] Essenhigh RH, Fundamentals of coal combustion, In: Chemistry of coal utilization – second supplementary volume, Elliott MA (ed), New York, USA, John Wiley and Sons, (1981) pp.1153–1312.
- [11] Smoot LD, Modeling of coal–combustion processes, Progress in Energy and Combustion Science, 10 (2), (1984) pp.229–272.
- [12] Smoot LD, Smith PJ, Coal combustion and gasification, New York, USA, Plenum Press, (1985) p.459.
- [13] Heap MP, Kramlich JC, Pershing DW, Pohl JH, Richter WF, Seeker WR, Effect of coal quality on power plant performance and costs – Volume 4: Review of coal science fundamentals, EPRI–CS–4283–Vol.4, Palo Alto, CA, USA, EPRI Technical Information Services, (1986) p.574.
- [14] Singer JG, Combustion fossil power – a reference book on fuel burning and steam

generation, Windsor, CN, USA, McGraw Hill, (1989) p.1010.

- [15] Jenkins RG, Nandi SP, Walker PL Jr., Reactivity of Heat-Treated Coals in Air at 500 deg C, *Fuel*, 52, (1973) p.288.
- [16] Snow CW, Wallace DR, Lyon LL, Crocker GR, Proc. of the Fourth Conf. On Carbon, Pergamon Press, New York, (1960) p.79.
- [17] Dutta S, Wen CY, Reactivity of Coal and Char, In Oxygen-Nitrogen Atmosphere, *Ind. Eng. Chem.*, 16, (1977) p.31.
- [18] Tseng HP, Edgar TF, Identification of the Combustion Behavior of Lignite Char Between 350 and 900 deg C, *Fuel*, 63, (1984) p.385.
- [19] Smith IW, The intrinsic Reactivity of Carbons to Oxygen, *Fuel*, 57, (1978) p.409.
- [20] Hengel TD, Walker PL Jr., Catalysis of Lignite Char by Exchangeable Calcium and Magnesium, *Fuel*, 63, (1984) p.1241.
- [21] Tong SB, Pareja P, Back MH, Correlation of the Reactivity, The Active Surface Area and Total Surface Area of Thin Films of Pyrolytic Carbon, *Carbon*, 20, (1982) p.191.
- [22] Radovic L, Walker PL Jr., Jenkins RG, Importance of Carbon Active Sites in The Gasification of Coal Chars, *Fuel* 62, (1983) p.849.
- [23] Chen SL, Heap MP, Pershing DW, Martin GB, Influence of Coal Composition on the Fate of Volatile and Char Nitrogen During Combustion, Nineteenth Symposium (International) on Combustion, The Combustion Institute, Pittsburgh, (1982) pp.1271-1280.
- [24] Habib MA, Elshafei M, Dajani M, Influence of combustion parameters on NO_x production in an industrial boiler, *Computers & Fluids*, 37 (1), (2008) pp.12-23.
- [25] Chaiklangmuang S, Jones JM, Pourkashanian M, Williams A, Conversion of volatile-nitrogen and char-nitrogen to NO during combustion, *Fuel*, 81 (18), (2002) pp.2363-2369.
- [26] Kim HS, Baek SW, Yu MJ, Formation characteristics of nitric oxide in a three staged air/LPG flame, *International Journal of Heat and Mass Transfer*, 46 (16), (2003) pp.2993-3008.
- [27] Man CK, Gibbins JR, Witkamp JG, Zhang J, Coal characterization for NO_x prediction in air-staged combustion of pulverized coals, *Fuel*, 84 (17), (2005) pp.2190-2195.
- [28] Backreedy RI, Jones JM, Ma L, Pourkashanian M, Williams A, Prediction of unburned carbon and NO_x in a tangentially fired power station using single coals and blends, *Fuel*, 84 (17), (2005) pp.2196-2203.
- [29] Förtsch D, Kluger F, Schnell U, Spliethoff H, Hein KRG, A Kinetic Model for the Prediction of No Emissions from Staged Combustion of Pulverized Coal, Twenty-seventh Symposium (International) on Combustion, The Combustion Institute, Pittsburgh, (1998) pp.3037-3044.
- [30] Staiger B, Unterberger S, Hein KRG, Development of an air staging technology to reduce NO_x emissions in grate fired boilers, *Energy*, 30 (8), (2005) pp.1429-1438.

- [31] Chae JO, Chun YN, Effect of two-stage combustion on NO_x emission in pulverized coal combustion, *Fuel*, 70 (6), (1991) pp.703–707.
- [32] Coda B, Kluger F, Förtsch D, Spliethoff H, Hein KRG, Coal–nitrogen release and NO_x evolution in air–staged combustion, *Energy Fuels*, 12 (6), (1998) pp.1322–1327.
- [33] Spliethoff H, Greul U, Rüdiger H, Hein KRG, Basic effects on NO_x emissions in air staging and reburning at a bench–scale test facility, *Fuel*, 75 (5), (1996) pp.560–564.
- [34] Li S, Xu TM, Hui SE, Zhou QL, Tan HZ, Optimization of air staging in a 1 MW tangentially fired pulverized coal furnace, *Fuel Processing Technology*, 90 (1), (2009) pp.99–106.
- [35] Costa M, Azevedo JLT, Experimental characterization of an industrial pulverized coal–fired furnace under deep staging conditions, *Combustion Science and Technology*, 179 (9), (2007) pp.1923–1935.
- [36] Ribeirete A, Costa M, Detailed measurements in a pulverized–coal–fired large–scale laboratory furnace with air staging, *Fuel*, 88 (1), (2009) pp.40–45.
- [37] Ren F, Li Z, Jing J, Zhang X, Chen Z, Zhang J, Influence of the adjustable vane position on the flow and combustion characteristics of a down–fired pulverized–coal 300 MWe utility boiler, *Fuel Processing Technology*, 89 (12), (2008) pp.1297–1305.
- [38] Shirai H, Tsuji H, Ikeda M, Kotsuji T, Influence of Combustion Conditions and Coal Properties on Physical Properties of Fly Ash Generated from Pulverized Coal Combustion, *Energy Fuels*, 23 (7), (2009) pp.3406–3411.
- [39] Cheng J, Zhou J, Liu J, Zhou Z, Huang Z, Cao X, Zhao X, Cen K, Sulfur removal at high temperature during coal combustion in furnaces: a review, *Progress in Energy and Combustion Science*, 29 (5), (2003) pp.381–405.
- [40] Zaugg SD, Blackham AU, Hedman PO, Smoot LD, Sulphur pollutant formation during coal combustion, *Fuel*, 68 (3), (1989), pp.346–353.
- [41] IEA Coal Industry Advisory Board, Coal quality and ash characteristics, Paris, France, OECD/IEA, (1985) p.63.
- [42] Jones ML, Benson SA, An overview of slagging/fouling with Western coals. In: *Effects of coal quality on power plants*, Atlanta, GA, USA, (1988) pp.13–15.
- [43] Barrett RE, Designing boilers to avoid slagging, fouling, *Power*, 134 (2), (1990) p.41–45.
- [44] Wibberley LJ, Characterization of coals for fly ash and sulfur oxide emissions. In: *An intensive course on the characterization of steaming coals*, Newcastle, NSW, Australia, (1985) pp.20–22.
- [45] Miller SF, Schobert HH, Effect of mineral matter particle size distribution during pilot–scale combustion of pulverized coal and coal–water slurry fuels, *Energy Fuels*, 7 (4), (1993) pp.532–541.
- [46] Benson SA, Jones ML, Harb JN, Ash formation and deposition. In: *Fundamentals of coal combustion for clean and efficient use*, Smoot LD (ed), Amsterdam, the Netherlands, Elsevier Science Publishers, (1993) pp.299–373.

- [47] Huffman GP, Huggins FE, Dunmyre GR, Investigation of the high-temperature behaviour of coal ash in reducing and oxidizing atmospheres, *Fuel*, 60, (1981) pp.585–597.
- [48] Gibson JR, Livingston WR, The Sintering and Fusion of Bituminous Coal Sshes. In *Inorganic Transformations and Ash Deposition during Combustion*, Benson SA (ed), United Engineering Foundation International Conf., Palm Coast, FL, (1991).
- [49] Bryant GW, Browning GJ, Emanuel H, Gupta SK, Gupta RP, Lucas JA, The fusibility of blended coal ash, *Energy Fuels*, 14, (2000) pp.316–325.
- [50] Winegartner EC, Rhodes BT, An empirical study of the relation of chemical properties to ash fusion temperatures, *Trans ASME J Eng Power*, 97, (1973) pp.395–401.
- [51] Seggiani M, Pannocchia G, Predication of coal ash thermal properties using partial least-squares regression, *Ind Eng Chem Res*, 42, (2003) pp.4919–4926.
- [52] Goni C, Helle S, Garcia X, Gordon A, Parra R, Kelm U, Coal blend combustion: fusibility ranking from mineral matter composition, *Fuel*, 82, (2003) pp.2087–2095.
- [53] Jak E, Predication of coal ash fusion temperatures with the FACT thermodynamic computer package, *Fuel*, 81, (2002) pp.1655–1668.
- [54] Harb JN, Munson CL, Richards GH, Use of Equilibrium Calculations To Predict The Behavior of Coal Ash in Combustion Systems, *Energy Fuels*, 7, (1993) pp.208–214.
- [55] Sage WL, McIroy JB, Relationship of coal ash viscosity to chemical composition, *Combustion*, 31, (1959) pp.41–48.
- [56] Schobert HH, Streeter RC, Diehl EK, Flow properties of low-rank coal ash slags implications for slagging gasfication, *Fuel*, 64, (1985) pp.1611–1617.
- [57] Buhre BJP, Browning GJ, Gupta RP, Wall TF, Measurement of the viscosity of coal-derived slag using thermomechanical analysis, *Energy Fuels*, 19, (2005) pp.1078–1083.
- [58] Bryant GW, Lucal JA, Gupta SK, Wall TF, Use of thermomechanical analysis to quantify the flux additions necessary fo slag flow in slagging gasifiers fired with coal, *Energy Fuels*, 12, (1998) pp.257–261.
- [59] Patterson JH, Hurst HJ, Ash and slag qualities of Australian bituminous coals for use in slagging gasifiers, *Fuel*, 79, (2999) pp.1671–1678.
- [60] Oh MS, Brooker DD, dePaz EF, Brady JJ, Decker TR, Effect of crystalline phase formation on coal slag viscosity, *Fuel Processing Technology*, 44, (1995) pp.191–199.
- [61] Raask E. *Mineral impurities in coal combustion*, Hemisphere Publishing Corporation, Washington, (1985) pp.169–189.
- [62] Walsh PM, Sayre AN, Loehden DO, Monroe LS, Beér JM, Sarofim AF, Deposition of bituminous coal ash on an isolated heat exchanger tube: Effects of coal properties on deposit growth, *Prog. Energy Combust. Sci.*, 16 (4), (1990), pp.327–345.
- [63] Baxter LL, Influence of ash deposit chemistry and structure on physical and transport properties, *Fuel Processing Technology*, 56 (1–2), (1998) pp.81–88.

- [64] Beer JM, Sarofim AF, Barta LE, Inorganic transformations and ash deposition during combustion. In: Engineering Foundation, Benson, S. A. (ed), ASME, New York, (1992).
- [65] Benson SA, Jones ML, Harb JN, Ash formation and deposition Chap.4. In: Smoot LD, editor. Fundamentals of coal combustion for Clean and Efficient Use, Elsevier Science, New York, (1993) p.299.
- [66] Naruse I, Kamihashira D, Khairil, Miyauchi Y, Kato Y, Yamashita T, Tominaga H, Fundamental ash deposition characteristics in pulverized coal reaction under high temperature conditions, *Fuel*, 84 (4), (2005) pp.405–410.
- [67] Vuthaluru HB, Wall TF, Ash formation and deposition from a Victorian brown coal modelling and prevention, *Fuel Processing Technology*, 53 (3), (1998) pp.215–233.
- [68] Li S, Whitty KJ, Effect of temperature and residual carbon, *Energy Fuels*, 23 (4), (2009) pp.1998–2005.
- [69] Bai J, Li W, Li B, Characterization of low–temperature coal ash behaviors at high temperatures under reducing atmosphere, *Fuel*, 87 (4–5), (2008) pp.583–591.
- [70] Abbott MF, Conn RE, Austin LG, Studies on slag deposit formation in pulverized–coal combustors: 5. Effect of flame temperature, thermal cycling of the steel substrate and time on the adhesion of slag drops to oxidized boiler steels, *Fuel*, 64 (6), (1985) pp.827–831.
- [71] Naganuma H, Ikeda N, Ito T, Sato F, Urashima K, Takuwa T, Yoshiie R, Naruse I, Elucidation of Ash Deposition Mechanism with Interfacial Reaction, *Journal of the Japan Institute of Energy*, 88, (2009) pp.816–822.
- [72] Hansen LA, Frandsen FJ, Dam–Johansen K, Ash fusion quantification by means of thermal analysis, An Engineering Foundation Conference on Impact of Mineral Impurities in Solid Fuel Combustion, Hawaii, Nov. (1997).
- [73] Ichikawa K, Oki Y, Inumaru J, Ashizawa M, Study on the predicting technique of ash deposition tendency in the entrained–flow coal gasifier, *Trans. Japan Soc. Mech. Eng., Ser. B*, 67, (2001) pp.144–150.
- [74] Song WJ, Tang LH, Zhu XD, Wu YQ, Zhu ZB, Koyama S, Effect of coal ash composition on ash fusion temperatures, *Energy Fuels*, 24 (1), (2009) pp.182–189.
- [75] Rushdi A, Sharma A, Gupta R, An experimental study of the effect of coal blending on ash deposition, *Fuel*, 83, (2004) pp.495–506.
- [76] Pohl JH, Creelman RA, Ward C, Borio R, Radway G, Larsen G, Mehta A, Wolsiffer S, Davis C, Expanded use of high–sulfur, low–fusion coals in utility boilers: effect of additives, *Proc. 26th Int. Tech. Conf. Coal Util. Fuel Syst.*, Florida, (2001) pp.597–608.
- [77] Libutti BL, Brandon JH, Effective use of oxide mixtures as fuel additives, *Pap. NACE Conf. (Natl. Assoc. Corros. Eng.)*, Toronto, (1975) p.162.
- [78] Williams GD, Cotton IJ, Energy and maintenance savings by use of fuel and fireside additive programs, *Proc. Refining Dep. Am. Pet. Inst.*, 55, (1976) pp.819–839.
- [79] Sinha RK, High–temperature fireside corrosion and its control by chemical additives,

- Mater Performance, 31 (4), (1992) pp.44–49.
- [80] Ninomiya Y, Wang, Q, Xu S, Teramae T, Awaya I, Evaluation of a Mg–Based Additive for Particulate Matter (PM)_{2.5} Reduction during Pulverized Coal Combustion, *Energy Fuels*, 24 (1), (2009) pp.199–204.
- [81] Katalambula H, Gupta R, Low–Grade Coals: A Review of Some Prospective Upgrading Technologies, *Energy Fuels*, 23 (7), (2009) pp.3392–3405.
- [82] Stevenson GG, Perlack RD, The prospects for coal briquetting in the Third World, *Energy Policy*, June (2009)
- [83] Lázaro MJ, Boyano A, Gálvez ME, Izquierdo MT, Moliner R, Low–cost carbon–based briquettes for the reduction of no emissions from medium–small stationary sources, *Catal. Today*, 119 (2007) pp.175–180.
- [84] Sheng C, Gupta R, Wall T, Investigation on Australian low–grade coals, A report prepared for Central Research Institute of Electric Power Industry (CRIEPI), Japan (2004)
- [85] Tosun YI, Clean fuel–magnesia bonded coal briquetting, *Fuel Processing Technology*, 88 (2007) pp.977–981.
- [86] Mangena SJ, du Cann VM, Binderless briquetting of some selected South African prime coking, blend coking and weathered bituminous coals and the effect of coal properties on binderless briquetting, *Int. J. Coal Geol.*, 71 (2007) pp.303–312.
- [87] Chen Z, Wu W, Agarwal PK, Steam–drying of coal. Part 1. Modeling the behavior of a single particle, *Fuel*, 79 (2000) pp.961–973.
- [88] Geoffrey D, Bongers W, Jackson R, Woskoboenko F, Pressurised steam drying of Australian low–rank coals: Part 1. Equilibrium moisture contents, *Fuel Processing Technology*, 57 (1998) pp.41–54.
- [89] Geoffrey D, Bongers W, Jackson R, Woskoboenko F, Pressurised steam drying of Australian low–rank coals: Part 2. Shrinkage and physical properties of steam dried coals, preparation of dried coals with very high porosity, *Fuel Processing Technology*, 64 (2000) pp.13–23.
- [90] Steel KM, Patrick JW, The production of ultra–clean coal by chemical demineralization, *Fuel*, 80 (2001) pp.2019–2023.
- [91] Yoshida T, Takanohashi T, Sakanishi K, Saito I, Fujita M, Mashimo K, The effect of extraction condition on “HyperCoal” production (1) –Under room temperature filtration, *Fuel*, 81 (2002) pp.1463–1469.
- [92] Okuyama N, Komatsu N, Shigehisa T, Kaneko T, Tsuruya S, Hyper–coal process to produce the ash–free coal, *Fuel Processing Technology*, 85 (2004) pp.947–967.

Chapter 2

Combustion and Emission Characteristics of UBC

2.1 Introduction

Kobe Steel, Ltd. has developed an UBC process based on a slurry dewatering technology [1–3]. The UBC stands for Upgraded Brown Coal. Although extensive knowledge can be obtained from large background of studies on coal combustion, the combustion characteristics of UBC produced by means of the slurry dewatering process with oil has not been elucidated yet. The UBC contains large volatile matter and possess the high heating value. This may influence the NO_X and SO_X generation and char burnout characteristics during combustion in the practical coal combustion boiler.

In this chapter, the combustion characteristics of Indonesian UBC, compared to a bituminous coal are evaluated. The volatilization and char combustion characteristics are analyzed, using thermo–gravimetric analysis (TG–DTA). Moreover, the combustion tests are conducted, using a refractory furnace, varying the parameters of the two–stage combustion ratio. The combustion characteristics of UBC and bituminous coal, their NO_X and SO_X emissions and the burnout characteristics are elucidated quantitatively.

2.2 Experimental Section

Four types of coal are used as samples, as shown in Table 2–1. UBC C1 and UBC D1 are upgraded from different types of raw brown coal. Coal A1 and Coal B1 are bituminous coal. The fuel ratio in the table denotes the content ratio of fixed carbon to volatile matter in coal. As seen from the table, the fuel ratio of UBC is less than 1.0, and the ash content of UBC is lower than Coal A1 and Coal B1. The moisture content is almost the same as that of bituminous coal. The nitrogen and sulfur content is also lower than Coal A1 and Coal B1. As for the ash composition, the UBC especially has low SiO_2 and high Fe_2O_3 in ash. In particular, UBC C1 contains the highest CaO in ash among those coal samples. The coal was pulverized, so that a mass fraction of 80 % formed particles with diameters less than $75 \mu\text{m}$ as shown in Figure 2–1.

TG–DTA tests were conducted using a TG8120 Rigaku apparatus in order to analyze the volatilization and char combustion characteristics as shown in Figure 2–2. Table 2–2 shows the test condition of volatilization under pyrolysis and combustion. The weight of sample placed in a platinum pan is 5.5 mg, the gas flow rate is kept at 150 ml/min, and heating rate is 20 K/min. The maximum experimental temperature is set at 1273 K. For the coal combustion test, air is used as the reaction gas, and it is heated up to 380 K and kept for 10 minutes in order to remove moisture in coal, then heated up to 1273 K and kept for 40 minutes. For the volatilization test under pyrolysis, nitrogen is used as the inert gas, and it is heated up to 380 K and kept for 10 minutes, then heated up to 1173 K and kept for 40 minutes. In the char combustion test, it is heated up to 380 K, and kept for 10 minutes, then heated up to 973 K or 1173 K and kept for 10 minutes using nitrogen gas, then the reaction gas is switched to air and it is kept for 40 minutes. From TG–DTA curves, each reaction rate of coal combustion and volatilization, char combustion is quantitatively obtained.

Next, combustion test were conducted, using a pilot–scale pulverized coal combustion refractory furnace, as shown in Figure 2–3. The dimensions of the furnace are 3.65 m long and

0.4 m in inner diameter. The furnace is insulated by refractory to reduce the heat loss. The pulverized coal weighed by the volumetric feeder is transported to the burner with nitrogen gas, and burnt in the furnace with the primary air at the ambient temperature and the preheated secondary air at 573 K. Table 2–3 shows the test condition. The heat load is fixed at a given value of 60.3 kW for all the tests. The oxygen concentration of the flue gas at the furnace outlet is fixed at a given value of 4.0 % at dry basis. The two–stage combustion air, which is heated up at 473 K, is supplied at a location of 1.8 m from the burner tile in order to elucidate the effect of NO_x reduction. The parameters of the two–stage combustion ratio are set at 0, 15 and 30 % in the total air flow rate. In the experiments, the thermocouples and the particle sampling probe are inserted into the furnace and outlet to measure the gas temperature and to sample the reacting particles, respectively. The gas sampling probe is also inserted into the furnace outlet to measure the gas compositions including NO_x and SO_x .

Table 2–1: Properties of coals tested.

Coal sample		UBC C1	UBC D1	Coal A1	Coal B1
Heating value [MJ/kg, dry]		26.90	28.48	29.49	30.75
Proximate analysis [wt%, air dry]	Moisture	4.0	7.7	3.6	8.4
	Ash	3.1	1.9	12.9	5.2
	Volatile matter	50.3	53.5	34.7	43.5
Proximate analysis [wt%, dry]	Fixed carbon	46.6	44.6	52.4	51.3
Fuel ratio [-]		0.93	0.83	1.51	1.18
Ultimate analysis [wt%, d.a.f]	Carbon	69.87	71.97	84.62	79.22
	Hydrogen	4.98	5.37	5.56	5.65
	Nitrogen	1.01	0.82	1.93	1.78
	Sulfur	0.12	0.16	0.67	0.56
	Oxygen (Balance)	24.01	21.67	7.23	12.78
Ash fusion temperature [K] (Oxidizing)	Initial deformation	1536	1743	1753	1603
	Hemispherical	1648	1838	1843	1693
	Fluid	1823	1843	1848	1698
Ash compositions [wt%]	SiO ₂	16.6	43.4	66.2	51.9
	Al ₂ O ₃	3.5	33.2	23.7	25.0
	CaO	21.1	2.1	1.0	2.6
	TiO ₂	0.3	0.4	1.1	0.5
	Fe ₂ O ₃	31.2	16.5	4.3	10.3
	MgO	11.1	0.5	0.6	2.4
	Na ₂ O	0.10	0.20	0.40	0.74
	K ₂ O	0.20	0.20	1.30	2.18
	P ₂ O ₅	0.0	0.0	0.2	0.4
	SO ₃	12.0	1.3	0.4	1.8

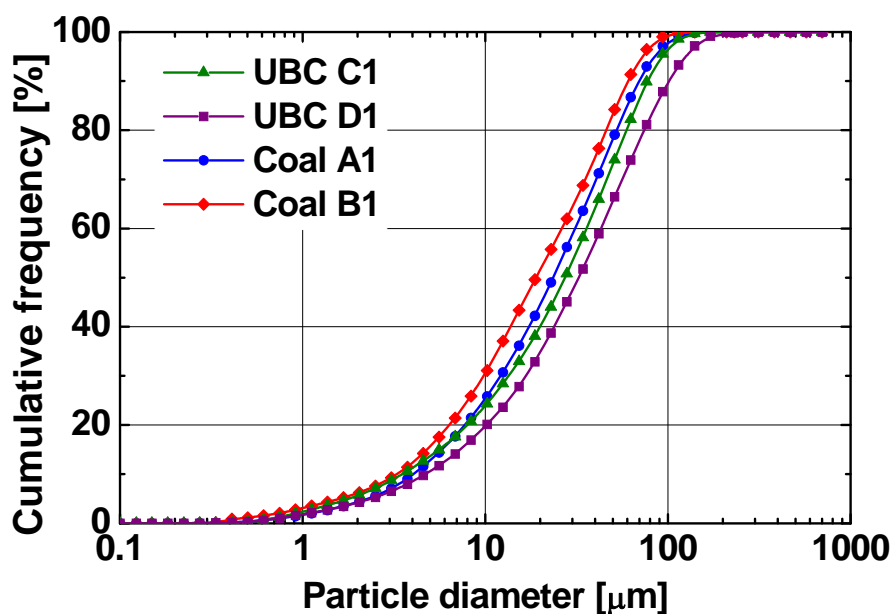


Figure 2–1: Particle diameter distributions for coal samples.

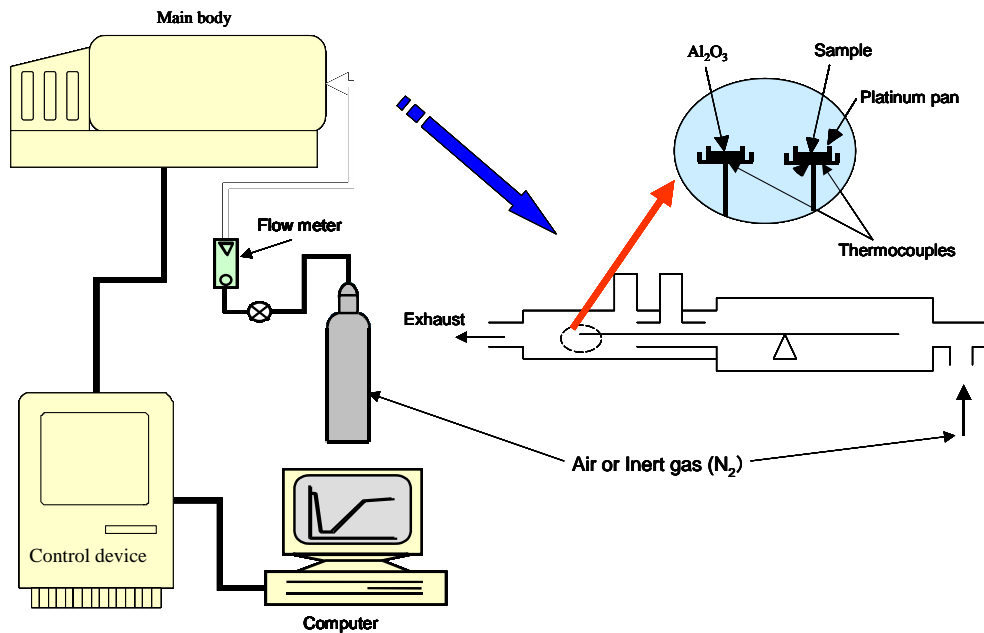


Figure 2-2: Apparatus of TG-DTA analysis.

Table 2-2: Test condition of volatilization under pyrolysis and combustion by TG-DTA analysis.

Coal sample	UBC C1, UBC D1, Coal A1, Coal B1
Sample amount [mg]	5.5
Atmosphere gas	Air(combustion), Nitrogen(pyrolysis)
Gas flow rate [ml/min]	150
Rate of temperature increase [K/min]	20
Program of temperature control	After holding for 10 min at 380 K, heat up until 1273 K and hold for 40 min.
Char combustion temperature [K]	973, 1173

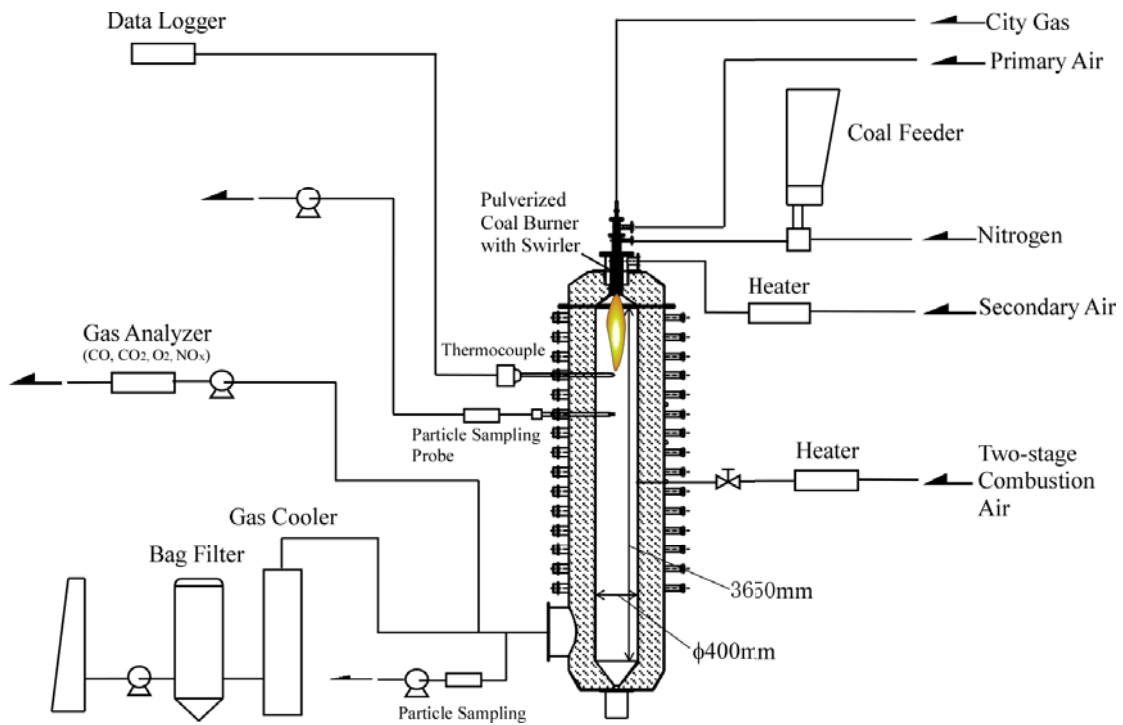


Figure 2-3: Schematic diagram of a pilot-scale pulverized coal combustion refractory furnace.

Table 2-3: Test condition using a pilot-scale pulverized coal combustion refractory furnace.

Coal sample	UBC C1, UBC D1, Coal A1, Coal B1
Heat load [kW]	60.3
Oxygen concentration at furnace outlet [%]	4.0
Primary air temperature [K]	310
Secondary air temperature [K]	573
Two-stage combustion air temperature [K]	473
Two-stage combustion rate [%]	0, 15, 30

2.3 Results and Discussion

2.3.1 Basic Combustion Behavior

The reaction rates of coal combustion, volatilization under pyrolysis and char combustion are analyzed, using TG–DTA. Figure 2–4 shows the combustion characteristics of four types of coal. The dimensionless parameter X means the conversion. Coal A1 and Coal B1 show similar combustion behavior. However, UBC C1 and UBC D1 start to react at lower temperatures, compared with Coal A1 and Coal B1. In particular, the reaction of UBC C1 starts at around 573 K. Figure 2–5 shows the volatilization characteristics under pyrolysis for four types of coal. Those results show that UBC C1 and UBC D1 contain a lot of volatile matter, which evolves at low temperature below 700 K, compared with Coal A1 and Coal B1. However, the kind of coal does not greatly affect the evolution rate of volatile matter. On the other hand, Figures 2–6 and 2–7 show the combustion characteristics of four types of char at 973 K and 1173 K in temperature, respectively. It is obviously observed that the char burnout time of UBC C1 and UBC D1 is shorter than that of Coal A1 and Coal B1. The result also shows that the reactivity of UBC C1 char is high under the low temperature around 973 K.

In the next step, the influence of the interaction between char configuration and char burnout characteristics is observed by SEM (Scanning Electron Microscope) photograph and specific surface area analysis of char. The specific surface area is measured by nitrogen adsorption B.E.T method. The char samples are prepared from the pulverized coal based on JIS M8812. Figure 2–8 shows the observation results. It is found that the char particle size of UBC C1 and UBC D1 is smaller than that of Coal A1 and Coal B1, but a lot of small asperity exist on the surface of the char particle of UBC C1 and UBC D1. This is because a lot of volatile matter discharged from the surface of coal particle. The specific surface area of UBC C1 and UBC D1 char is approximately 20 to 55 times as large as that of Coal A1 and Coal B1 char. Therefore, the char burnout time tends to be shortened as the specific surface area of char increased.

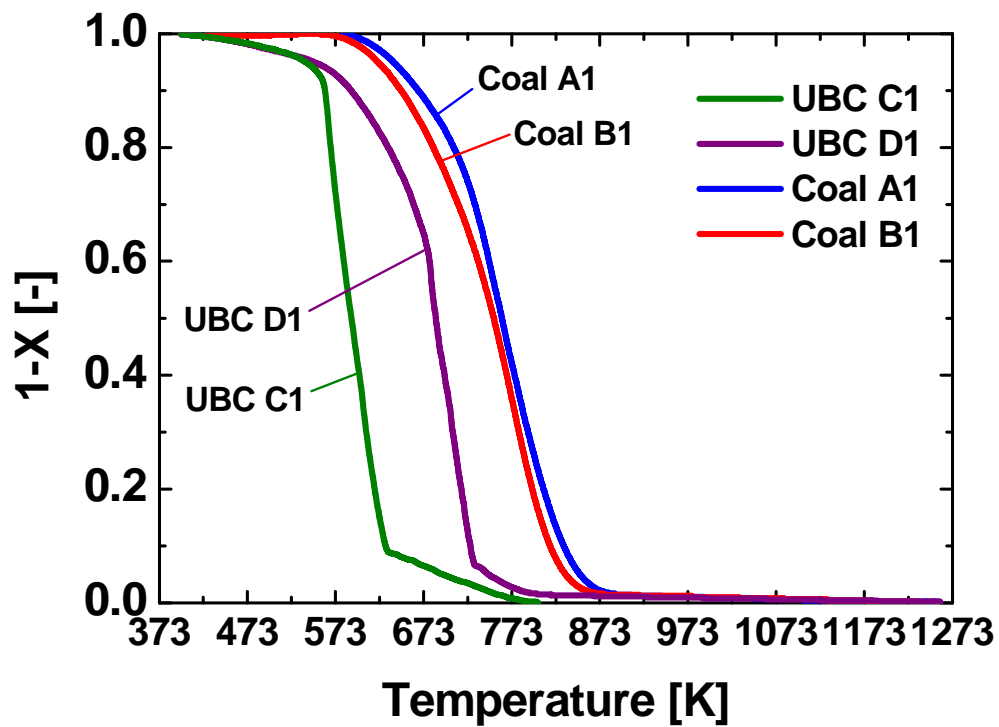


Figure 2-4: Combustion characteristics of four types of coal by TG-DTA.

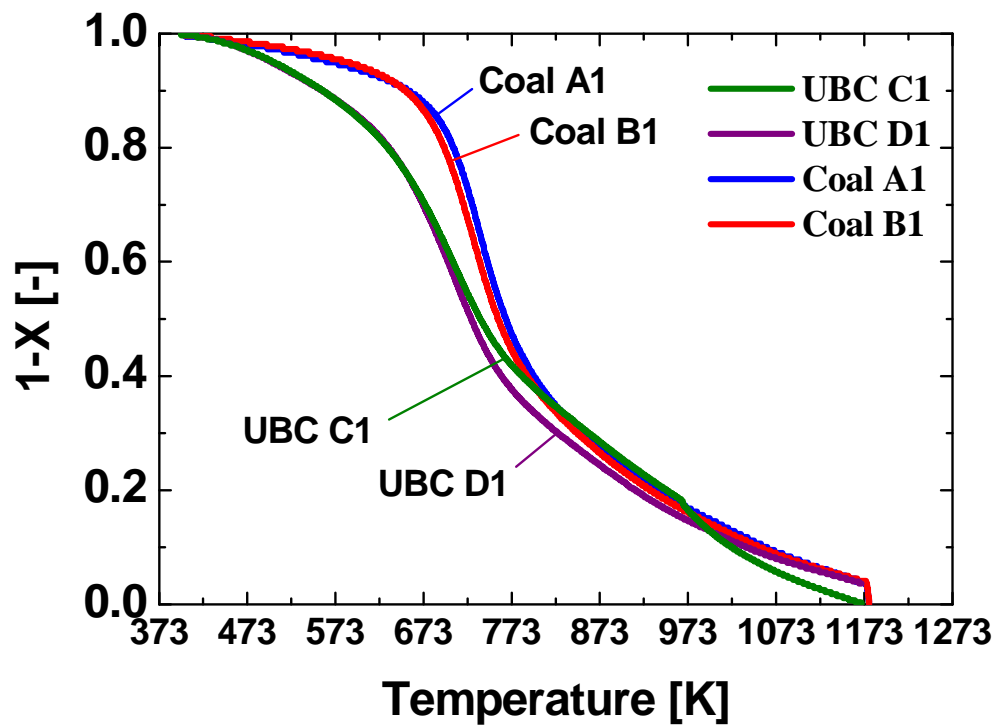


Figure 2-5: Volatilization characteristics under pyrolysis for four types of coal by TG-DTA.

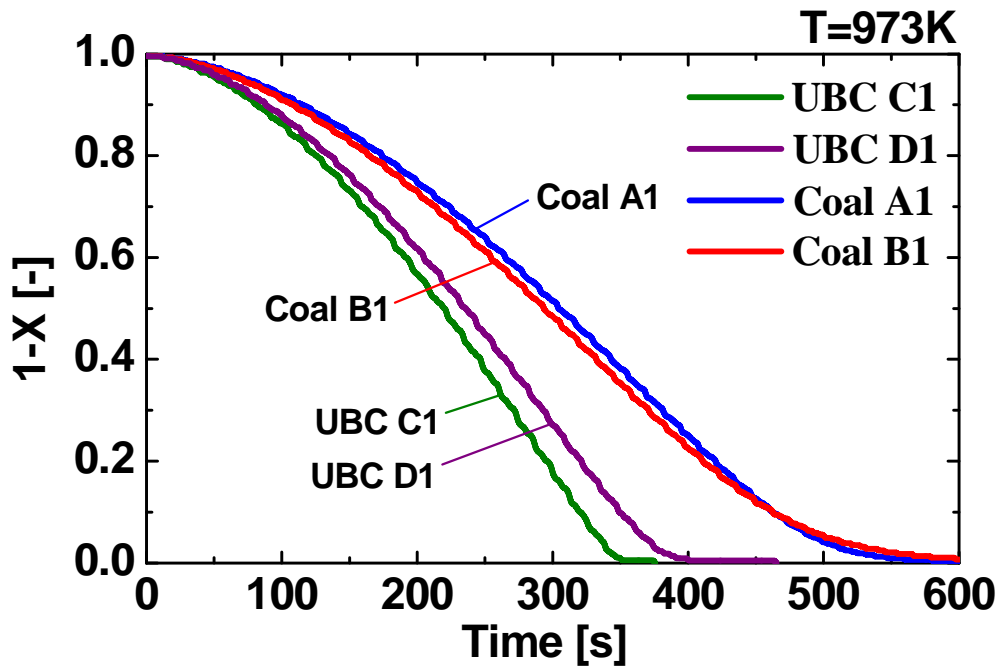


Figure 2-6: Char combustion characteristics of four types of coal by TG-DTA at 973 K.

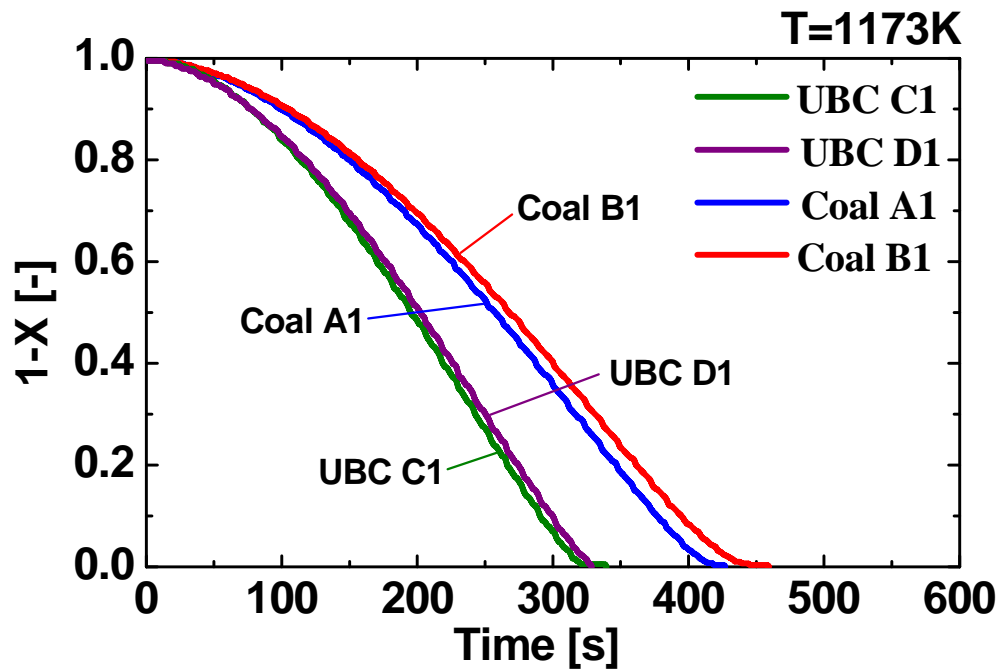


Figure 2-7: Char combustion characteristics of four types of coal by TG-DTA at 1173 K.

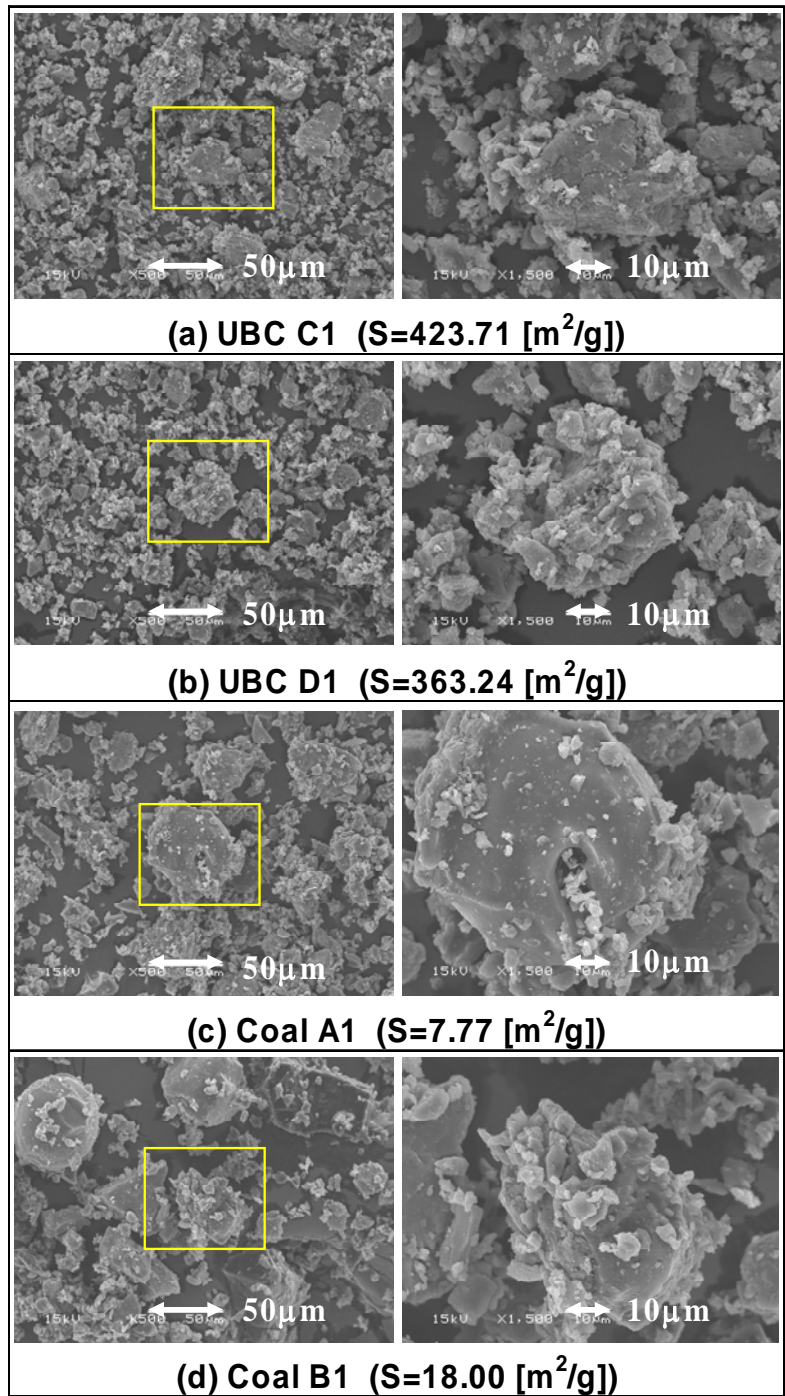


Figure 2–8: SEM images and specific surface area of four types of char.

2.3.2 Burnout Characteristics under Single-stage Combustion

The combustion tests were conducted, using the pilot-scale refractory furnace under single-stage combustion. Figure 2-9 shows the temperature profiles along the central furnace axis. The maximum temperature indicates approximately 1473 K and the temperature profiles are similar, not depending on coal samples. The unburnt fraction defined as Eq.(2-1) is used for the evaluation of combustion characteristics.

$$U_c^* = 100 - \eta = \frac{U_c}{1 - U_c} \times \frac{C_{Ash}}{100 - C_{Ash}} \times 100 \quad (2-1)$$

where U_c^* [%] is the unburnt fraction, η [%] is the combustion efficiency, U_c [%] is the unburnt carbon concentration in fly ash and C_{Ash} [%] is the ash content in coal. Figure 2-10 shows the relationship between the unburnt fraction at the furnace outlet and fuel ratio. The fuel ratio denotes the content ratio of fixed carbon to volatile matter in coal. From this result, the unburnt fraction of UBC C1 and UBC D1 indicate extremely small values. Additionally, the unburnt fraction decreases with decreasing of the fuel ratio. Figure 2-11 shows the unburnt fraction profiles along the central furnace axis. The unburnt fraction of four types of coal decreases as the distance from burner tile becomes long. In particular, the unburnt fraction of UBC C1 and UBC D1 indicates very low values even if the residence time of coal in the furnace is short. It is considered that the reactivity of UBC char with large specific surface area is high enough, as shown in the previous section of 2.3.1. It is thought that a lot of volatile matters in coal contribute to the large surface area of char particle when volatile matters discharge. Consequently, it is understood that UBC with low fuel ratio has good burnout characteristics, compared to the bituminous coal with high fuel ratio, and it contributes to improving the combustion efficiency.

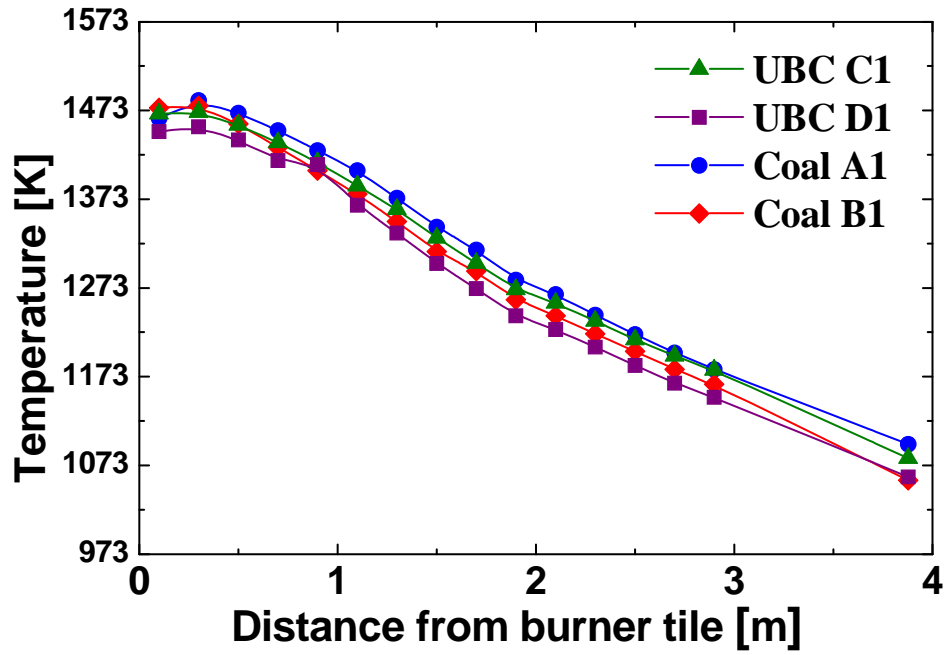


Figure 2-9: Temperature profiles along the central furnace axis.

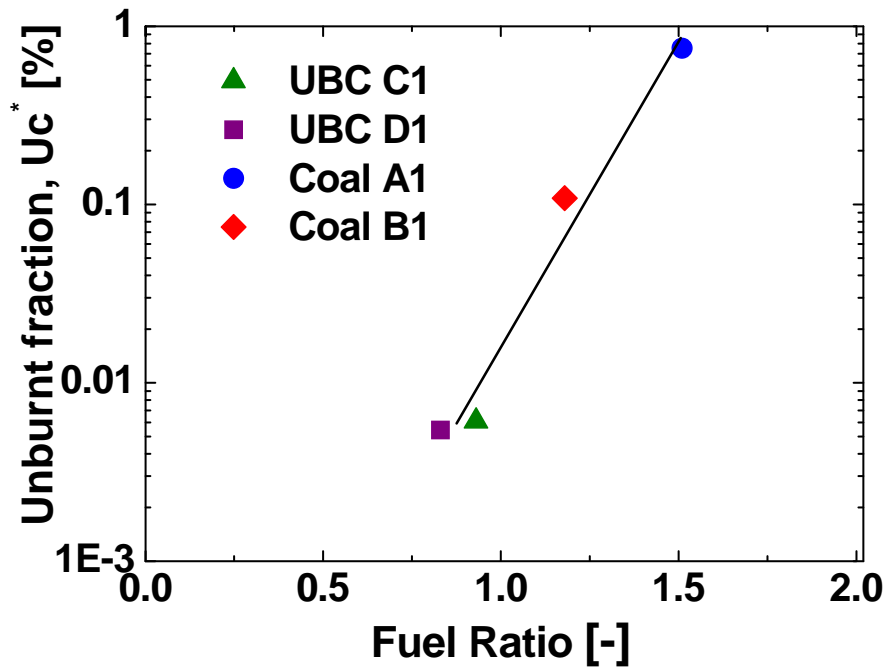


Figure 2-10: Relationship between unburnt fraction and fuel ratio.

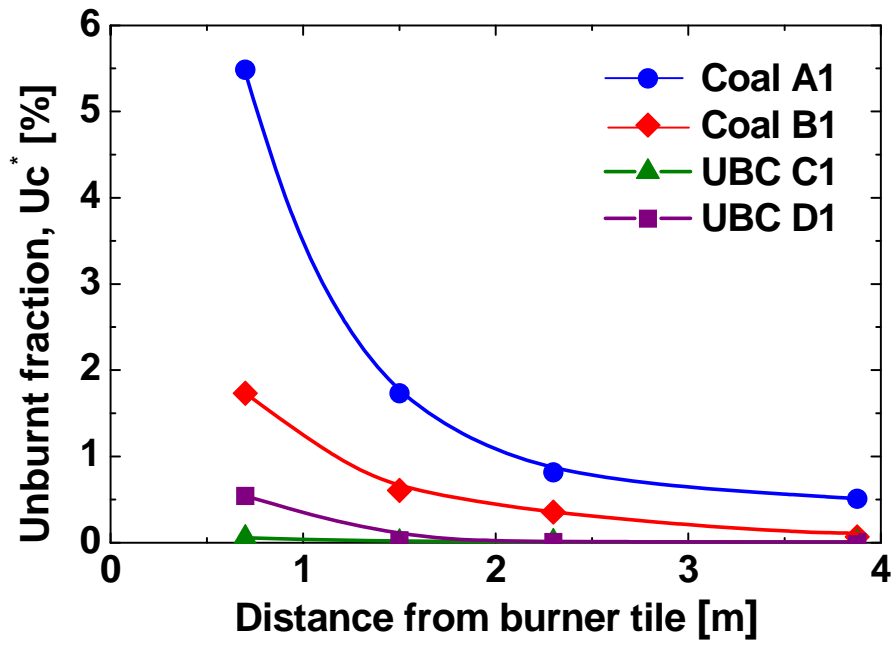


Figure 2-11: Unburnt fraction profiles along the central furnace axis.

2.3.3 NO_X and SO_X Emission Characteristics under Single-stage Combustion

Figure 2–12 shows the results of NO_X concentration and NO_X conversion at the furnace outlet. In pulverized coal combustion, NO_X is mainly formed from fuel bound nitrogen. Here, NO_X conversion, NO_X_CR [–], defined as Eq.(2–2) is used for the evaluation of NO_X emission characteristics

$$NO_X_CR = \frac{C_{NO_X}}{\left(\frac{2.24 \times 10^{-2} \times \frac{FN}{1.4 \times 10^{-2}}}{V_{dry}} \right)} \quad (2-2)$$

where C_{NO_X} [–] is the NO_X concentration at the furnace outlet, FN [–] is the fuel bound nitrogen, and V_{dry} [(m³/h)/(kg/h)] is the flow rate of dry air per feeding rate of coal. From this figure, the NO_X concentration decreases as the fuel-bound nitrogen decreases. However, NO_X conversion increases as the fuel-bound nitrogen decreases. It is considered that NO_X conversion of UBC increases because the unburnt fraction of UBC is extremely low and the reduction of NO_X by char particles is inhibited during combustion.

On the other hand, Figure 2–13 shows the results of SO_X concentration and SO_X conversion at the furnace outlet. In pulverized coal combustion, SO_X is formed from fuel-bound sulfur and pyrite. Here, SO_X conversion, SO_X_CR [–], defined as Eq.(2–3) is used for the evaluation of SO_X emission characteristics

$$SO_X_CR = \frac{C_{SO_X}}{\left(\frac{2.24 \times 10^{-2} \times \frac{FS}{3.2 \times 10^{-2}}}{V_{dry}} \right)} \quad (2-3)$$

where $C_{SO_x} [-]$ is the SO_x concentration at the furnace outlet, $FS [-]$ is the sulfur content in coal, and $V_{dry} [(m^3/h)/(kg/h)]$ is the flow rate of dry air per feeding rate of coal. From this figure, the SO_x concentration decreases as the sulfur content decreases. In particular, the SO_x conversion becomes zero value for the UBC C1. Here, the Ca/S mole ratio for each coal is shown in Figure 2–14. The result shows that the Ca/S mole ratio of UBC C1 indicates extremely higher value of 3.4, compared with those of other coals. For the UBC C1, it is considered that the calcium component in coal reacts with the sulfur constituent during combustion, and the solid compound containing sulfur like $CaSO_4$ is generated. As a result, the generation of SO_x is controlled.

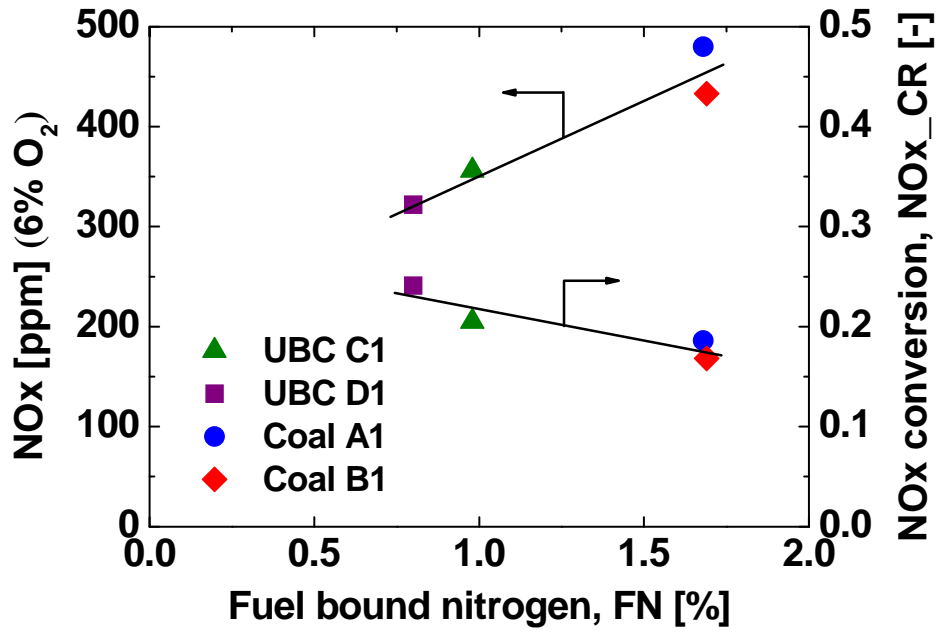


Figure 2-12: Results of NO_x concentration and NO_x conversion at the furnace outlet.

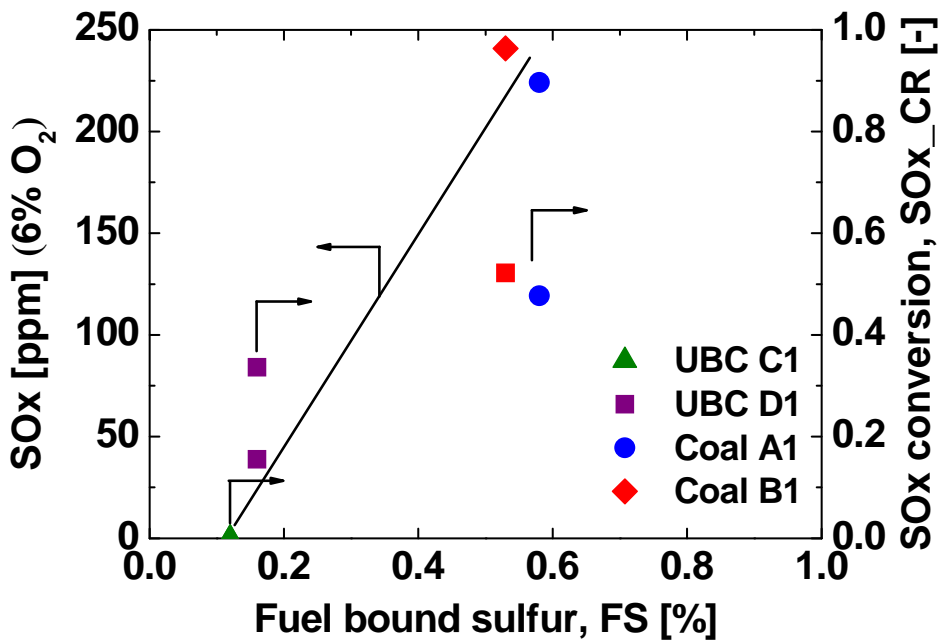


Figure 2-13: Results of SO_x concentration and SO_x conversion at the furnace outlet.

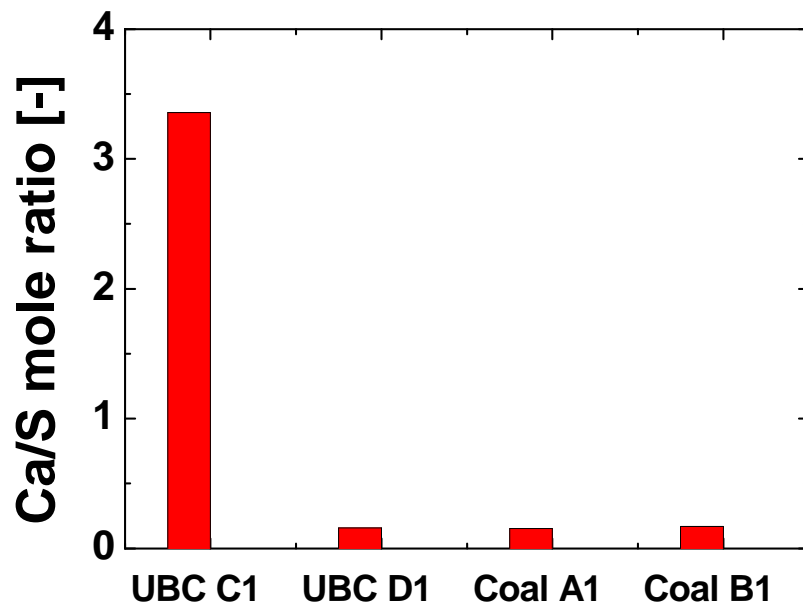


Figure 2-14: Ca/S mole ratio for four types of coal.

2.3.4 Effect of Two-stage Combustion on Burnout and NO_x Emission Characteristics

The combustion tests are conducted, using a refractory furnace, varying the parameters of the two-stage combustion ratio. In the previous study, it was reported that the unburned carbon content in the fly ash increased when the operations to reduce the emission of NO_x were performed in pulverized coal-fired boilers [4–7]. Figure 2–15 shows the effects of two-stage combustion on NO_x concentration and unburnt fraction at the furnace outlet. The NO_x concentration decreases with increasing of the two-stage combustion ratio for four types of coal as the reducing atmosphere is formed in the furnace. On the other hand, the unburnt fraction of Coal A1 and Coal B1 increases with increasing of the two-stage combustion ratio. However, the unburnt fraction of UBC C1 and UBC D1 indicates almost zero even if the two-stage combustion ratio increased. It is thought that the char burnout rate of UBC is fast enough even if the residence time is short. Consequently, it is concluded that UBC has good burnout characteristics compared to the bituminous coal and it contributes to both improvement of the combustion efficiency and NO_x reduction even if the two-stage combustion ratio increased.

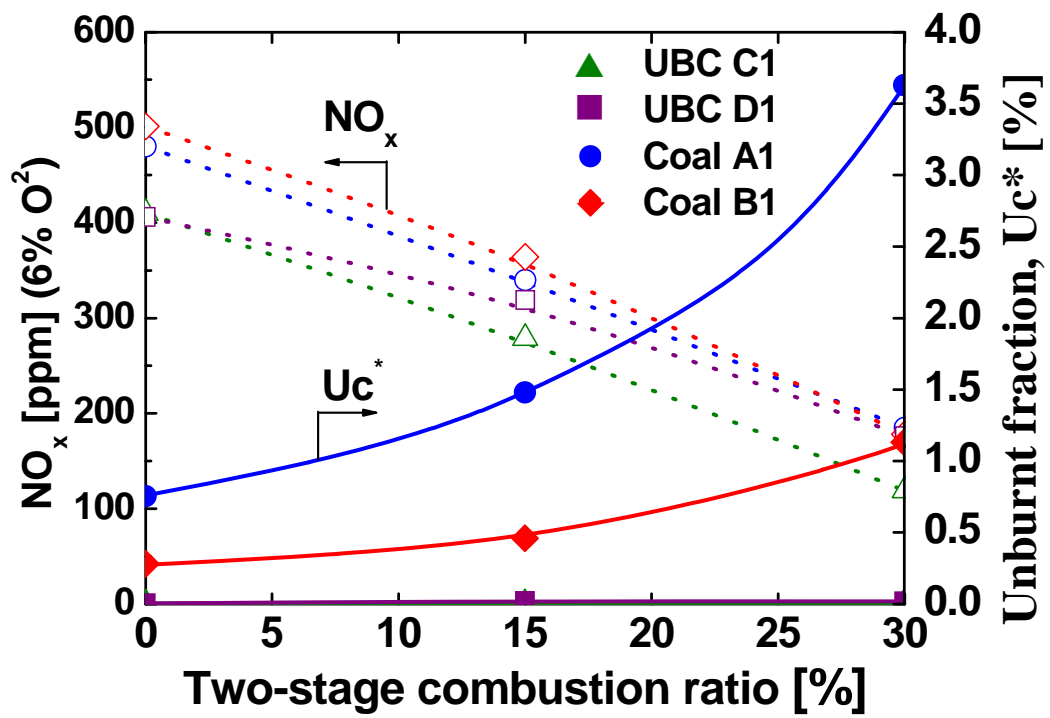


Figure 2–15: Effects of two–stage combustion on NO_x concentration and unburnt fraction.

2.4 Conclusions

Thermo-gravimetric analysis and combustion test, using the pilot-scale pulverized coal combustion refractory furnace, are conducted to elucidate the combustion characteristics of UBC and bituminous coal, their NO_x and SO_x emissions and the burnout characteristics quantitatively. The following results are obtained:

- UBC contains a lot of volatile matter which evolves at low temperature below 700 K, compared with the bituminous coal. However, the coal type does not greatly affect the evolution rate of volatile matter.
- The char burnout time of UBC is considerably shorter than that of bituminous coal, because the specific surface area of UBC is larger than that of bituminous coal.
- NO_x conversion of UBC increases because the unburnt fraction of UBC is extremely low and the reduction of NO_x by char particles is inhibited during combustion. However, the NO_x concentration of UBC is relatively lower than that of bituminous coal since UBC contains only a little nitrogen.
- The generation of SO_x depends on both the sulfur content and Ca/S mole ratio in coal.
- UBC has good burnout characteristics, compared to the bituminous coal. This contributes to both improvement of the combustion efficiency and NO_x reduction even if the two-stage combustion ratio increases.

References

- [1] S. Sugita, T. Deguchi, T. Shigehisa, S. Katsushima, Demonstration of UBC process in Indonesia, ICCS&T, Okinawa, Japan, (2005) Oct.
- [2] S. Sugita, T. Deguchi, T. Shigehisa, Demonstration of a UBC (Upgrading of Brown Coal) Process in Indonesia, Kobe Steel Engineering Reports, 56 (2) (2006) pp.23–26.
- [3] S. Yamamoto, S. Sugita, Y. Mito, T. Deguchi, T. Shigehisa, Y. Otaka, Development of Upgraded Brown Coal Process, The Institute for Briquetting and Agglomeration (IBA), Savannah, GA, (2007) Oct.
- [4] Costa M, Azevedo JLT, Experimental characterization of an industrial pulverized coal-fired furnace under deep staging conditions, Combustion Science and Technology, 179 (9), (2007) pp.1923–1935.
- [5] Ribeirete A, Costa M, Detailed measurements in a pulverized-coal-fired large-scale laboratory furnace with air staging, Fuel, 88 (1), (2009) pp.40–45.
- [6] Ren F, Li Z, Jing J, Zhang X, Chen Z, Zhang J, Influence of the adjustable vane position on the flow and combustion characteristics of a down-fired pulverized-coal 300 MWe utility boiler, Fuel Processing Technology, 89 (12), (2008) pp.1297–1305.
- [7] Shirai H, Tsuji H, Ikeda M, Kotsuji T, Influence of Combustion Conditions and Coal Properties on Physical Properties of Fly Ash Generated from Pulverized Coal Combustion, Energy Fuels, 23 (7), (2009) pp.3406–3411.

Chapter 3

Elucidation of Ash Deposition Behavior of UBC, Bituminous Coal and their Blended Coal

3.1 Introduction

Ash deposition phenomena are known to be influenced by the coal type (ash constituents, melting temperature, distribution of mineral matter, etc.), reaction atmosphere, particle temperature, surface temperature of the heat exchanger tube and its surface material, flow dynamics and so forth. However, precise and quantitative knowledge on the deposition of coal ash with a low-melting temperature during coal combustion has been insufficient yet. Additionally, Rushdi *et al.* [1] studied the effect of the coal blending on ash deposition during combustion, and concluded that the behavior of the blends was not additive in nature. Consequently, it is necessary to elucidate the key parameters controlling the ash deposition characteristics and to predict them quantitatively even when a blend of several types of coal are burned.

In this chapter, the relationship between the ash deposition characteristics and the ash melting characteristics under the coal blending conditions is elucidated. Indonesian UBC and two types of bituminous coal with different melting temperatures and ash compositions are

used for the combustion tests. The ash deposition tests were conducted using a refractory furnace. A water-cooled tube was inserted into the furnace to make the ash adhere to it. The molten slag fraction in ash was calculated with chemical equilibrium calculations.

3.2 Experimental Section

Figure 3–1 shows a schematic diagram of the pilot-scale pulverized coal combustion refractory furnace used in this study. The furnace was 3.65 m long and 0.4 m in inner diameter. It was insulated by refractory material to reduce the heat loss. The pulverized coal weighed by the volumetric feeder was transported to the burner with nitrogen gas. The primary air (at ambient temperature) and secondary air (at 573 K) were supplied separately. City gas was supplied to the furnace in order to heat it to 1750 K. Three types of coal were used as the samples, as shown in Table 3–1. UBC D2 is the upgraded brown coal from Indonesia. Coal A2 and Coal B2 are the bituminous coal of Australia and Indonesia, respectively. As seen from the table, the fuel ratio of UBC D2 was the lowest and the ash melting temperature of Coal A2 was the highest among the three coals. Ash produced from UBC D2 especially had a low SiO₂ content and high Fe₂O₃ content. The coal was pulverized so that a mass fraction of 85 % formed particles with diameters less than 75 μm. Table 3–2 shows the experimental conditions. The heat load was fixed at a given value of 149 kW for all the tests. The oxygen concentration of the flue gas at the furnace outlet was fixed at a given value of 1.0 % on a dry basis. The oxygen concentration at the ash deposition tube inserted was between 1.0 % and 2.0 % on a dry basis. A deposition probe, made of stainless steel (SUS304), was inserted 1.9 m from the burner tile where the temperature was around 1573 K. The temperature around the ash-deposition tube was similar to that in the slagging area near the burner in the pulverized coal combustion boiler. The length and outer diameter of the ash deposition tube were 0.2 and 0.0318 m, respectively.

The deposition probe mainly consisted of a test piece for deposition and a water-cooled probe as shown in Figure 3-2. It is assumed that the temperature measured by these thermocouples was almost the same as the surface temperature of the test piece for deposition. The surface temperature was controlled to 773 K by adjusting the flow rate of the cooling water inside the tube. The cross-sectional structure and compositions of ash deposit on the tube was observed, using a scanning electron microscope (SEM) and an energy dispersive X-ray spectroscopy (EDX) apparatus. In the experiments, the thermocouple and gas sampling probe were inserted into the furnace to measure the gas temperature and gas concentrations, respectively.

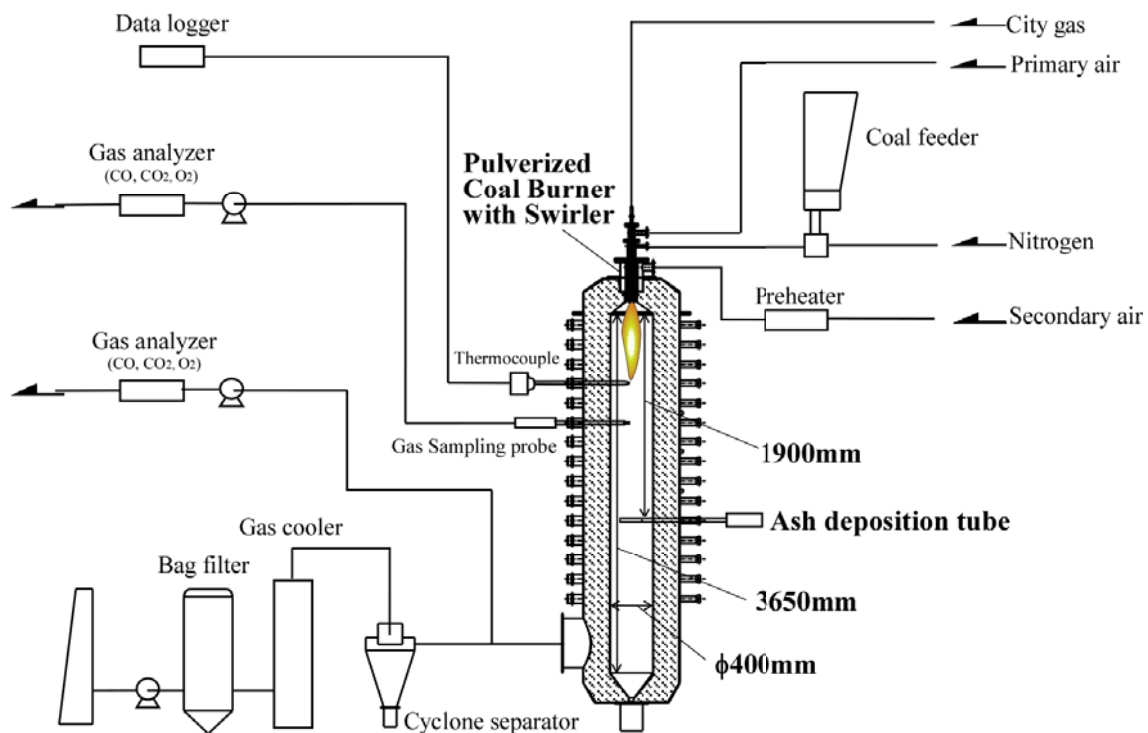


Figure 3-1: Schematic diagram of pilot-scale pulverized coal combustion refractory furnace

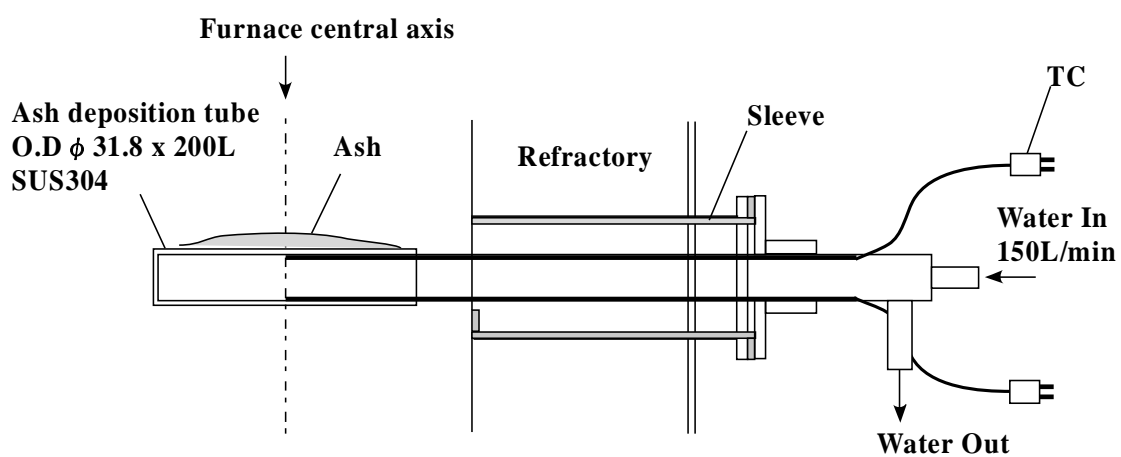


Figure 3-2: Water-cooled ash deposition probe.

Table 3-1: Properties of coals tested.

Coal sample		UBC D2	Coal A2	Coal B2
Heating value [MJ/kg]		27.17	28.89	27.53
Proximate analysis [wt%, dry]	Ash	1.76	12.53	6.23
	Volatile matter	54.76	33.54	43.31
	Fixed carbon	43.55	53.93	50.46
Fuel ratio [-]		0.80	1.61	1.17
Total sulfur [wt%, d.a.f.]		0.22	0.54	0.75
Ultimate analysis [wt%, d.a.f.]	Carbon	71.15	82.70	79.64
	Hydrogen	5.39	5.30	5.76
	Nitrogen	0.92	1.87	1.83
	Sulfur	0.18	0.50	0.70
	Oxygen (Balance)	22.35	9.61	12.06
Ash fusion temperature [K] (Oxidizing)	Initial deformation	1452	1441	1326
	Hemispherical	1687	>1823	1614
	Fluid	1804	>1823	1687
Ash compositions [wt%]	SiO ₂	40.00	69.80	56.90
	Al ₂ O ₃	27.85	20.73	23.00
	CaO	3.70	0.48	2.19
	TiO ₂	0.56	1.03	0.57
	Fe ₂ O ₃	19.95	4.95	11.80
	MgO	1.21	0.66	2.27
	Na ₂ O	0.14	0.25	0.04
	K ₂ O	0.40	0.98	0.44
	P ₂ O ₅	0.05	0.20	0.34
	MnO	0.27	0.05	0.03
	V ₂ O ₅	0.05	0.05	0.05
	SO ₃	3.80	0.40	1.27

Table 3-2: Experimental conditions

Coal sample	UBC D2, Coal A2, Coal B2
Heating value [kW]	149
Combustion stoichiometric ratio [-]	1.05
Oxygen concentration at furnace outlet [%]	1.0
Oxygen concentration around ash deposition tube [%]	1.0~2.0
Gas and mean particle temperature around ash deposition tube [K]	1534~1545
Gas velocity at 1540 K [m/s]	~2.6
Surface temperature of ash deposition tube [K]	773
Ash deposition tube diameter [mm]	31.8
Ash deposition tube length [mm]	200
Exposure time for ash deposition [min]	30, 60, 100

3.3 Results and Discussion

3.3.1 Ash Deposition Behavior

Figure 3–3 shows the temperature profiles for three types of coal along the central furnace axis measured with a thermocouple. The temperature profiles for each case are similar. The temperature at the location, where the ash deposition tube was inserted, is between 1534 and 1545 K. The maximum particle temperature measured with a two–color pyrometer reaches 2000 K at a location 0.3 m from the burner tile. Photos of ash deposition on the tube surface for three types of coal after 100 min of exposure are shown in Figure 3–4. For Coal A2, numerous fine gray particulates seem to deposit on the surface, and some particulates agglomerate with each other. For Coal B2, numerous fine brown particles deposit on the surface, and some of the deposited ashes are in a molten state. For UBC D2, on the other hand, most of the deposited ashes are in a molten state, and a very thin layer of molten slag forms on the surface of the tube. Figure 3–5 shows the cross–sectional structure and compositions of the deposit on the tube for the three types of coal. In those figures, the light gray layer indicates the oxidized thin film of the tube made of stainless steel (SUS304). The gray particles show the ash. For Coal A2, there are many spherical ash particles on the layer of the oxidized thin film on the tube. Some ash particles with SiO_2 and Al_2O_3 also locally exist in the layer of the oxidized thin film. For Coal B2, there are a few ash particles in the layer of the oxidized thin film. However, for UBC D2, there are no particles in the oxidized thin film on the tube. Additionally, the ash particles with SiO_2 and Al_2O_3 uniformly exist in the layer of the oxidized thin film. It is thought that the molten slag from the UBC ash reacts with the oxidized thin film and forms a homogeneously decentralized molten slag layer on the tube.

Figure 3–6 shows the time dependence of the deposition fraction of ash (ϕ_{ash}) for the three types of coal. The deposition fraction of ash is defined as the following equations:

$$\phi_{ash} = \frac{D_{ash}}{F_{ash-probe} \cdot t} \quad (3-1)$$

$$F_{ash-probe} = \frac{A_p}{A_f} F_{ash-furnace} \quad (3-2)$$

In Eqs. (3-1) and (3-2), D_{ash} denotes the deposition mass of ash for a certain exposure time (t). $F_{ash-probe}$ and $F_{ash-furnace}$ mean the mass flow rate of ash in the cross-sectional areas of the probe (A_p) and furnace (A_f), respectively. The profile of deposition fraction of ash depends on the coal type as shown in Figure 3-6. The initial deposition fractions of ash for three types of coal have high values and become steady after 100 min. Therefore, the exposure time for evaluating the deposition fraction of ash is defined as 100 min. It is found that the deposition fractions of ash after 100 min are high in the order of UBC D2, Coal B2 and Coal A2. In particular, the deposition fraction of UBC D2 is relatively higher, even though the ash content is lower. It is assumed that some factors such as particle size, momentum and viscosity affect the deposition fractions of ash. However, it is confirmed that the ash particle size distributions of three types of coal measured by the particle size analyzer are almost the same. Consequently, the molten state of ash particles affects the ash deposition fraction on the surface of the tube. From those results, the ash compositions such as SiO_2 , Al_2O_3 , Fe_2O_3 and alkali metals and molten state of slag will affect the behavior of ash deposition on the tube.

Figure 3-7 shows the experimental results of the deposition fraction of ash under coal blending conditions. The deposition fraction of ash ($\phi_{ash, t=100}$) after 100 min corresponding to the mixing ratio of ash is measured in the experiment with blended coal combustion. In the figure, the deposition fractions of ash produced from a mixture with UBC D2 show a curve with a local maximum value. In particular, the deposition fraction of ash produced from a mixture of Coal B2 and UBC D2 indicates the highest value when the mixing ratio of UBC ash is around 60%.

From those results, the deposition fraction of ash under coal blending conditions affects the molten state of ash.

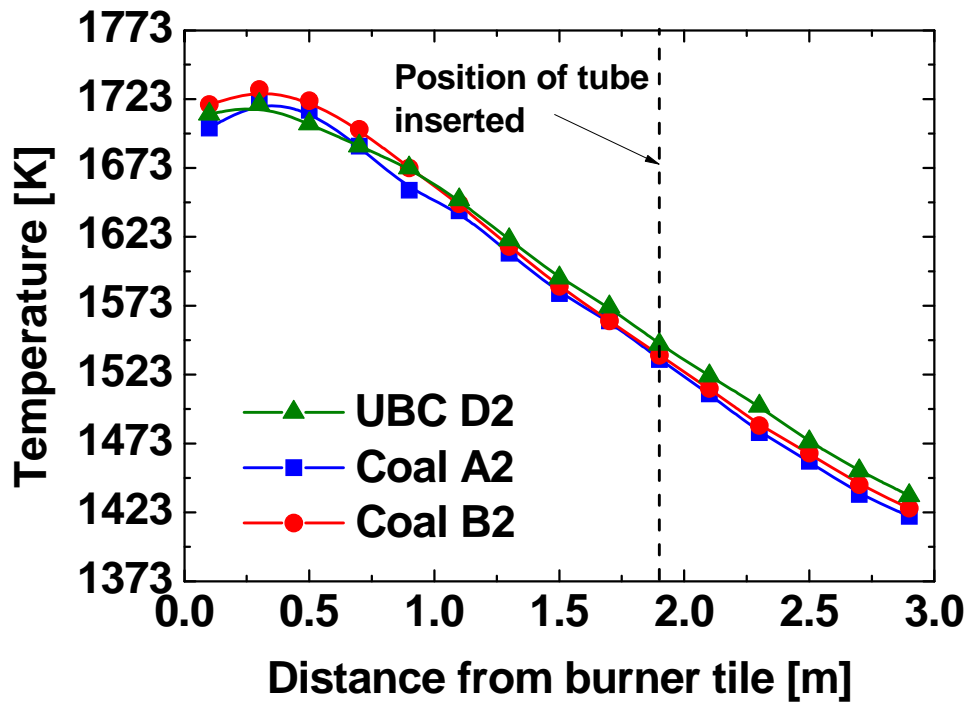


Figure 3-3: Temperature profiles for three types of coal along the central furnace axis.

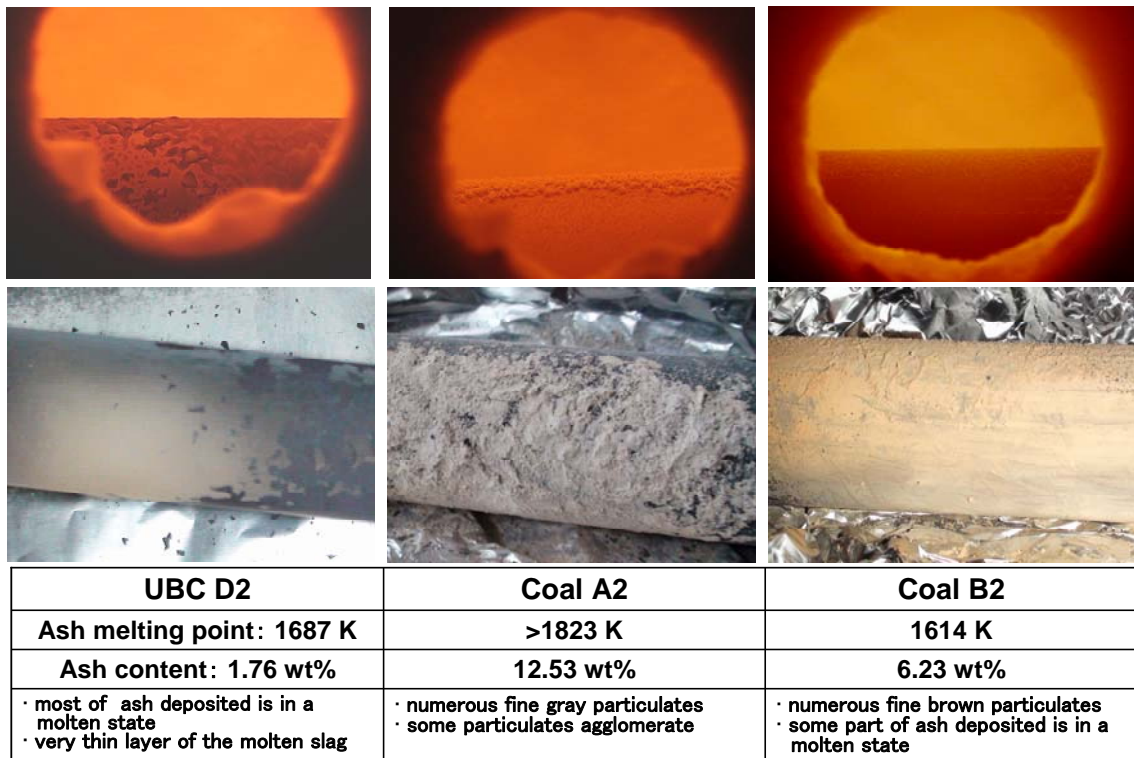


Figure 3-4: Photos of ash deposition on the tube surface for three types of coal after 100 min. (upper photos: tubes in the furnace; bottom photos: tubes out of the furnace)

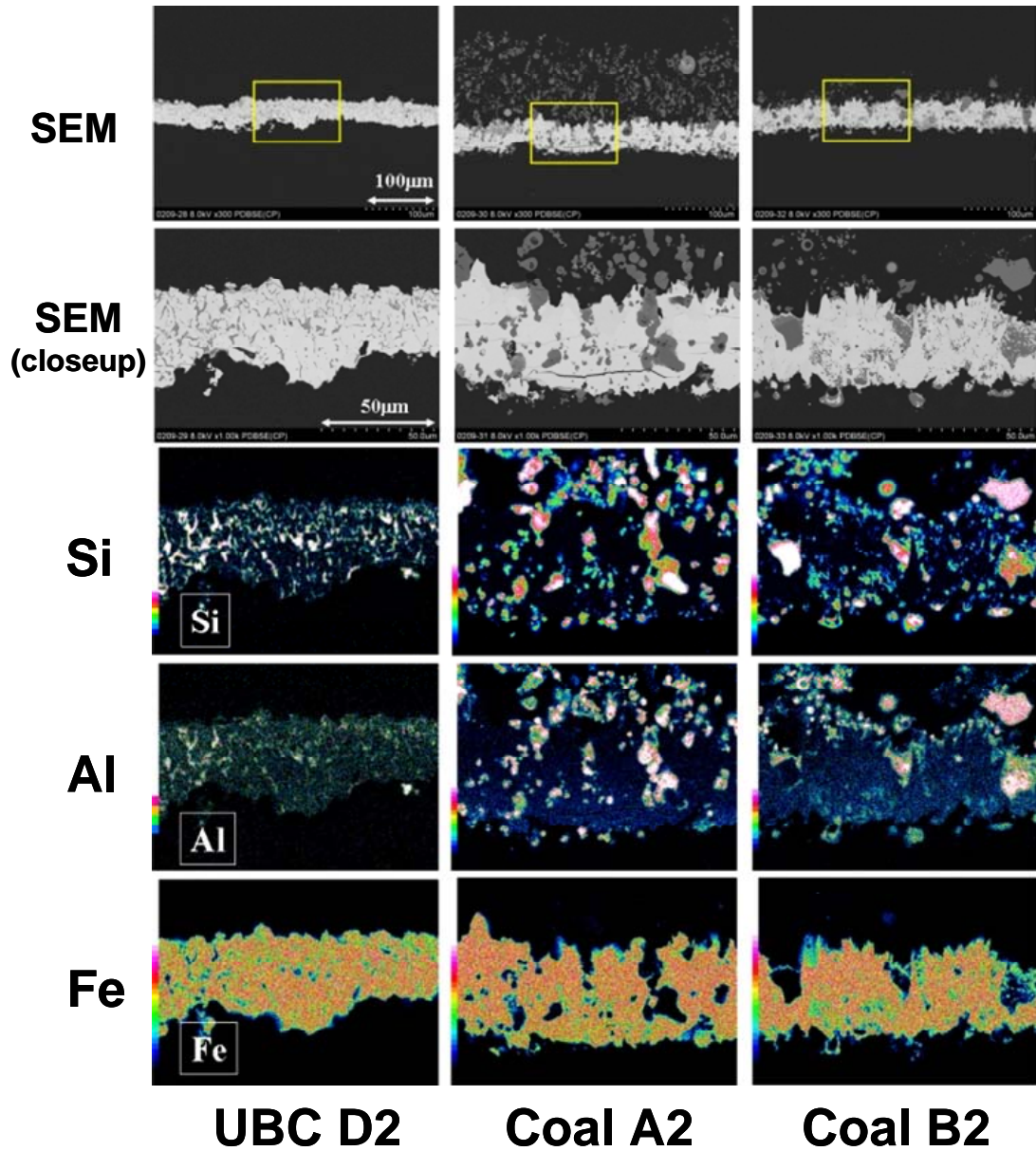
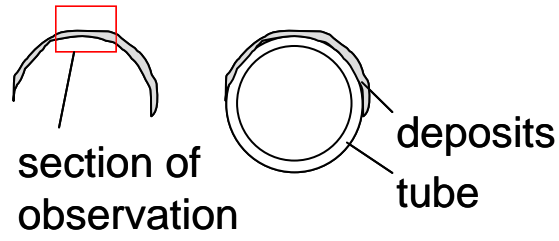


Figure 3-5: Cross-sectional structure and compositions of deposit on the tube for three types of coal.

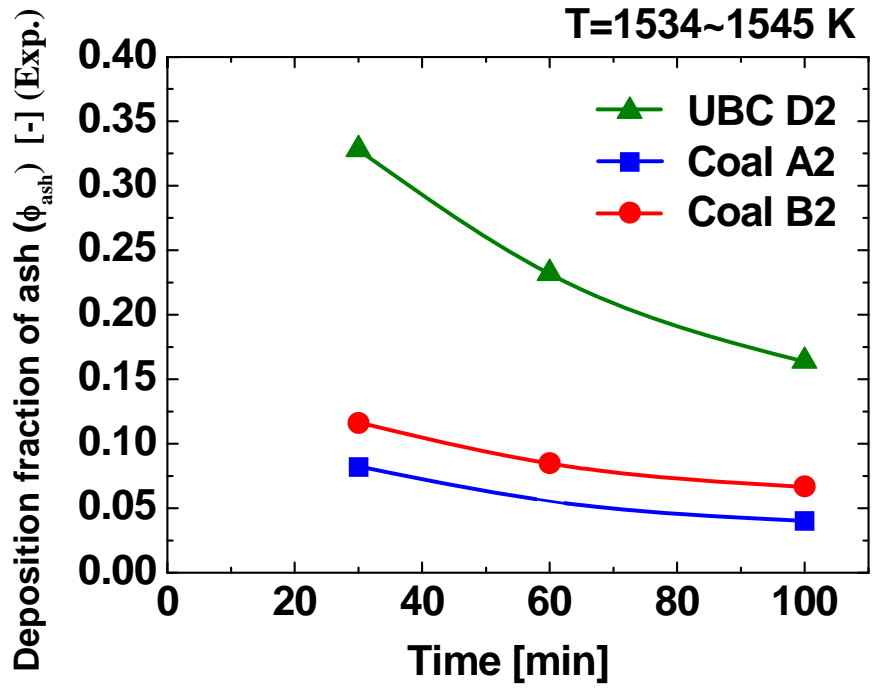


Figure 3-6: Time dependence of the deposition fraction of ash (ϕ_{ash}) for the three types of coal.

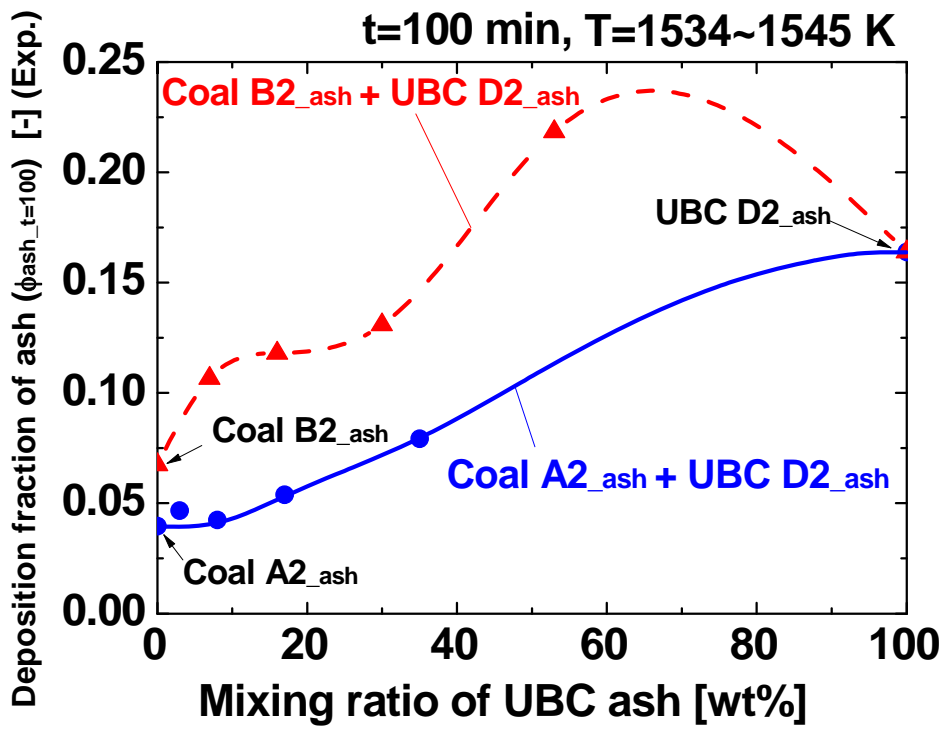


Figure 3-7: Experimental results of deposition fraction of ash under coal blending conditions.

3.3.2 Chemical Equilibrium Calculations

In this calculation, I tried to evaluate the molten fraction of each ash by chemical equilibrium theory, using Fact Sage Ver. 5.5 software [2,3]. This software has special thermodynamic databases on non-ideal liquid species, so it can simulate the compositions of non-ideal liquid species in terms of the minimization of the Gibbs's free energy of all phases as functions of temperature and the initial composition. Table 3-3 shows the conditions of the chemical equilibrium calculations. In the calculations, the ash compositions of the blended coal were assumed to be uniform. The gaseous compositions given were assumed to be near a burner in the pulverized coal combustion boiler. The ash deposition area is always exposed to the flue gas as shown in Table 3-3. These calculations were performed at 50 K increments to determine the mass percentage of molten slag in the ash in the temperature range 1273–2073 K.

Figure 3-8 shows the calculated molten slag fractions for the three types of coal ash. The molten slag fraction is defined as the content ratio of molten slag to total ash. The molten slag formation for the three types of ash starts between 1273 and 1473 K. The molten slag fraction of UBC D2 ash rapidly increases between 1473 and 1523 K; however, its growth trend decreases at temperatures of 1523 K or higher. Although the molten slag fraction for Coal B2 ash also increases over 1473 K, the growth trend does not decrease around 1523 K. For Coal A2 ash, the growth trend of the molten slag fraction in ash increases very slowly up to 1623 K. The coal ash compositions and calculated results of the molten slag compositions at 1573 K for the three types of coal ash are shown in Table 3-4. For the Coal A2 ash, all of CaO, Na₂O and K₂O are contained in the molten slag, but the major components like SiO₂, Al₂O₃ and Fe₂O₃ are little contained in the molten slag. However, for the Coal B2 and UBC D2 ashes, the major components like SiO₂, Al₂O₃ and Fe₂O₃ are contained in the molten slag. Those calculated molten slag fractions in ash shown in Figure 3-8 correlate well with the experimental results of

the deposition fraction of ash, as shown in Figure 3–6. According to Table 3–4, the phase change of the main components in ash like SiO_2 , Al_2O_3 and Fe_2O_3 from solid to slag phase may relate to easiness of the ash deposition. As the result of Table 3–4 suggests that the stable slag compositions are obtained thermodynamically, the molten slag fraction in ash obtained by the chemical equilibrium calculations is a useful index for predicting the deposition fraction of ash. Figure 3–9 shows the calculated results of molten slag fraction in ash at a temperature of 1573 K under ash blending conditions. In this figure, the molten slag fractions show curves with the local maximum value when there is a mixture with UBC D2 ash. In particular, the molten slag fraction in ash produced from a mixture of Coal B2 ash with UBC D2 ash shows the highest value when the mixing ratio of UBC D2 ash is around 60%. Those calculation results correlate well with the experimental results, as shown in Figure 3–7. Figure 3–10 shows the relationship between the molten slag fraction in ash and the deposition fraction of ash. It is clearly confirmed that the deposition fraction of ash increases as the molten slag fraction in ash increases. In particular, the deposition fraction in ash rapidly increases if the molten slag fraction in ash becomes over around 60%. As a result, the molten slag fraction in ash obtained by the chemical equilibrium calculation correlates with the deposition fraction of ash obtained by experiments even under mixing conditions of UBC to bituminous coal. Therefore, the molten slag fraction in ash obtained by the chemical equilibrium calculations is one of the useful indices to predict the blending method with UBC to reduce the deposition fraction of ash.

Table 3-3: Condition of chemical equilibrium calculation for three types of coal ash and their blends.

Temperature (K)	1273 ~ 2073	
Gas composition (%)	O ₂	1.0
	CO ₂	19.0
	N ₂	80.0
Ash composition (wt%)	SiO ₂ , Al ₂ O ₃ , CaO, TiO ₂ , Fe ₂ O ₃ , MgO, Na ₂ O, K ₂ O, P ₂ O ₅ , MnO, V ₂ O ₅ , SO ₃	

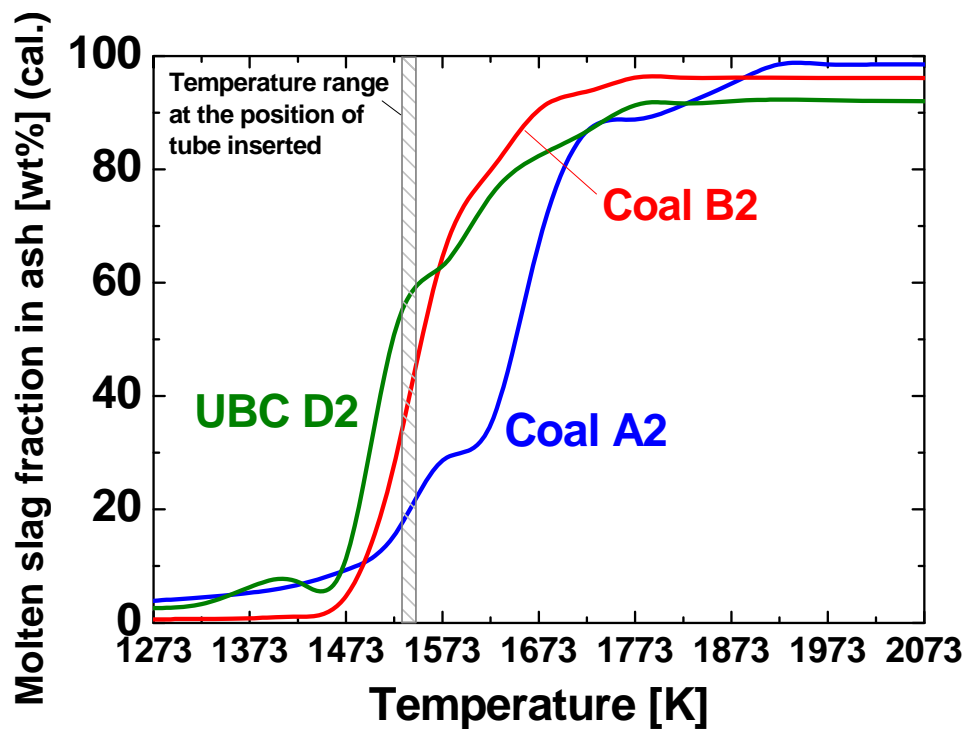


Figure 3-8: Calculated results of molten slag fraction in ash for three types of coal ash.

Table 3-4: Coal ash composition and calculated results of molten slag composition at 1573 K for three types of coal ash.

	UBC D2(ash)	UBC D2(slag)	Coal A2(ash)	Coal A2(slag)	Coal B2(ash)	Coal B2(slag)
SiO ₂	40.00	33.99	69.80	22.48	56.90	35.69
Al ₂ O ₃	27.85	13.07	20.73	2.88	23.00	12.90
CaO	3.70	3.70	0.48	0.48	2.19	2.19
TiO ₂	0.56	0.56	1.03	1.03	0.57	0.57
Fe ₂ O ₃	19.95	2.68	4.95	0.03	11.80	3.07
FeO	0.00	7.41	0.00	0.38	0.00	7.86
MgO	1.21	1.08	0.66	0.08	2.27	2.22
Na ₂ O	0.14	0.14	0.25	0.25	0.04	0.04
K ₂ O	0.40	0.08	0.98	0.98	0.44	0.07
P ₂ O ₅	0.05	0.00	0.20	0.00	0.34	0.00
MnO	0.27	1.08	0.05	0.05	0.03	2.22
V ₂ O ₅	0.05	0.00	0.05	0.00	0.05	0.00
SO ₃	3.80	0.00	0.40	0.00	1.27	0.00

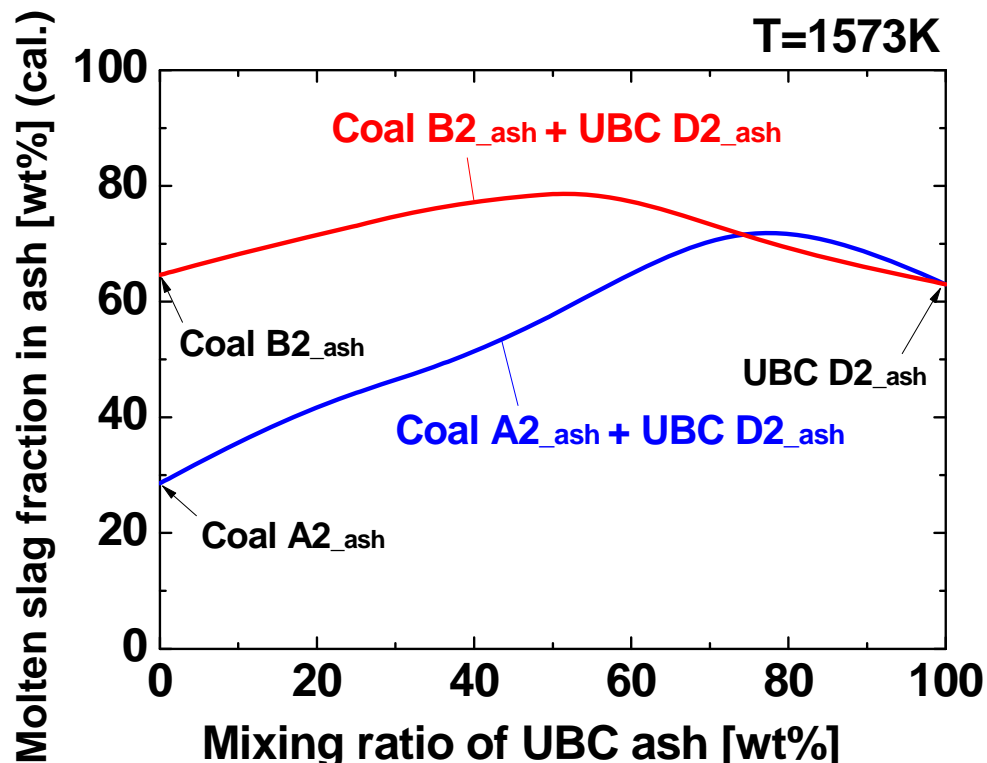


Figure 3-9: Calculated molten slag fractions in ash under ash blending conditions.

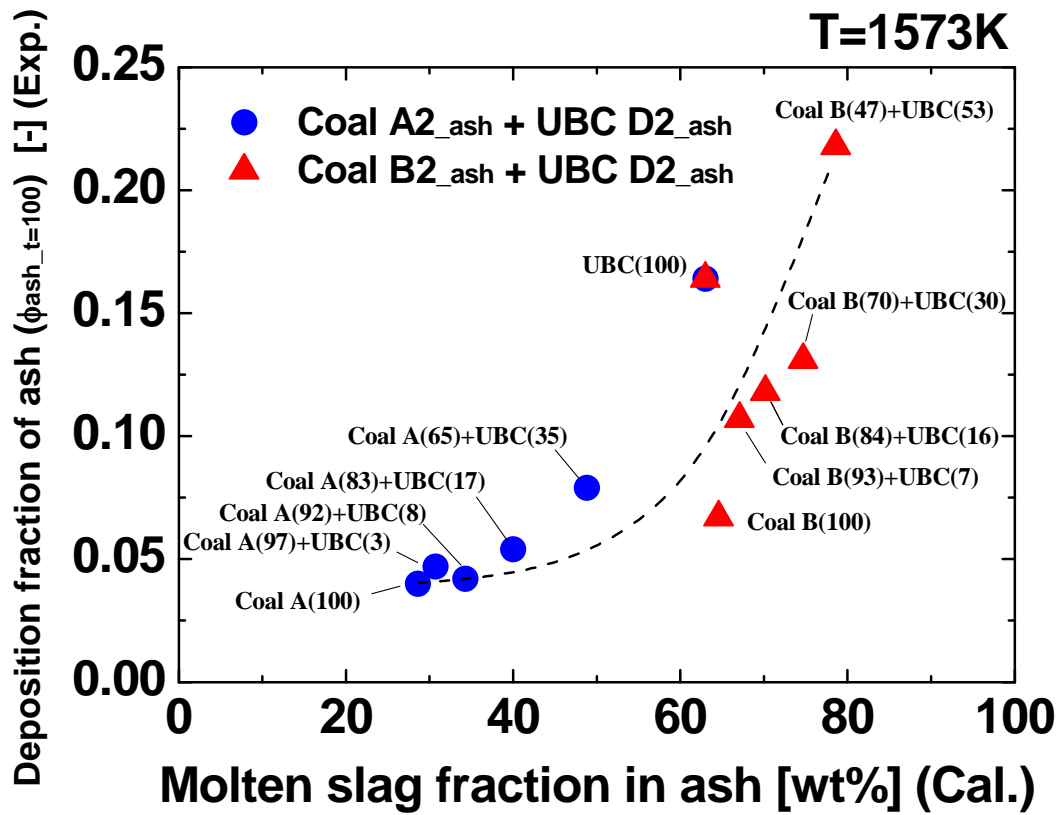


Figure 3–10: Relationship between molten slag fraction in ash and deposition fraction of ash.

3.4 Conclusions

Ash deposition tests are conducted and chemical equilibrium calculations are carried out for three types of coal in this study. The following findings are obtained:

- The ash deposition characteristics have a close relationship with the ash melting characteristics.
- The molten slag fraction in ash obtained by the chemical equilibrium calculation correlates with the deposition fraction of ash obtained in experiments even under mixing conditions of UBC to bituminous coal.
- The molten slag fraction in ash obtained by the chemical equilibrium calculations is one of the useful indices to predict the blending method with UBC to reduce the deposition fraction of ash.

References

- [1] Rushdi A, Sharma A, Gupta R, An experimental study of the effect of coal blending on ash deposition, *Fuel*, 83, (2004) pp.495–506.
- [2] FACT, www.crct.polymtl.ca
- [3] Bale CW, Chartrand P, Deckerov SA, Eriksson G, Hack K, Mahfoud RB, Melançon J, Pelton AD, Petersen S, FactSage thermochemical software and databases, *Calphad Journal*, 62, (2002) pp.189–228.

Chapter 4

Elucidation of Mechanisms of the Reduction of Ash Deposition Using Additive

4.1 Introduction

In Chapter 3, it has been proven that the molten slag fraction in ash obtained by chemical equilibrium calculations is one of the useful indices to predict the coal blending method to reduce the deposition fraction of ash. On the other hand, there exist a lot of power stations using low-rank coals with low ash melting point such as sub-bituminous, lignite and brown coal alone in Indonesia, China, Germany and so on. Therefore, it is also desired to develop the technologies that can reduce the ash deposition using additive to coal in order to utilize low-rank coals including UBC as much as possible. It is considered that this technology contributes to the effective utilization of unused fossil fuel resources in the near future.

First, the influence of each ash constituent on the molten slag fraction is evaluated in order to determine the proper component as an additive. From this study, it is understood that MgO is most effective in controlling the molten slag fraction of ash. Several papers relating to Mg-based fuel additives for boilers have already been reported. Pohl *et al.* [1] investigated the effect of the injection of Mg(OH)₂ slurry on the reduction of slagging in a coal-fired boiler, while

Libutti *et al.* [2], Williams *et al.* [3], and Sinha [4] studied the effect of the injection of MgO additives on the reduction of fireside corrosion in an oil-fired boiler. Ninomiya *et al.* [5] evaluated the addition of a Mg-based additive to coal on the emission/reduction of particulate matter (PM) during coal combustion. Even in those references, however, the mechanisms by which MgO addition to the coal affects the reduction of ash deposition were not elucidated.

In this chapter, the objectives are to evaluate the effect of MgO addition to the coal on the reduction of ash deposition for UBC and to understand the mechanisms of this reduction of ash deposition. The melting temperature of UBC ash is 1494 K, which is lower than that of bituminous coal ash. Before the actual ash-deposition experiments, the molten slag fraction in the UBC ash was estimated by means of chemical equilibrium calculations for different mixing mass ratios of MgO to coal ash. In the next step, ash-deposition tests were also conducted, using a pilot-scale pulverized coal combustion furnace equipped with a refractory wall.

4.2 Chemical Equilibrium Calculations

For the calculations, the UBC E of Indonesian UBC and the Coal A3 of Australian bituminous coal with different melting temperatures and ash compositions are selected, as shown in Table 4-1. As seen from the table, the hemispherical melting temperature of UBC E ash under oxidizing conditions is extremely lower than that of Coal A3 ash. The prominent features of UBC E ash are higher CaO and Fe₂O₃ contents in the ash. The ash particles tend to adhere more on the tube as the number of molten particles increases. In this calculation, therefore, the molten fraction of each ash is estimated by chemical equilibrium theory, using Fact Sage Ver. 6.1 software [6,7]. Table 4-2 shows the conditions of the chemical equilibrium calculations. The gaseous compositions given were assumed to be near a burner in the pulverized coal combustion boiler. The ash-deposition area is always exposed to the reducing

gas. Therefore, the partial pressures of CO, CO₂ and H₂ gas are fixed in the calculations. These calculations are performed at 50 K increments to determine the mass percentage of molten slag in the ash in the temperature range 1273–2073 K.

Table 4-1: Properties of coals tested.

Coal sample		UBC E	Coal A3	
Heating value [MJ/kg]		25.27	29.02	
Proximate analysis [wt%, dry]	Ash	6.27	12.18	
	Volatile matter	49.09	32.83	
	Fixed carbon	44.64	54.99	
Fuel ratio [-]		0.91	1.67	
Ultimate analysis [wt%, d.a.f]	Carbon	72.91	81.39	
	Hydrogen	5.65	5.26	
	Nitrogen	1.05	1.83	
	Sulfur	0.34	0.50	
	Oxygen (Balance)	20.05	11.02	
Ash fusion temperature [K]	Oxidizing	Initial deformation	1440	1753
		Hemispherical	1494	>1823
		Fluid	1651	>1823
	Reducing	Initial deformation	1433	1607
		Hemispherical	1453	1821
		Fluid	1473	>1823
Ash compositions [wt%]	SiO ₂	41.10	65.90	
	Al ₂ O ₃	12.50	22.90	
	CaO	10.30	1.08	
	Fe ₂ O ₃	16.30	4.58	
	MgO	8.36	0.79	
	Na ₂ O	0.13	0.47	
	K ₂ O	1.50	1.37	
	SO ₃	8.34	0.62	
	P ₂ O ₅	0.04	0.31	
	TiO ₂	0.64	1.37	
	V ₂ O ₅	0.03	0.07	
	MnO	0.26	0.03	

Table 4-2: Conditions of the chemical equilibrium calculations.

Temperature (K)	1273 ~ 2073	
Gas composition (%)	O ₂	8.3 x 10 ⁻⁸
	CO ₂	12.3
	CO	8.2
	H ₂	1.5
	N ₂	70.6
	H ₂ O	7.4
Ash composition (wt%)	SiO ₂ , Al ₂ O ₃ , CaO, Fe ₂ O ₃ , MgO, Na ₂ O, K ₂ O, SO ₃ P ₂ O ₅ , TiO ₂ , V ₂ O ₅ , MnO	

4.3 Experimental Section

Figure 4–1 shows a schematic diagram of the pilot–scale pulverized coal combustion refractory furnace used in this study. The furnace has a length of 3.65 m and an inner diameter of 0.4 m, and it is insulated by a refractory material to reduce heat loss. The pulverized coal weighed by the volumetric feeder is transported to the burner with nitrogen gas. The primary air (at ambient temperature) and secondary air (at 573 K) are supplied separately. City gas is supplied to the furnace in order to heat it to 1750 K. In the experiments, a thermocouple and a gas sampling probe are inserted into the furnace to measure the gas temperature and gaseous concentrations, respectively. The coal is pulverized so that a mass fraction of 85 % forms particles with diameters less than 75 μm .

MgO solid with a mean particle diameter of 0.2 μm and purity of 99.9 % is used as an additive for the UBC E. The pulverized UBC E and MgO additive are mixed using a mixer before the ash–deposition test. Table 4–3 shows the experimental conditions. The heat load is fixed at 149 kW for all the tests. The oxygen concentration of the flue gas at the furnace outlet is fixed at 1.0 % as a dry basis. The oxygen concentration at the inserted ash deposition tube is approximately 1.5 % as a dry basis. The deposition probe made of stainless steel SUS304 is inserted at a distance of 1.9 m from the burner tile, where the temperature is about 1573 K. The temperature around the ash deposition tube is similar to that in the slagging area near the burner in the pulverized coal combustion boiler. The length and outer diameter of the ash–deposition tube are 0.2 and 0.0318 m, respectively. The deposition probe mainly consists of a test piece for deposition and a water–cooled probe. Two thermocouples are installed between the test piece and the water–cooled probe. It is assumed that the temperature measured by these thermocouples is almost the same as the surface temperature of the test piece for deposition. The surface temperature is controlled to 773 K by adjusting the flow rate of the cooling water inside the tube. The cross–sectional structures and compositions of ash particles

before adherence to the tube and the deposition layer on the tube are observed using scanning electron microscopy (SEM) and electron-probe microanalysis (EPMA), respectively. The ash particles are also collected in the filter just before their adherence to the tube, using a water-cooled sampling probe and a suction pump.

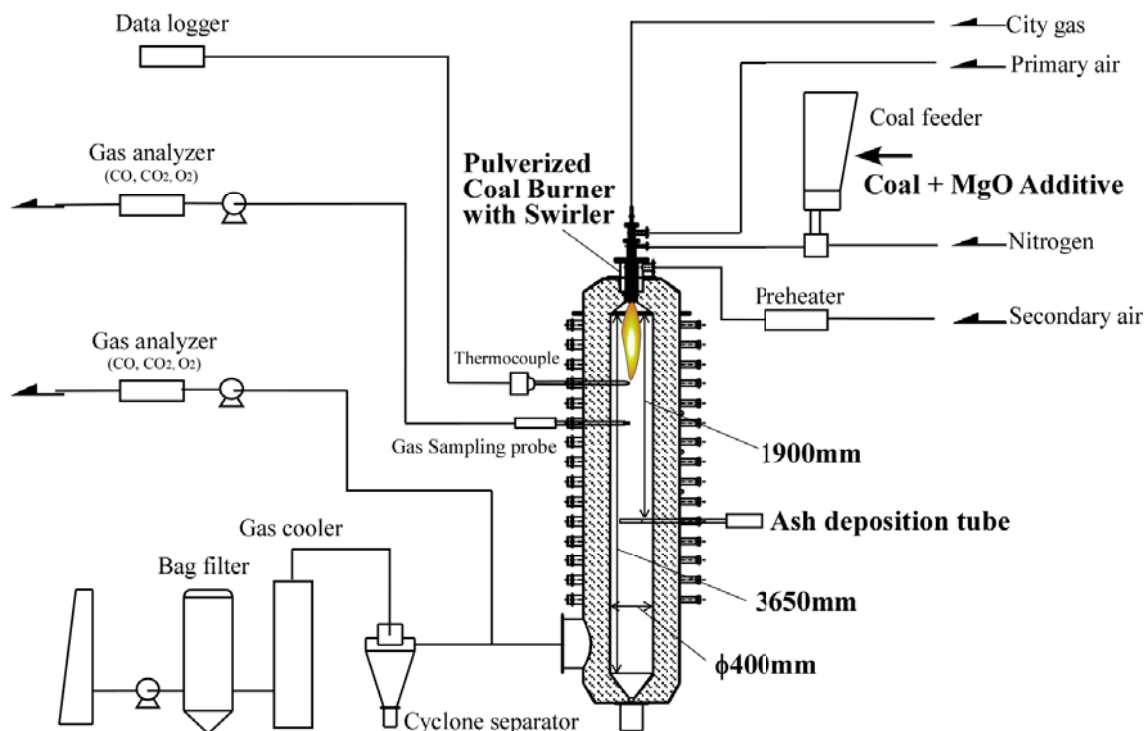


Figure 4–1: Schematic diagram of a pilot-scale pulverized coal combustion refractory furnace.

Table 4–3: Experimental conditions.

Coal sample	UBC E
Heating value [kW]	149
Combustion stoichiometric ratio [-]	1.05
Oxygen concentration at furnace outlet [%]	1.0
Oxygen concentration around ash deposition tube [%]	1.5
Gas and mean particle temperature around ash deposition tube [K]	1573
Gas velocity at 1573 K [m/s]	~2.6
Surface temperature of ash deposition tube [K]	773
Ash deposition tube diameter [mm]	31.8
Ash deposition tube length [mm]	200
Exposure time for ash deposition [min]	100
Mean particle diameter of MgO [μm]	0.2, 5
Additive fraction of MgO to UBC ash [wt%]	0, 25, 50

4.4 Results and Discussion

4.4.1 Fraction of Molten Slag with and without MgO Addition Obtained by Chemical Equilibrium Calculations

Figure 4–2 shows the calculated results of the molten slag fraction in ash for two types of coal ash. The molten slag fraction is defined as the content of molten slag in the total ash. For UBC E ash, the molten slag forms at relatively low temperatures. For Coal A3 ash, however, the molten slag does not form at temperatures lower than 1273 K.

Figure 4–3 shows the relationship between the additive fraction of each component in coal ash to UBC E ash and the increase/decrease mass ratio of the molten slag. In the calculations, each ash component was simply added to UBC E ash sample. The increase/decrease mass ratio of molten slag is defined as the mass ratio of the molten slag with the additive to that without the additive. Therefore, the ratio of less than one means that the production of molten slag actually decreases even if an additive is added to the ash. This figure shows that MgO or Al₂O₃ addition is effective for UBC E ash. With 25 wt% MgO addition, particularly, the production of molten slag in UBC E ash is almost halved. On the contrary, it is found that an addition of FeO, SiO₂, Na₂O, or CaO component to UBC E ash make the molten slag mass increase.

Figure 4–4 shows the relationship between the additive fraction of MgO and the molten slag fraction in the ash with MgO at 1573 K. In the calculations, the MgO is simply added to the UBC E ash sample. From the figure, it is seen that the molten slag fractions of UBC E ash are large, with values over 90%. The molten slag fraction in Coal A3 ash is relatively low at around 40%. However, the molten slag fraction in ash with MgO decreases as the additive fraction of MgO in the three types of coal ash increases. As for UBC E ash, the molten slag fraction in ash with MgO becomes almost the same as that of Coal A3 ash when the additive fraction of MgO is 25 %. Therefore, the addition of MgO to coal ash plays a role in decreasing the molten slag fraction in the ash.

Figure 4–5 shows the calculated results of the compositions in both the molten slag and solid phases for the UBC E ash with and without MgO at 1573 K. The additive fraction of MgO to UBC E ash is 25 wt%. The minor components with less than 0.1 wt% in both phases are negligible in this figure. For the UBC E ash without MgO addition, SiO₂ slag is significant in the slag phase formed. When MgO is added, the fraction of the molten slag phase decreases, and some aluminosilicate compounds are produced. As a result, the large amount of molten slag, including SiO₂ and FeO, decreases through the addition of MgO to the UBC E ash. As a result, it is understood that MgO as an additive is most effective in controlling the molten slag fraction of ash.

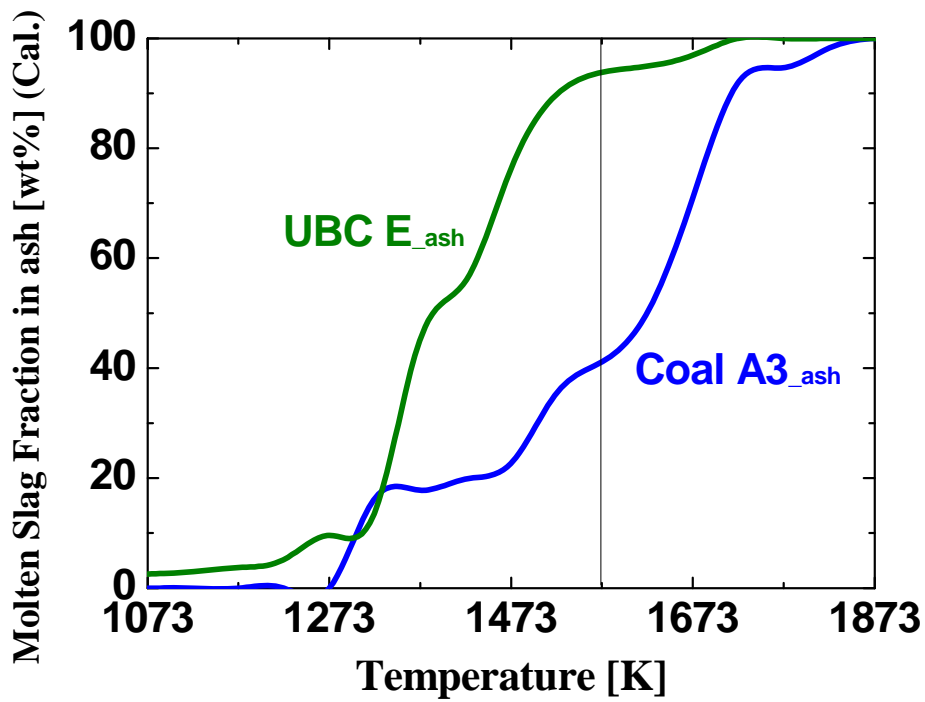


Figure 4-2: Calculated results of the molten slag fraction in ash for two types of coal ash.

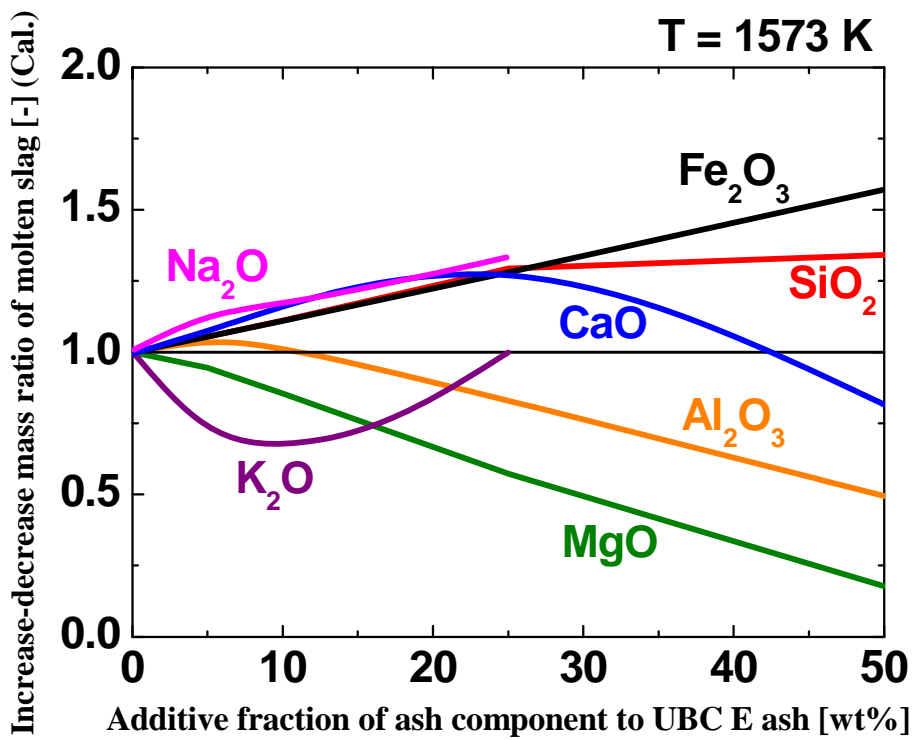


Figure 4-3: Relationship between additive fraction of ash component to UBC E ash and the increase-decrease mass ratio of molten slag.

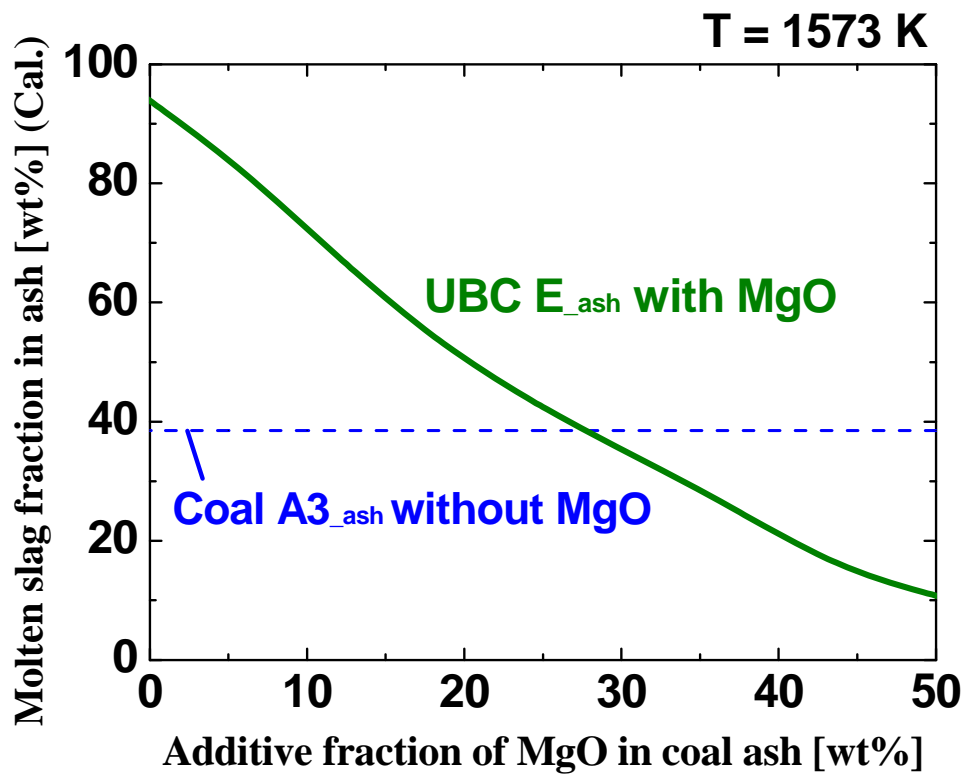
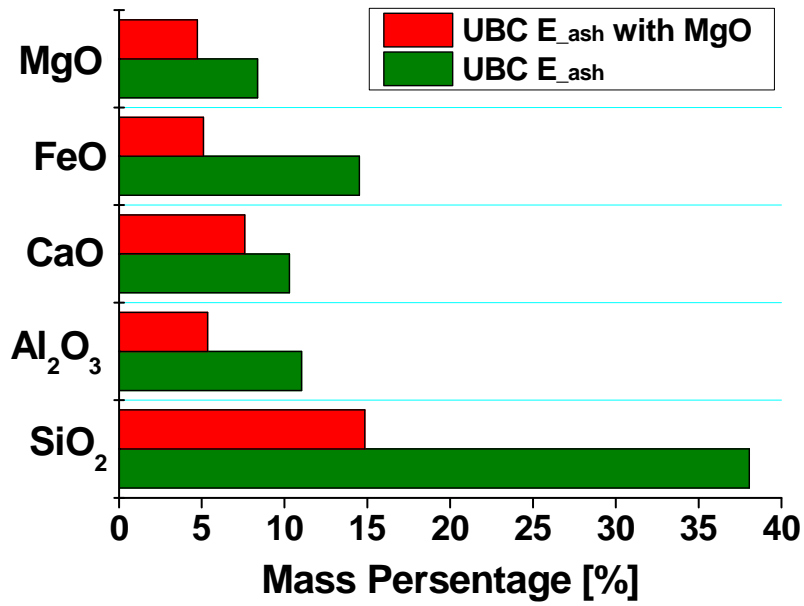
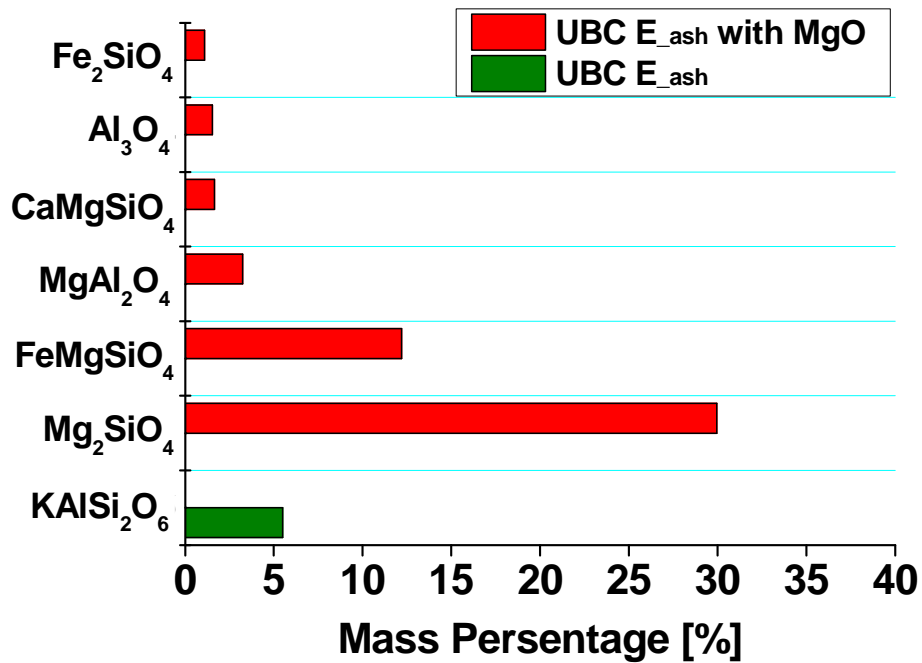


Figure 4-4: Relationship between the additive fraction of MgO and the molten slag fraction in the ash with MgO at 1573 K.



(a) Compositions in the molten slag phase.



(b) Compositions in the solid phase.

Figure 4–5: Calculated results of the compositions in both the molten slag and solid phases for the UBC E ash with and without MgO at 1573 K.

4.4.2 Ash Deposition Behavior during Coal Combustion

Figures 4–6 and 4–7 show the profiles of the temperatures and gaseous concentrations and unburnt fraction U_c^* along the central axis of the furnace during UBC combustion, respectively. The temperature at the location of the ash–deposition tube is approximately 1573 K. The unburnt fraction is defined as:

$$U_c^* = 100 - \eta = \frac{U_c}{1 - U_c} \times \frac{C_{Ash}}{100 - C_{Ash}} \times 100 \quad (4-1)$$

where U_c^* [%] is the unburnt fraction, η [%] is the combustion efficiency, U_c [%] is the unburnt carbon concentration in the fly ash, and C_{Ash} [%] is the ash content in the coal. At the probe insertion position, the unburnt carbon in the reacting particles is almost zero, and only a little CO remains. As for O₂ profile, after the oxygen concentration takes minimum value at the position whose distance from the burner tile is 0.3 m, the local maximum value is indicated near the probe insertion position. This is because air is supplied from surroundings during combustion due to the turbulent combustion using a burner with swirlers.

Figure 4–8 shows photographs of ash deposition on the tube for the UBC E with and without MgO after an exposure time of 100 min. For the UBC E without MgO, most of the deposited ash is in the molten state, and the deposition layer on the tube is very thin. For the UBC E with MgO, on the other hand, the ash–deposition layer is mainly composed of fine brown particles.

Figure 4–9 shows the relationship between the calculated molten slag fraction in the ash and the deposition fraction of ash (ϕ_{ash}) obtained experimentally. Here, ϕ_{ash} is defined as:

$$\phi_{ash} = \frac{D_{ash}}{F_{ash-probe} \cdot t} \quad (4-2)$$

$$F_{ash-probe} = \frac{A_p}{A_f} F_{ash-furnace} \quad (4-3)$$

In Eqs. (4-2) and (4-3), D_{ash} denotes the deposition mass of ash for a certain exposure time t . $F_{ash-probe}$ and $F_{ash-furnace}$ are the mass flow rates of ash in the cross-sectional areas of the probe (A_p) and the furnace (A_f), respectively. The term of $\phi_{ash, t=100}$ is the experimental result after 100 min. As seen from the figure, the deposition fraction of ash also decreases with a decrease in the calculated molten slag fraction. This result suggests that MgO addition to UBC E can contribute to reducing the ash deposition to the same level as that of Coal A3.

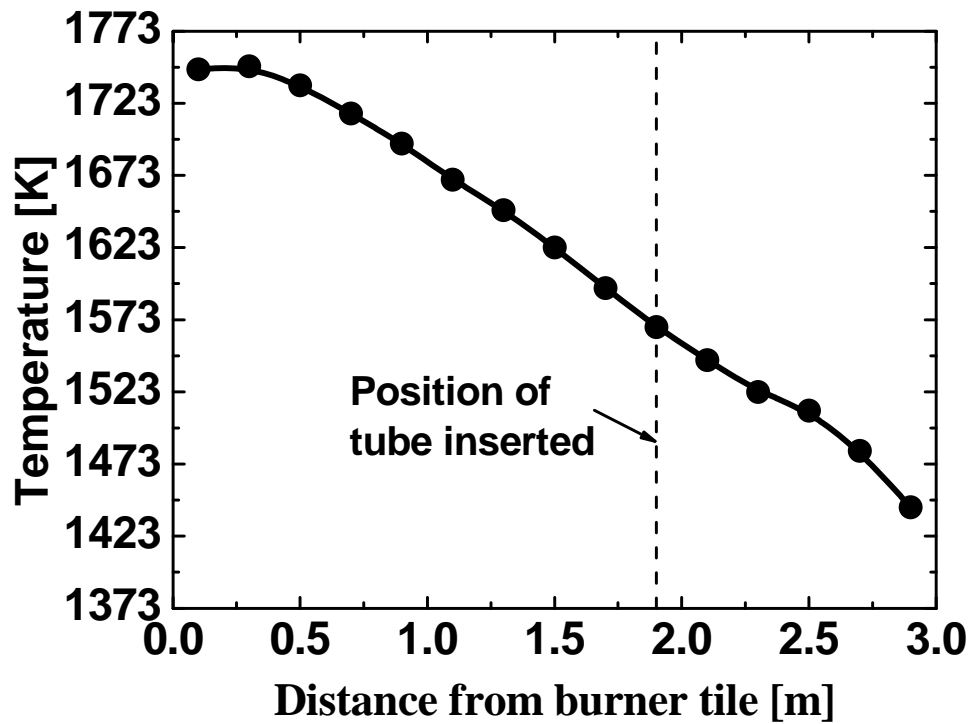


Figure 4-6: Temperature profiles along the central axis of the furnace.

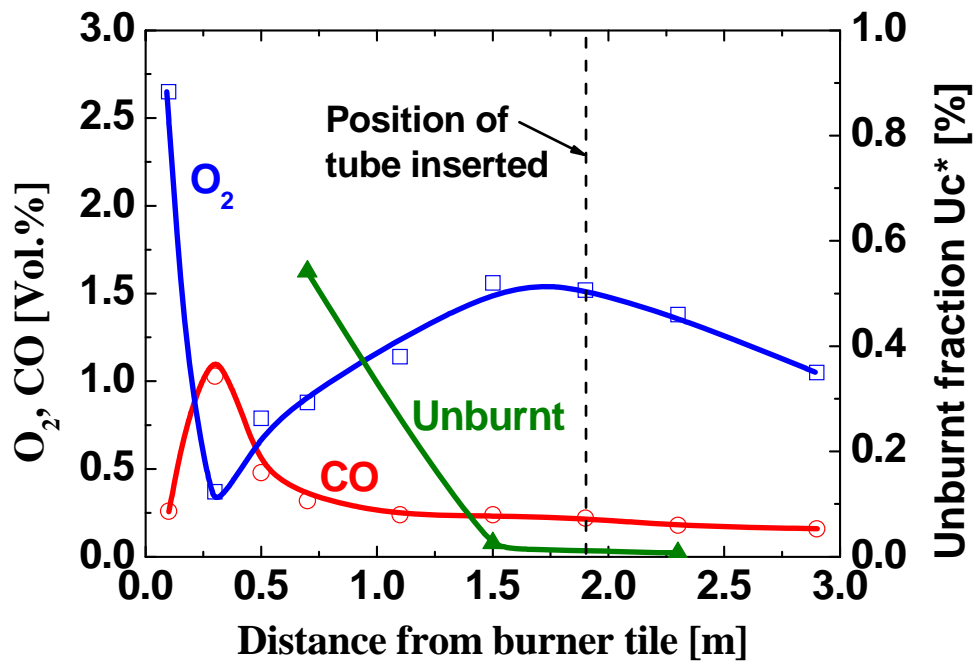


Figure 4-7: Profiles of gaseous concentrations and the unburnt fraction along the central axis of the furnace.

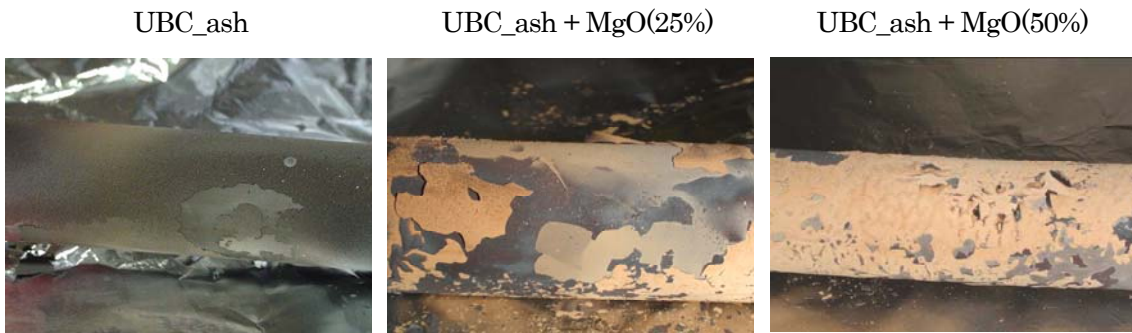


Figure 4–8: Photos of ash deposition on the tube after 100 min.

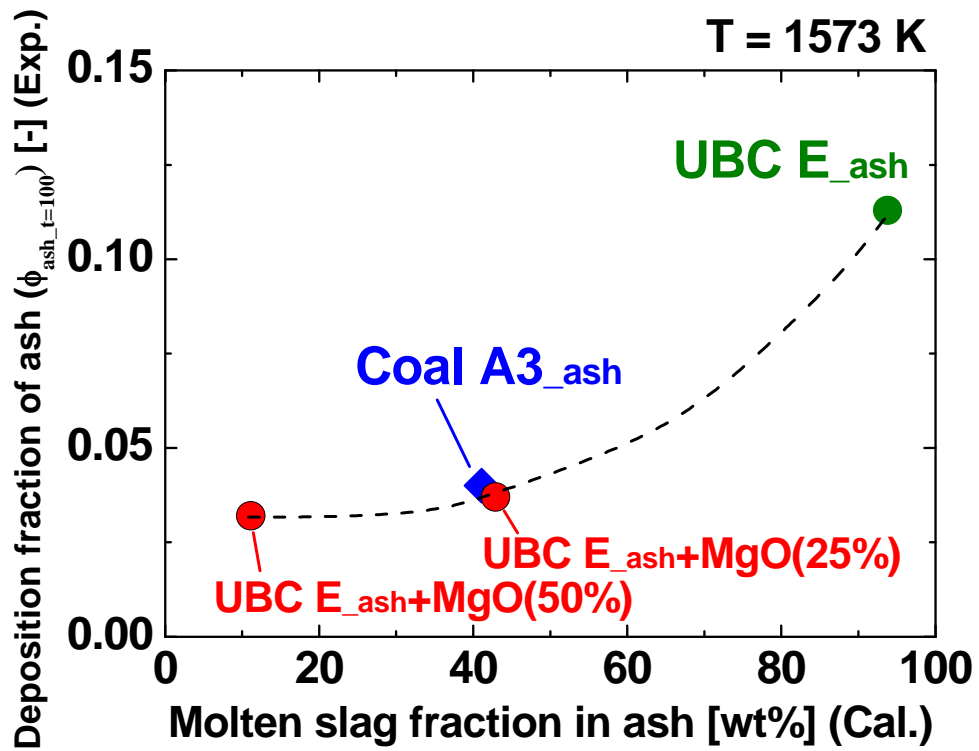


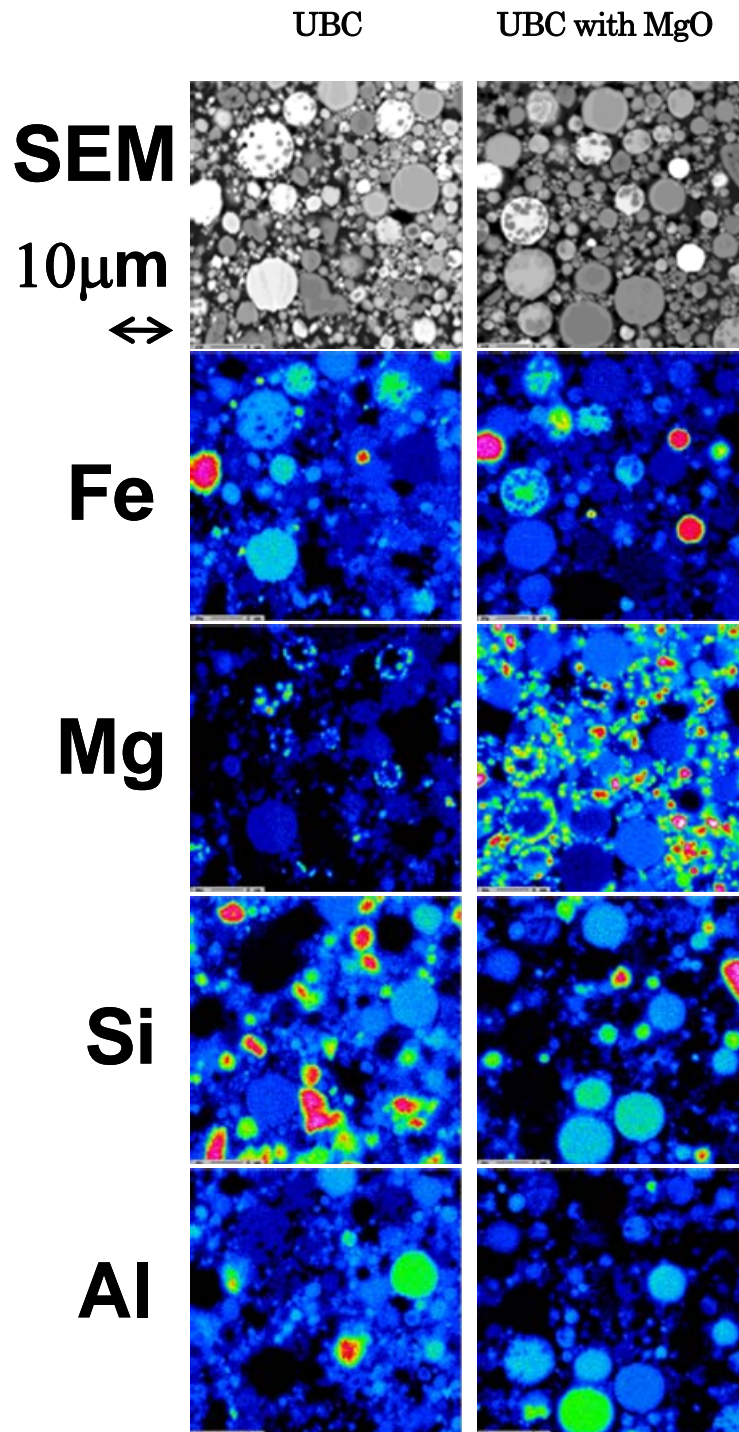
Figure 4–9: Relationship between molten slag fraction in ash and the deposition fraction of the ash.

4.4.3 Mechanisms for the Reduction of Ash Deposition

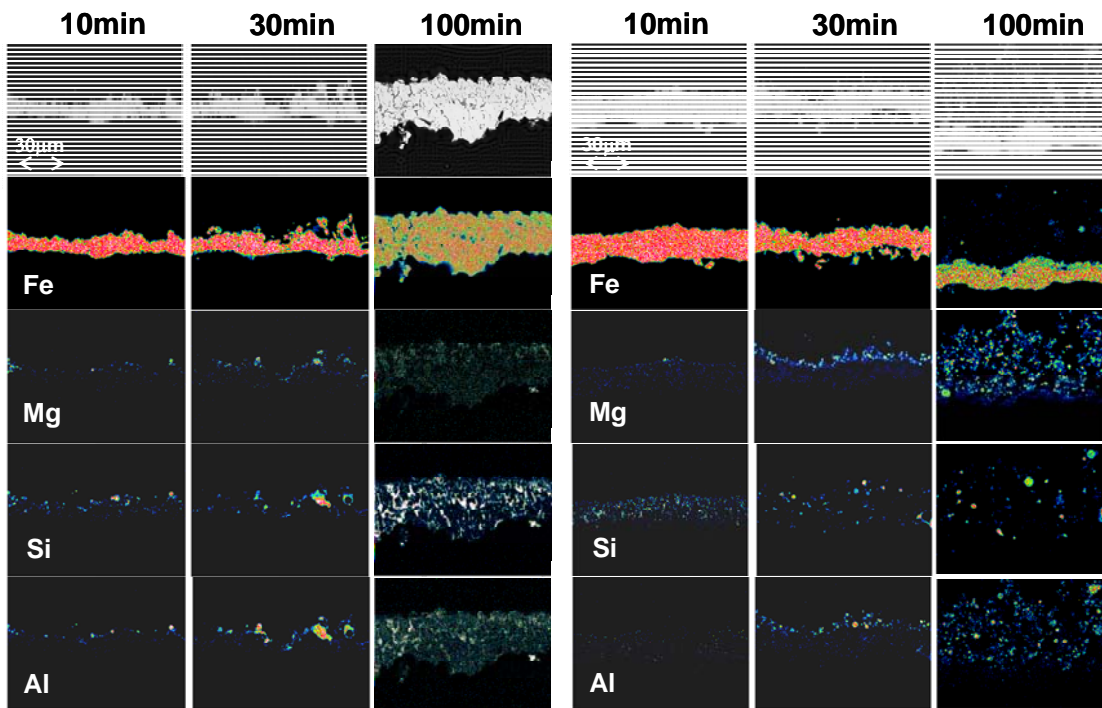
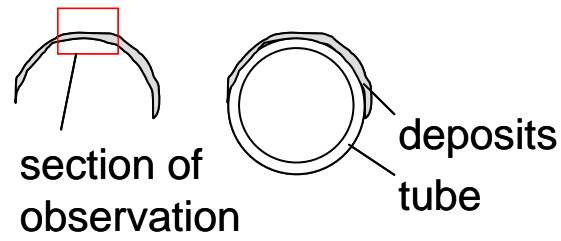
Figure 4–10 shows the cross-sectional structures and compositions of the ash particles just before their adherence to the ash deposition tube. The additive fraction of MgO in the UBC ash is 25 wt%, and the mean particle diameter of the added MgO is 0.2 μm . Comparing the Mg distributions for the UBC ash with and without MgO, it is found that, for the UBC ash with MgO, Mg deposits on the surface of the ash particles.

Figure 4–11 shows the cross-sectional structures and compositions of the deposits on the tube. The samples of ash deposits on the tube are collected after exposure times of 10, 30 and 100 min. Comparing the results after 100 min for the UBC ash with and without MgO, a thicker layer of Fe is produced for the UBC ash without MgO. This thick layer is mainly composed of Fe, Si and Al. For the UBC ash with MgO, on the other hand, the layer is thinner, and is not enriched by Si and Al. As MgO is added to the UBC, the MgO concentration in the deposit increases.

Figure 4–12 summarizes the mechanisms for the reduction of the ash deposition for the UBC ash with MgO on the basis of the above observations. For the UBC ash without MgO, the UBC ash reacts directly with the tube to produce an oxidized film that contains Fe, Si and Al. For the UBC ash with MgO, on the contrary, the existence of MgO inhibits direct reactions between the molten slag deposits and the tube surface. According to the results of the chemical equilibrium calculations mentioned above, MgO addition to the UBC can reduce the production of molten slag. In other words, the surface state of the deposit would always be dry, so that the UBC ash with MgO would not adhere to the tube easily. Consequently, it is concluded that MgO addition can reduce not only the ash deposition on tube but also the corrosion of the tube.



Figures 4–10: Cross-sectional structures and compositions of ash particles just before adhering to the ash deposition tube.



(a) UBC ash

(b) UBC ash with MgO addition

Figure 4-11: Cross-sectional structures and compositions of the deposits on the tube.

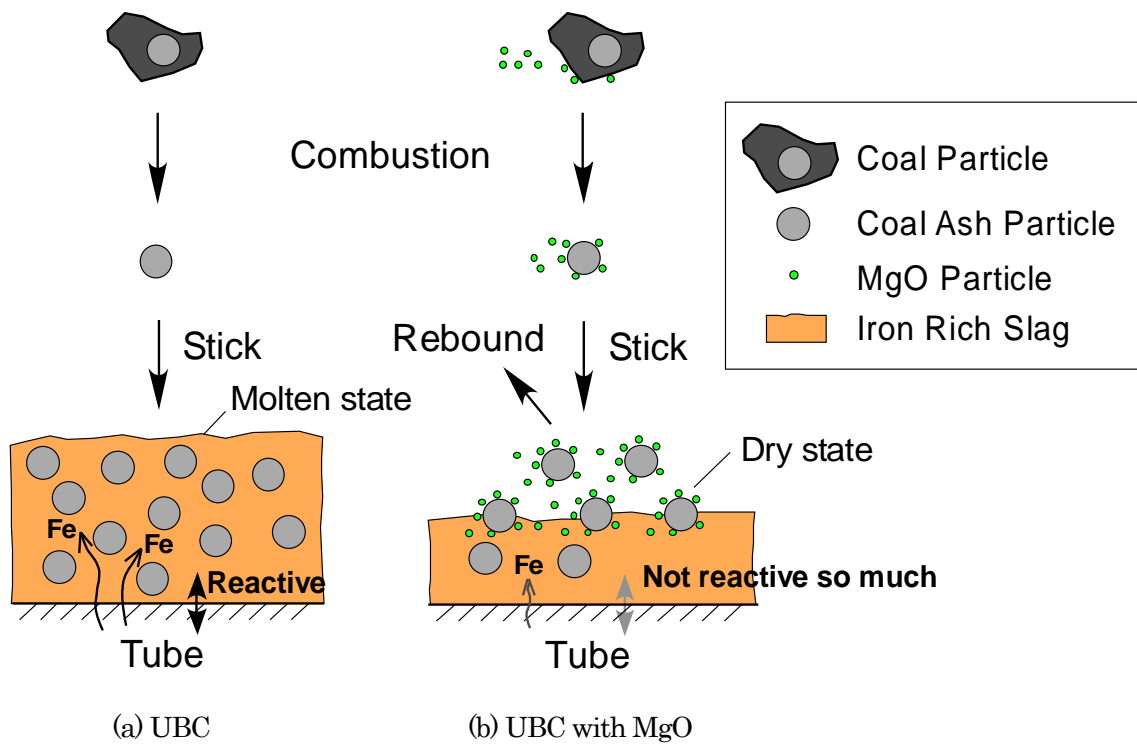


Figure 4–12: Mechanisms for the reduction of the ash deposition for the UBC ash with MgO.

4.5 Conclusions

Chemical equilibrium calculations and ash-deposition tests are conducted in order to evaluate the effects of MgO addition to coal on the reduction of ash deposition for UBC, and to understand the mechanisms of this reduction of ash deposition. The following findings are obtained:

- MgO as an additive is most effective in controlling the molten slag fraction of ash.
- One of the reduction mechanisms due to MgO addition involve the production of solid-phase aluminosilicates, and play a role in decreasing the molten slag fraction in the ash on the tube.
- The amount of ash deposition for UBC with MgO is relatively diminished. This is because the MgO inhibited the production of molten slag on the tube. In other words, the surface state of the deposit would always be dry, so that the UBC ash with MgO would not adhere to the tube easily.
- MgO addition also inhibits direct reactions between the molten slag deposits and the tube surface. Consequently, it is considered that MgO addition can reduce not only the ash deposition on tube but also the corrosion of the tube.

References

- [1] Pohl JH, Creelman RA, Ward C, Borio R, Radway G, Larsen G, Mehta A, Wolsiffer S, Davis C, Expanded use of high-sulfur, low-fusion coals in utility boilers: effect of additives, Proc. 26th Int. Tech. Conf. Coal Util. Fuel Syst., Florida, (2001) pp.597–608.
- [2] Libutti BL, Brandon JH, Effective use of oxide mixtures as fuel additives, Pap. NACE Conf. (Natl. Assoc. Corros. Eng.), Toronto, (1975) p.162.
- [3] Williams GD, Cotton IJ, Energy and maintenance savings by use of fuel and fireside additive programs, Proc. Refining Dep. Am. Pet. Inst., 55, (1976) pp.819–839.
- [4] Sinha RK, High-temperature fireside corrosion and its control by chemical additives, Mater Performance, 31 (4), (1992) pp.44–49.
- [5] Ninomiya Y, Wang, Q, Xu S, Teramae T, Awaya I, Evaluation of a Mg-Based Additive for Particulate Matter (PM)_{2.5} Reduction during Pulverized Coal Combustion, Energy Fuels, 24 (1), (2009) pp.199–204.
- [6] FACT, www.crct.polymtl.ca
- [7] Bale CW, Chartrand P, Deckerov SA, Eriksson G, Hack K, Mahfoud RB, Melançon J, Pelton AD, Petersen S, FactSage thermochemical software and databases, Calphad Journal, 26, (2002) pp.189–228.

Chapter 5

Demonstration of UBC Combustion in 145MW Practical Coal Combustion Boiler

5.1 Introduction

In Chapter 2, it is concluded that UBC has good burnout characteristics, compared to the bituminous coal and this contributes to both improvement of the combustion efficiency and NO_x emission even if the two-stage combustion ratio increases.

In Chapter 3, it is confirmed that the ash deposition characteristics have a close relationship with the ash melting characteristics. Consequently, it has been proven that the molten slag fraction in ash obtained by chemical equilibrium calculations is one of the useful indices to predict the coal blending method to reduce the deposition fraction of ash.

In this Chapter, the objectives are to evaluate both the combustion characteristics such as NO_x and SO_x emissions and the burnout, and the ash deposition behavior such as slagging for the blended coal with UBC in a 145 MW practical coal combustion boiler. The demonstration test of UBC combustion that is operated for 8 days is conducted, using the blended coal consisting 20 wt% of UBC and 80 wt% of bituminous coal. The coal blending condition is decided by the method developed in Chapter 3.

5.2 Coal Samples

An Indonesian UBC of UBC F and an Australian bituminous coal of Coal G were selected as samples. The UBC briquettes' samples of 1500 tons were manufactured in the 600 ton/day demonstration plant in South Kalimantan of Indonesia, and shipped to Japan. Then, the UBC samples were blended with Australian bituminous coal. The blended coal of 7500 tons contains 20 wt% of UBC and 80 wt% of bituminous coal. Figure 5–1 shows the photo of blended coal pile. Those properties are also shown in Table 5–1. As seen from the table, the fuel ratio of UBC is less than 1.0. The nitrogen and sulfur content of UBC F is also lower than that of Coal G. The moisture content of UBC F and Coal G has not large difference. The ash content of UBC F is lower than Coal G. As for the ash compositions, the UBC F especially has low SiO_2 and high CaO and Fe_2O_3 in ash. The hemispherical temperature of UBC F under oxidizing conditions is 230 K lower than that of the Coal G. Figure 5–2 shows the particle diameter distributions of coal ash sample, which is measured based on JIS M 8812. It is found that the UBC F ash contains relatively small particles, compared with Coal G ash.

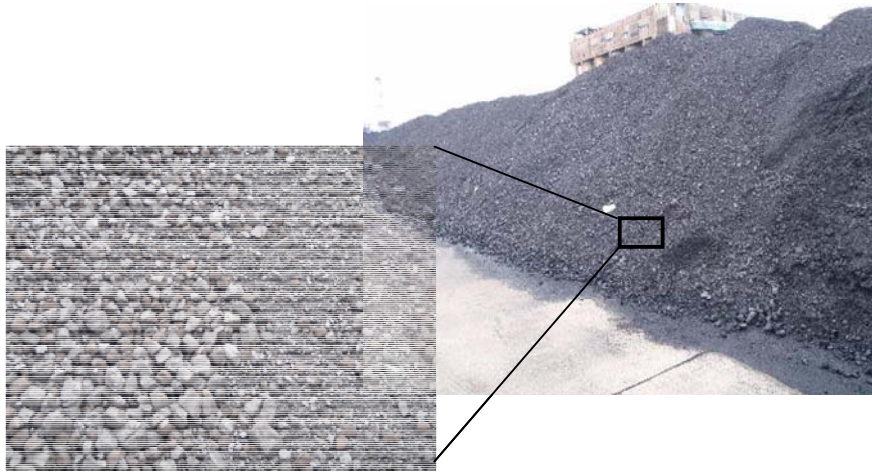


Figure 5–1: Photo of blended coal pile contains 20 wt% of UBC and 80 wt% of bituminous coal.

Table 5–1: Properties of coals tested.

Coal sample		UBC F	Coal G(80%)+UBC F(20%)	Coal G	
Heating value [MJ/kg]		24.22	28.60	29.70	
Proximate analysis [wt%, air dry]	Moisture	8.8	10.2	10.6	
Proximate analysis [wt%, dry]	Ash	4.60	10.12	11.50	
	Volatile matter	48.70	38.22	35.60	
	Fixed carbon	45.98	50.43	51.54	
Fuel ratio [-]		0.94	1.35	1.45	
Ultimate analysis [wt%, daf]	Carbon	72.77	81.30	83.43	
	Hydrogen	5.70	5.76	5.78	
	Nitrogen	1.08	1.70	1.86	
	Sulfur	0.11	0.61	0.73	
	Oxygen (Balance)	20.34	10.63	8.20	
Ash fusion temperature [K]	Oxidizing	Initial deformation	1426	1586	1329
		Hemispherical	1523	1689	1753
		Fluid	1658	1694	>1823
	Reducing	Initial deformation	1340	1499	1293
		Hemispherical	1503	1603	1725
		Fluid	1610	1608	1804
Ash compositions [wt%]	SiO ₂	40.70	56.78	60.80	
	Al ₂ O ₃	12.10	22.90	25.60	
	CaO	11.90	4.61	2.79	
	Fe ₂ O ₃	16.00	7.06	4.83	
	MgO	10.20	2.89	1.06	
	Na ₂ O	0.11	0.21	0.23	
	K ₂ O	0.83	0.93	0.95	
	SO ₃	7.80	3.00	1.80	
	P ₂ O ₅	0.05	0.19	0.22	
	TiO ₂	0.67	1.15	1.27	
	V ₂ O ₅	0.07	0.10	0.11	
	MnO	0.37	0.11	0.04	

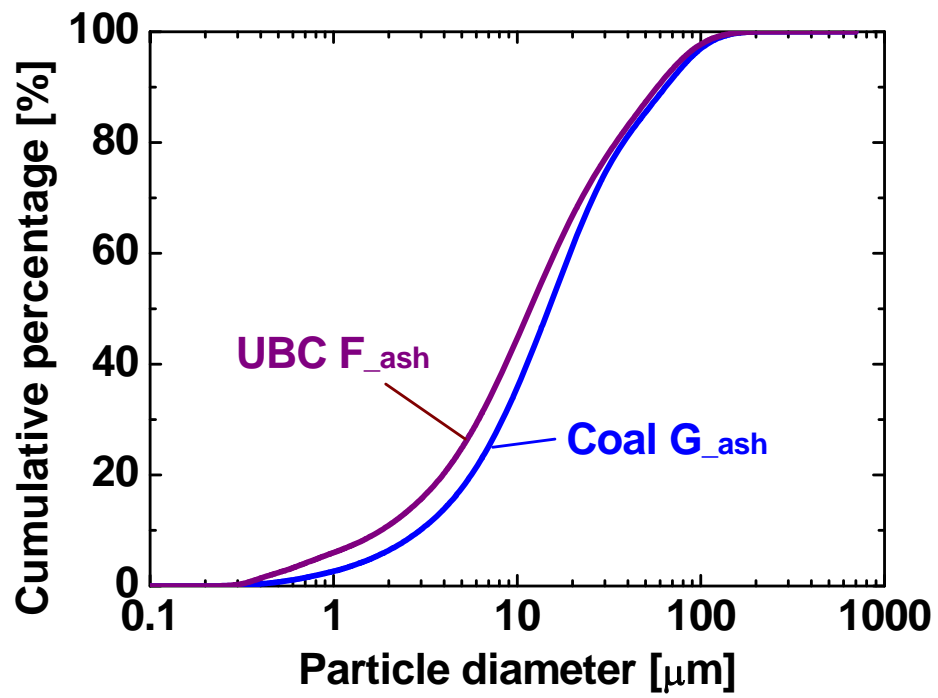


Figure 5-2: Particle diameter distributions of coal ash samble which is made based on JIS M 8812.

5.3 Chemical Equilibrium Calculations

The molten fractions of each ash were calculated by a chemical equilibrium theory, using Fact Sage Ver. 6.1 software [1,2]. Table 5–2 shows the conditions of the chemical equilibrium calculations. The gaseous compositions given are assumed to be near a burner in the pulverized coal combustion boiler. The ash deposition area is always exposed to the reducing gas. Therefore, the partial pressures of CO, CO₂ and H₂ gas are fixed in the calculations. The calculations are carried out in 50 K increments to determine the mass percentage of molten slag in the ash in the temperature range of 1273 – 2073 K.

Table 5–2: Conditions of chemical equilibrium calculations.

Temperature (K)	1273 ~ 2073	
Gas composition (%)	O ₂	8.3 x 10 ⁻⁸
	CO ₂	12.3
	CO	8.2
	H ₂	1.5
	N ₂	70.6
	H ₂ O	7.4
Ash composition (wt%)	SiO ₂ , Al ₂ O ₃ , CaO, Fe ₂ O ₃ , MgO, Na ₂ O, K ₂ O, SO ₃ P ₂ O ₅ , TiO ₂ , V ₂ O ₅ , MnO	

5.4 Experimental Section

Figure 5–3 shows a flow diagram and photo of the 145 MW coal combustion power station used in this study. This power station is located in the Kakogawa Works of Kobe steel, Ltd., and was designed to burn bituminous coal. The coal is unloaded from vessel and piled in the yard. Then, it is fed into the coal mill and pulverized. The pulverized particle diameter is less than 75 μm , and its mass fraction is more than 80 wt%. The flue gas passes through the de-NO_x tower, air heater, electric precipitator and de-SO_x tower.

Figure 5–4 shows a schematic diagram of the boiler and locations of the ash deposition tests. It is a tangential firing boiler, equipped with 16 pulverized coal burners arranged in four rows on the walls of the furnace. The combustion air is separated into primary air and over-fired air (OFA). The ash deposits are collected from the furnace wall beside the top burner at 1523 K. This position is called “slagging area”. Table 5–3 shows the boiler operational conditions. Both Coal G and the blended coal of Coal G with UBC F are burned in the combustion tests. The heat load is fixed at 145 MW for each test. The oxygen concentration in the flue gas is kept at 2.9 % on a wet basis. The ratio of over-fired air to total combustion air is 34.5 %. The ash deposition tube, which is made of stainless steel (SUS304), is inserted into the boiler to collect the slagging deposits as shown in Figures 5–5 and 5–6. The length and outer diameter of the ash deposition tube are 0.2 and 0.0318 m, respectively. The deposition probe mainly consists of a test piece for deposition and a water-cooled probe. Two thermocouples are installed between the test piece and the water-cooled probe. The surface temperatures of the test piece of deposition are assumed to be the temperatures measured by those thermocouples. The surface temperature is controlled at 723 K by adjusting the flow rate of cooling water inside the probe. The cross-sectional structures and configurations of ash particles on the tube are observed and analyzed, using scanning electron microscopy (SEM) and image processing software (Image Hyper 2), respectively. Furthermore, the combustion characteristics of both Coal G and the

blended coal of Coal G with UBC F, their NO_x and SO_x emissions and the burnout characteristics are quantitatively elucidated.

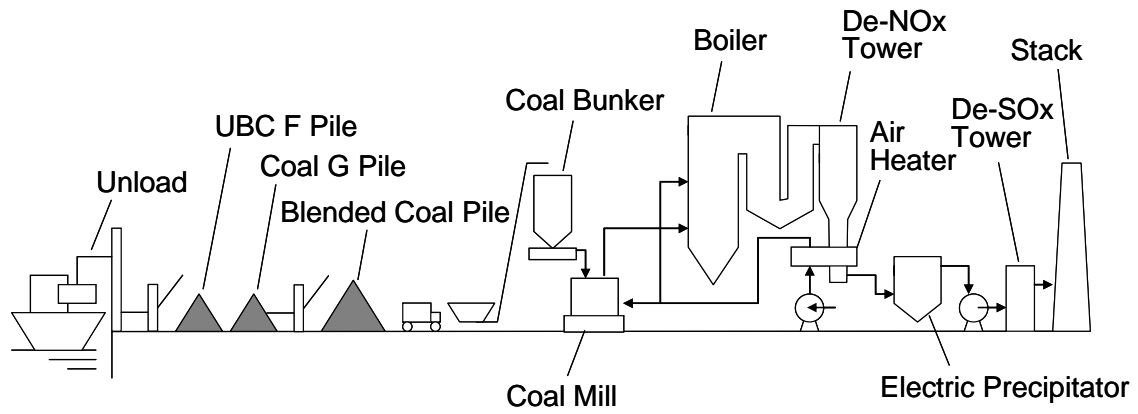


Figure 5-3: Flow diagram and photo of 145 MW coal combustion power station.

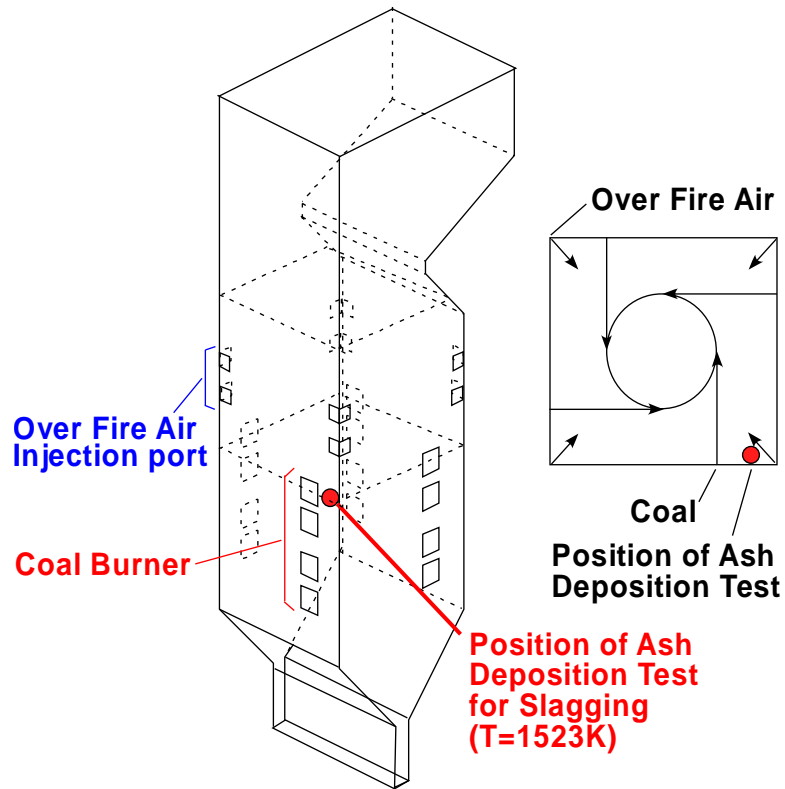


Figure 5-4: Schematic diagram of the boiler and location of the ash deposition tests.

Table 5-3: Boiler operational conditions.

Coal	Coal G, Coal G(80)+UBC F(20)
Heat load [MW]	145
Quantity of evaporation [t/h]	450
Feed rate of coal [t/h]	55
Oxygen concentration at boiler outlet [wet-%]	2.9
Combustion stoichiometric ratio at boiler outlet [-]	1.18
Ratio of over fire air to total combustion air [%]	34.5



Figure 5-5: Photo of the ash deposition test probe inserted in the boiler.

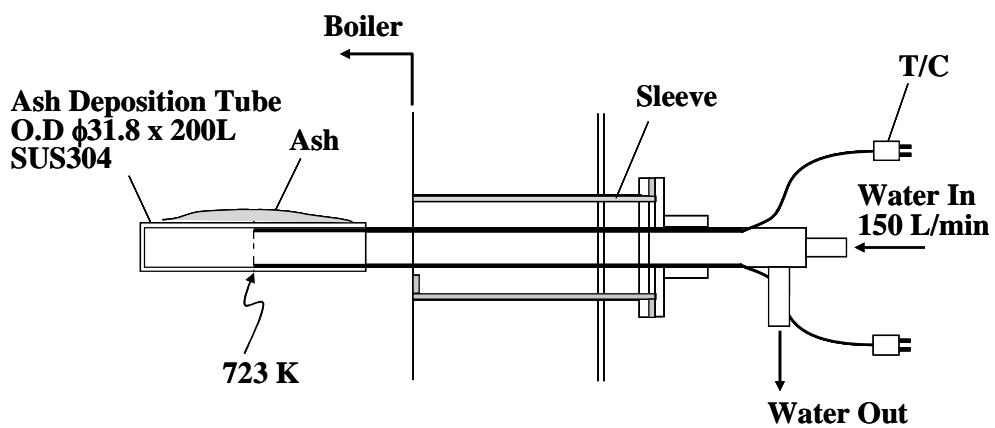


Figure 5-6: Schematic diagram of the ash deposition test probe.

5.5 Results and Discussion

5.5.1 Fraction of the Molten Slag Obtained by Chemical Equilibrium Calculations

The previous studies [3–6] reported that the ash deposition and growth in the boiler were greatly influenced by ash melting characteristics such as ash melting point and viscosity. Our previous studies proved that the ash deposition rate dramatically increased if the molten slag fraction in ash obtained by chemical equilibrium calculations was over 60 %, as shown in Chapter 3.

Figure 5–7 shows the calculated results of the molten slag fraction in ash for Coal G, UBC F and their blended coal. The molten slag fraction is defined as the content of molten slag in the total ash. For the UBC F ash, the molten slag forms at relatively low temperatures, and the molten slag fraction rapidly increases between 1323 and 1573 K. For the Coal G ash, however, the molten slag does not form at temperatures less than 1273 K, and the molten slag fraction gradually increases between 1273 and 1673 K. When the mixing mass ratio of UBC F to Coal G increases by 20 wt%, additionally, the molten slag fraction in ash increases between 1323 and 1873 K.

Figure 5–8 shows the relationship between the mixing fraction of UBC F with Coal G and the molten slag fraction in ash at 1523 K. In this figure, the molten slag fraction of UBC F ash reaches approximately 90 %. For the blended coal consisting of 20 wt% of UBC F and 80 wt% of Coal G, however, it attains 50 % only, which is close to the value of 43 % for Coal G. The calculation results mean that this coal blending plays a role in reducing the molten slag fraction.

Figure 5–9 shows the calculated results of the compositions in (a) the molten slag and (b) the solid phases for UBC F ash, Coal G ash and their blended coal ash at 1523 K. The minor components with less than 0.1 wt% in both phases are negligible in this figure. For the UBC F

ash alone, the SiO_2 slag is significant in the slag phase formed. When the Coal G ash is mixed with the UBC F ash, the fraction of the molten slag phase decreases, and some aluminosilicates compounds are produced. As a result, the amount of molten slag, including SiO_2 , FeO and CaO is greatly reduced by mixing the Coal G ash into the UBC F ash.

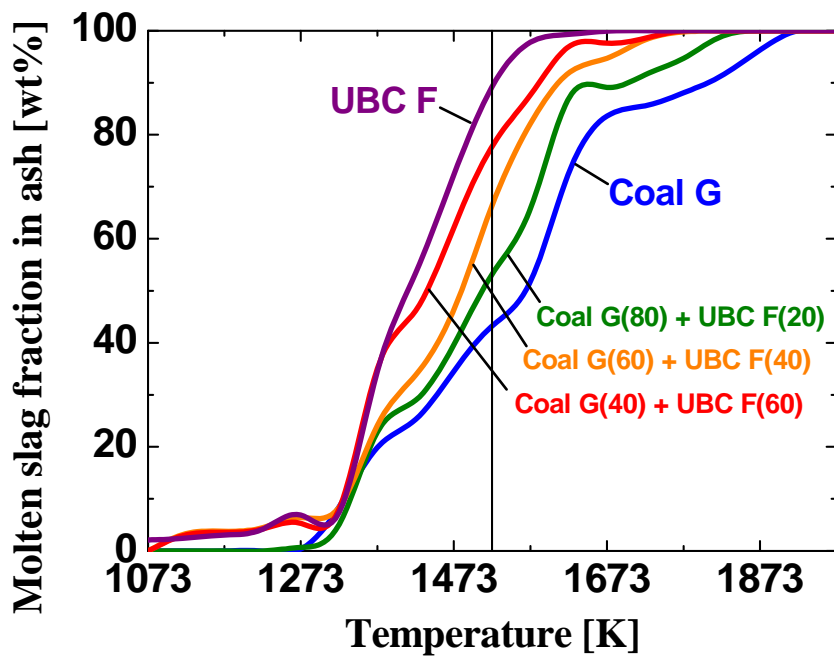


Figure 5-7: Calculated results of molten slag fraction in ash for the blended coal of Coal G and UBC F.

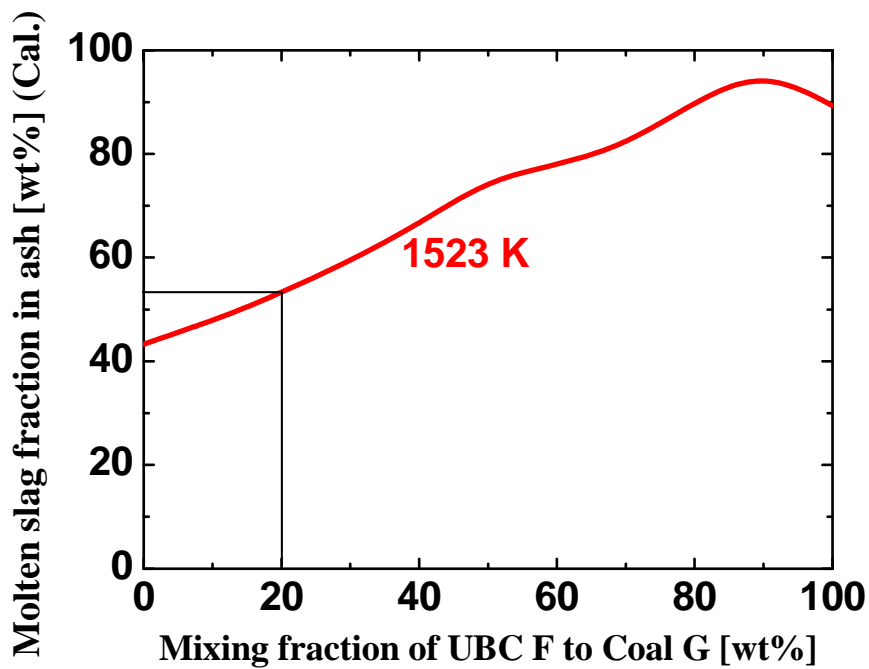
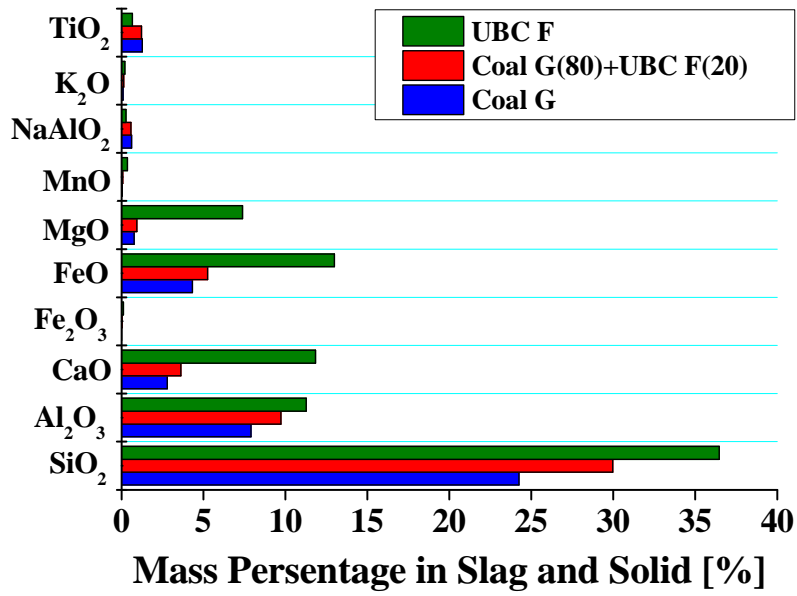
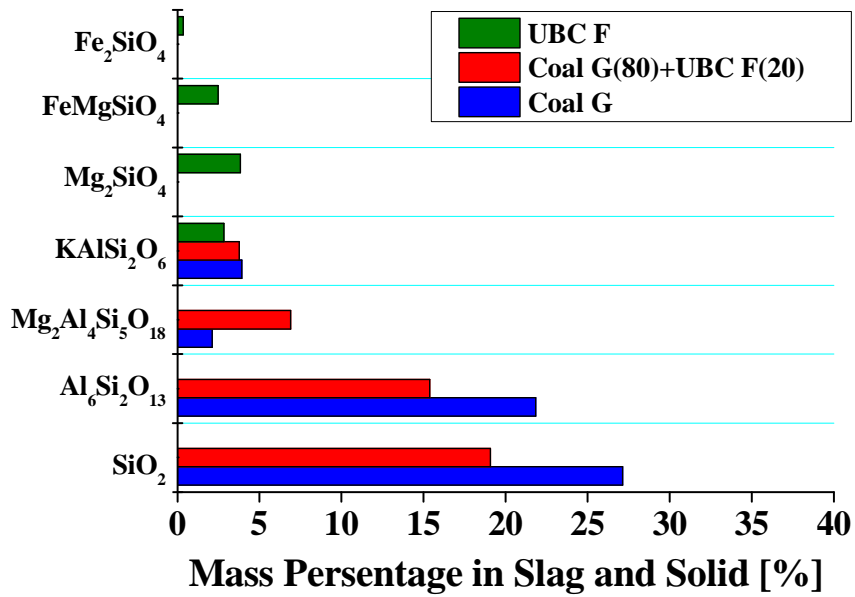


Figure 5-8: Relationship between the mixing fraction of UBC F with Coal G and the molten slag fraction in ash at 1523 K.



(a) Compositions in the molten slag phase



(b) Compositions in the solid phase

Figure 5-9: Calculated results of the compositions in the molten slag and solid phases for the UBC F ash, Coal G ash and their blended coal ash at 1523 K.

5.5.2 Ash Deposition Behavior in the Boiler

Figure 5–10 shows photos of the slagging area at around 1523 K in the boiler. The level of ash deposition on the wall was observed, using a water-cooled CCD camera. The ash particles adhere around the burner for both Coal G and the blended coal. However, they do not grow until a large clinker. Additionally, it is not observed that the ash adheres strongly on the wall around the slagging area in the boiler.

Photos of the ash deposition on the tube after an exposure time of 100 min are shown in Figure 5–11. For Coal G, numerous fine gray particulates seem to deposit on the surface, and some particulates agglomerate with each other. For the blended coal, the color of the deposited ash turns brown. Because the original color of UBC ash is brown, and the UBC ash is mixed with gray ash of Coal G. But, there is no large difference between Coal G and the blended coal.

Figure 5–12 shows the results of mass of the deposited ash measured and deposition fraction of ash on the tube at 1523 K after an exposure time of 100 min. The deposition fraction of ash is defined as the ratio of mass of the deposited ash on the test tube to the supplied coal amount in the boiler during 100 min. Both the mass of deposited ash and deposition fraction of ash for the blended coal increase, compared with that for Coal G. As the molten slag fraction in ash for the blended coal at 1523 K increased, as shown in Figure 5–8, the surface of deposited ash will become sticky. However, no slagging problems occurred during the 8 days of boiler operation.

Figure 5–13 shows the cross-sectional structures of the deposit on the tube at 1523 K. The lower side images are the closeup near the tube surface. The white layer, which is located below of the image, shows the tube. The gray color particle indicates the ash. The black color area is resin for specimen preparation. There are a lot of spherical ash particles on the tube for the blended coal. From those observations, there seems to be more spherical and larger particles in the blended coal ash deposits, compared with the Coal G ash deposits. This is because the

molten slag fraction in ash for the blended coal at 1523 K is higher than that for Coal G. Even for the blended coal, however, no sintering phenomenon occurred in the ash deposition layer.

Next, the particle configuration of both the deposited ash was quantitatively analyzed, using an image processing software. Figure 5–14 shows the images of deposited ash on the tube, which is adjusted for the image processing. Table 5–4 shows the analytical results of mean value of circularity coefficient and mean area ratio of particle. The circularity coefficient (C_c) is defined as the following equations:

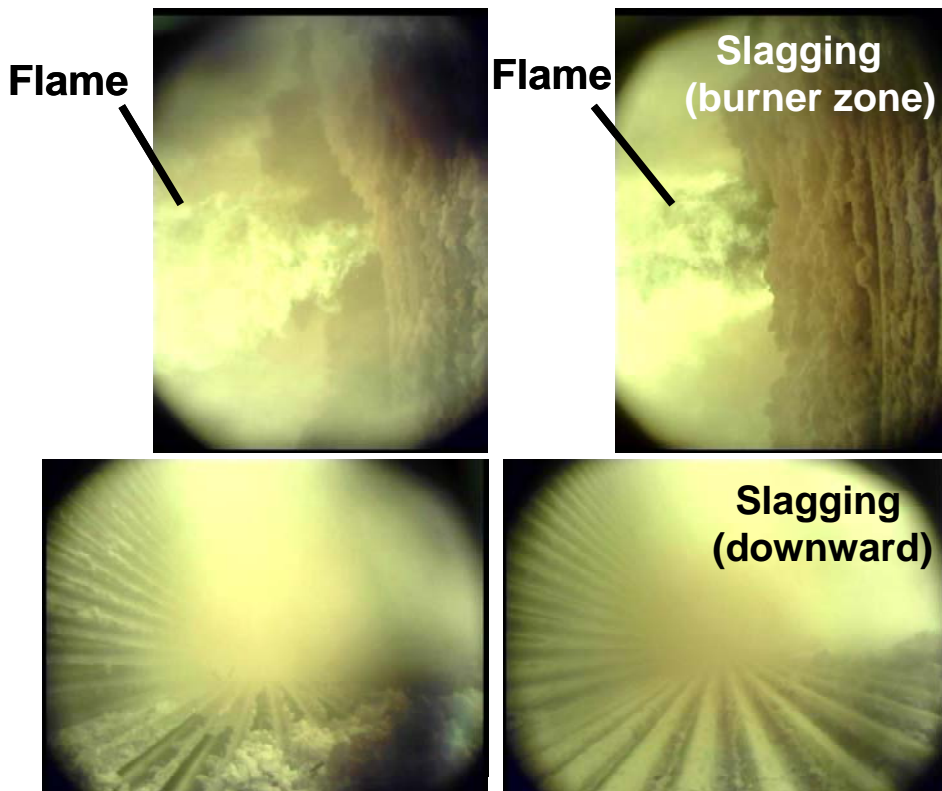
$$C_c = \frac{4\pi \times A}{L^2} \quad (5-1)$$

where A is the area of particle, L is the peripheral length of particle. The circularity coefficient becomes the maximum value of 1.0 when a particle is circle. The mean value of circularity coefficient is the average of the circularity coefficient for all the particles. The mean area ratio of particle is defined as the ratio of mean projected area of ash deposits to that of the Coal G ash deposits. It is clear that the circularity coefficient of the blended coal ash deposits is higher than that of the Coal G ash deposits. Additionally, the mean area ratio of particle of blended coal ash deposits is 1.17. On the other hand, the particle diameter distributions of coal ash sample, which is measured based on JIS M 8812, indicates that the UBC F ash contains relatively small particles, compared with Coal G ash, as shown in Figure 5–2. Consequently, if it is assumed that the ash particles of blended coal with UBC F is molten, coalesce with each other happens and the particles become large. It is also understood that the blended coal ash particles are solidified on the tube with spherical shape kept by the surface tension after they melt.

Based on those observations, the mechanisms of ash deposition in the boiler are summarized as follows. The slagging behavior involves the coal ash being partly fragmented

and becoming molten during combustion, and then it adheres to the tube surface. The blended coal ash particles react with each other on the tube because the residence time of the ash particles before they adhere to the tube is short. According to the results of the chemical equilibrium calculations mentioned above, the deposited ash particles on tube become large and spherical when the molten slag fraction in ash increases. Additionally, it is thought that the deposited ash becomes the mass of molten slag called clinker when the molten slag fraction in ash increases more and more.

In the present study, Coal G is able to reduce the production of molten slag by being blended with UBC F. In other words, blending makes the surface state of the deposit dry, and so the UBC F ash does not adhere to the tube strongly. Therefore, this result suggests that appropriate blending of UBC with bituminous coal enables UBC to be used without any ash deposition problems in the boiler.



(a) Coal G

(b) Coal G (80) + UBC F (20)

Figure 5–10: Photos of slagging area at around 1523 K in the boiler during combustion.



(a) Coal G

(b) Coal G (80) + UBC F (20)

Figure 5–11: Photos of ash deposition on the tube after 100 min.

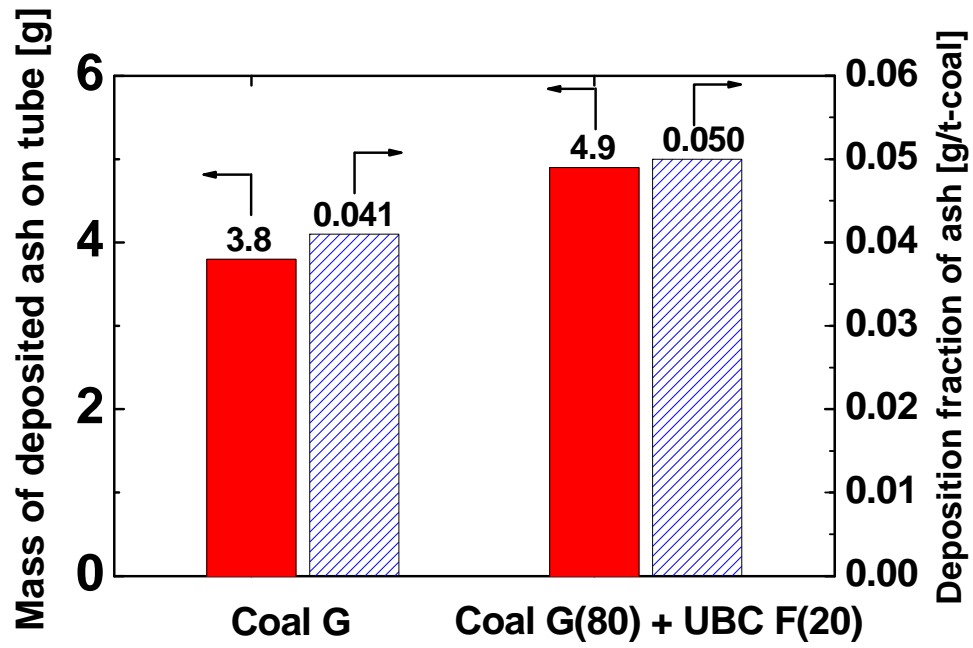
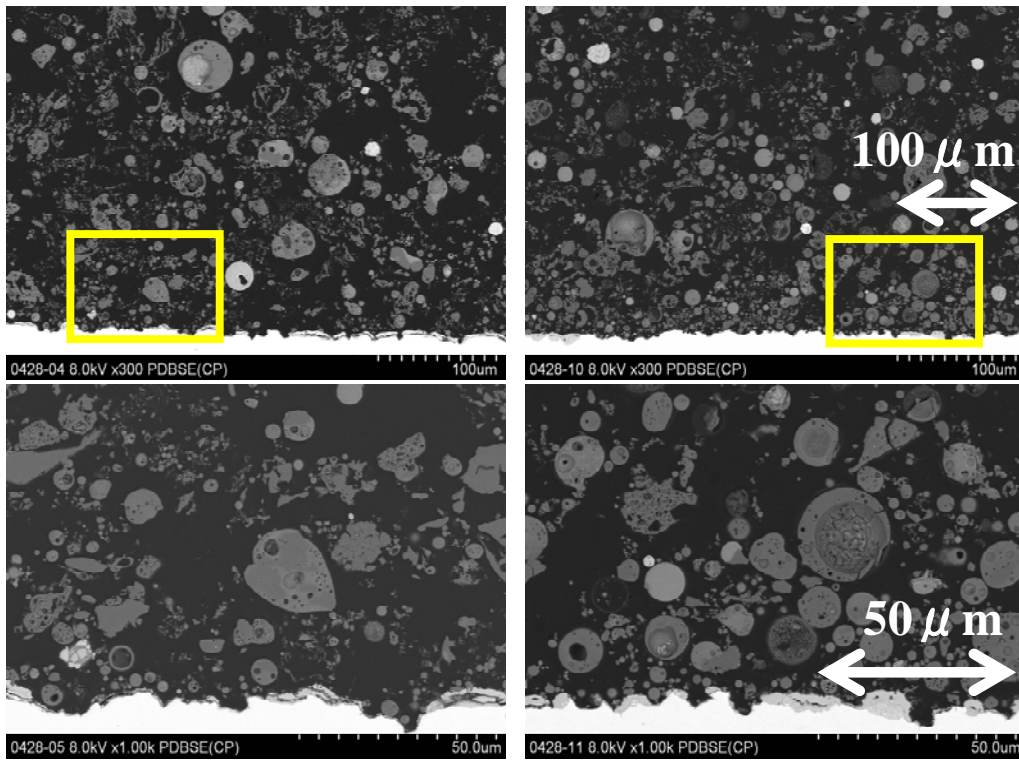
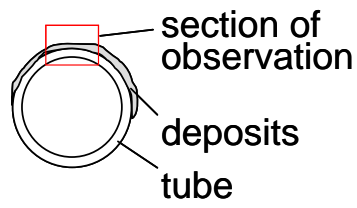


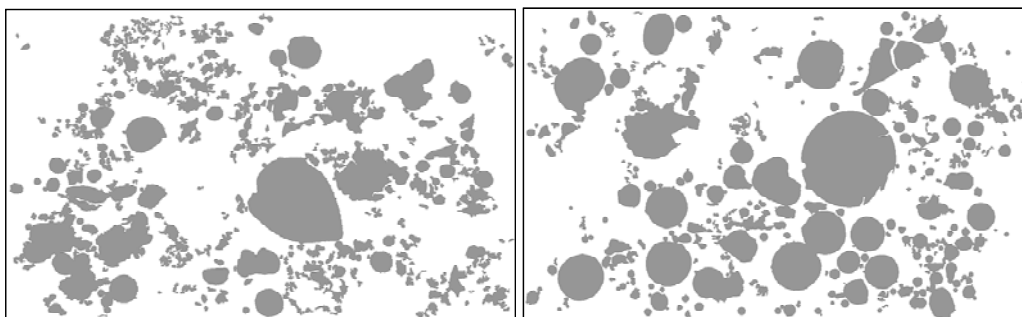
Figure 5–12: Results of examining the mass of the deposited ash and deposition fraction of ash on the tube at 1523 K.



(a) Coal G

(b) Coal G (80) + UBC F (20)

Figure 5-13: Cross-sectional structures of the deposit on the tube at 1523 K.



(a) Coal G

(b) Coal G (80) + UBC F (20)

Figure 5-14: Images of deposited ash on tube which is adjusted for image processing.

Table 5-4: Analytical results of particle configuration.

Coal	Coal G	Coal G(80)+UBC F(20)
Mean value of circularity coefficient [-]	0.541	0.719
Mean area ratio of particle [-]	1.0	1.17

5.5.3 Combustion and Emission Characteristics

The fly ash samples are collected from the electric precipitator in order to evaluate the unburnt fraction for both Coal G and the blended coal. The unburnt fraction defined as Eq.(5-2) is used for the evaluation of combustion characteristics.

$$U_c^* = 100 - \eta = \frac{U_c}{1 - U_c} \times \frac{C_{Ash}}{100 - C_{Ash}} \times 100 \quad (5-2)$$

where U_c^* [%] is the unburnt fraction, η [%] is the combustion efficiency, U_c [%] is the unburnt carbon concentration in fly ash and C_{Ash} [%] is the ash content in coal. For the NO_x emission, NO_x concentration in flue gas at outlet of the boiler, which is located upstream of de- NO_x tower, is monitored and averaged during combustion. For the SO_x emission, SO_x concentration in flue gas at upstream of de- SO_x tower is monitored and averaged during combustion.

Figure 5-15 shows the results of unburnt fraction, NO_x and SO_x concentration during combustion. All the values of unburnt fraction, NO_x and SO_x concentration of blended coal are reduced, compared to Coal G alone. Those results prove the considerations for combustion and emission characteristics in Chapter 2. In particular, it is elucidated that UBC has good burnout characteristics, compared to the bituminous coal and this contributes to both improvement of the combustion efficiency and NO_x emission even if the two-stage combustion are conducted.

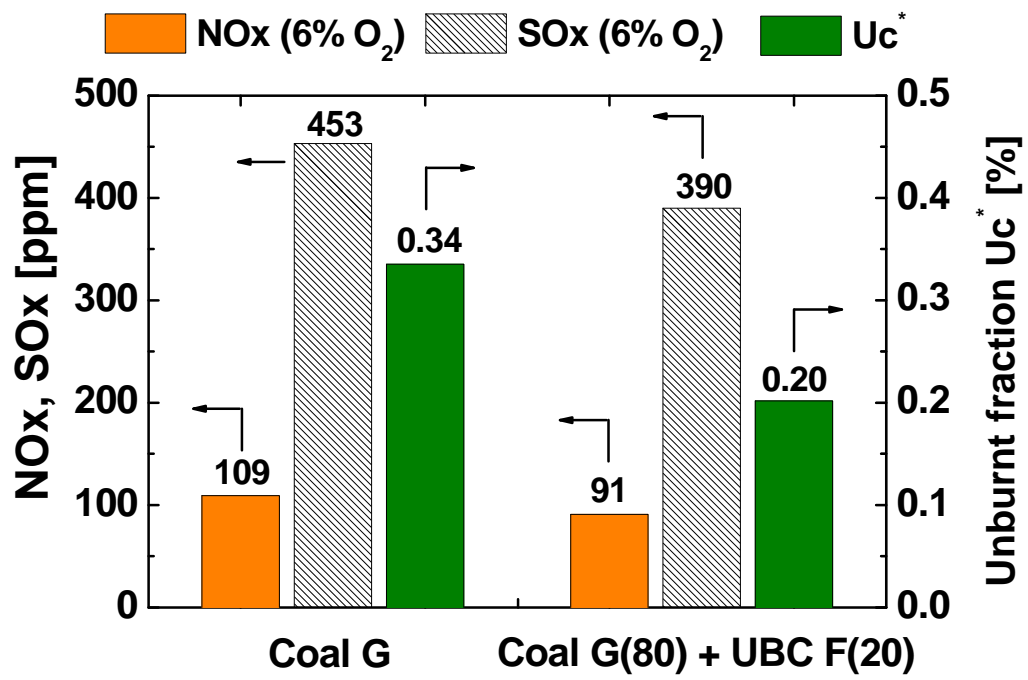


Figure 5-15: Results of unburnt fraction, NO_x and SO_x concentration.

5.6 Conclusions

The demonstration tests of UBC combustion in a 145 MW practical coal combustion boiler are conducted on blended coal consisting 20 wt% of UBC and 80 wt% of bituminous coal. Both the combustion characteristics such as NO_X and SO_X emissions and the burnout, and the ash deposition behavior such as slagging are elucidated. The following conclusions are obtained:

- UBC has good burnout characteristics compared to bituminous coal and this contributes to both improvement of the combustion efficiency and NO_X reduction for the blended coal even if the two-stage combustion were conducted.
- The emission of SO_X for blended coal decreases compared to bituminous coal since the sulfur content in UBC is low.
- Blending UBC with bituminous coal plays a role in reducing the molten slag fraction. This is because the solid phase compositions of aluminosilicates are produced due to the bituminous coal blending. As a result of ash deposition tests, the deposited ash particles on tube for the blended coal become larger and more spherical than those of bituminous coal. However, the mass of the deposited ash for the blended coal does not greatly increase and no slagging problems occur during the 8 days of boiler operation under the present blending conditions. Therefore, appropriate blending of UBC with bituminous coal enables UBC to be used with a low ash melting point without any ash deposition problems in a practical boiler.

References

- [1] FACT, www.crct.polymtl.ca
- [2] Bale CW, Chartrand P, Deckerov SA, Eriksson G, Hack K, Mahfoud RB, Melançon J, Pelton AD, Petersen S, FactSage thermochemical software and databases, *Calphad Journal*, 62, (2002) pp.189–228.
- [3] Raask E. *Mineral impurities in coal combustion*, Hemisphere Publishing Corporation, Washington, (1985) pp.169–189.
- [4] Walsh PM, Sayre AN, Loehden DO, Monroe LS, Beér JM, Sarofim AF, Deposition of bituminous coal ash on an isolated heat exchanger tube: Effects of coal properties on deposit growth, *Prog. Energy Combust. Sci.*, 16 (4), (1990), pp.327–345.
- [5] Beer JM, Sarofim AF, Barta LE, Inorganic transformations and ash deposition during combustion. In: *Engineering Foundation*, Benson, S. A. (ed), ASME, New York, (1992).
- [6] Benson SA, Jones ML, Harb JN, Ash formation and deposition Chap.4. In: Smoot LD, editor. *Fundamentals of coal combustion for Clean and Efficient Use*, Elsevier Science, New York, (1993) p.299.

Chapter 6

Conclusions

The purpose of this study is to develop the ecological and highly efficient combustion technology, which enables Indonesian UBC to be utilized in the practical coal combustion boiler. First, the NO_x and SO_x emissions and the burnout characteristics are evaluated quantitatively. Second, the method to control ash deposition using both coal blending and MgO additives into coal is built up after the relationship between ash deposition characteristics and ash melting characteristics is clarified. Additionally, the reduction mechanisms of ash deposition is elucidated. Finally, the practical combustion tests both the combustion characteristics such as NO_x and SO_x emissions and the burnout, and the ash deposition behavior such as slagging for the blended coal of UBC with bituminous coal are performed in a 145 MW coal combustion boiler. The conclusions obtained in each chapter are as follows:

In Chapter 2, thermo-gravimetric analysis and combustion test, using the pilot-scale pulverized coal combustion refractory furnace, are conducted to elucidate the combustion characteristics of UBC and bituminous coal, their NO_x and SO_x emissions and the burnout characteristics quantitatively. The following results are obtained:

- UBC contains a lot of volatile matter which evolves at low temperature below 700 K, compared with the bituminous coal. However, the coal type does not greatly affect the evolution rate of volatile matter.
- The char burnout time of UBC is considerably shorter than that of bituminous coal, because the specific surface area of UBC is larger than that of bituminous coal.
- NO_x conversion of UBC increases because the unburnt fraction of UBC is extremely low and the reduction of NO_x by char particles is inhibited during combustion. However, The NO_x concentration of UBC is relatively lower than that of bituminous coal since UBC contains only a little nitrogen.
- The generation of SO_x depends on both the sulfur content and Ca/S mole ratio in coal.
- UBC has good burnout characteristics, compared to bituminous coal. This contributes to both improvement of the combustion efficiency and NO_x reduction even if the two-stage combustion ratio increases.

In Chapter 3, ash deposition tests are conducted and chemical equilibrium calculations are carried out for three types of coal tested in the present study. The following findings are obtained:

- The ash deposition characteristics have a close relationship with the ash melting characteristics.
- The molten slag fraction in ash obtained by the chemical equilibrium calculation correlates with the deposition fraction of ash obtained in experiments even under mixing conditions of UBC to bituminous coal.
- The molten slag fraction in ash obtained by the chemical equilibrium calculations is one of the useful indices to predict the blending method with UBC to reduce the deposition

fraction of ash.

In Chapter 4, chemical equilibrium calculations and ash–deposition tests are conducted in order to evaluate the effects of MgO addition to coal on the reduction of ash deposition for UBC, and to understand the mechanisms of this reduction of ash deposition. The following findings are obtained:

- MgO as an additive is most effective in controlling the molten slag fraction of ash.
- One of the reduction mechanisms due to MgO addition involved the production of solid–phase aluminosilicates, and plays a role in decreasing the molten slag fraction in the ash on the tube.
- The amount of ash deposition for UBC with MgO is relatively diminished. This is because the MgO inhibited the production of molten slag on the tube. In other words, the surface state of the deposit would always be dry, so that the UBC ash with MgO would not adhere to the tube easily.
- MgO addition also inhibited direct reactions between the molten slag deposits and the tube surface. Consequently, it is considered that MgO addition can reduce not only the ash deposition on tube but also the corrosion of the tube.

In Chapter 5, the demonstration tests of UBC combustion in a 145 MW practical coal combustion boiler are conducted on blended coal consisting 20 wt% of UBC and 80 wt% of bituminous coal. Both the combustion characteristics such as NO_x and SO_x emissions and the burnout, and the ash deposition behavior such as slagging are elucidated. The following conclusions are obtained:

- UBC has good burnout characteristics compared to the bituminous coal and this contributes to both improvement of the combustion efficiency and NO_x reduction for the blended coal even if the two-stage combustion are conducted.
- The emission of SO_x for blended coal decreases compared to the bituminous coal since the sulfur content in UBC is low.
- Blending UBC with the bituminous coal plays a role in reducing the molten slag fraction. This is because the solid phase compositions of aluminosilicates are produced due to the bituminous coal blending. As a result of ash deposition tests, the deposited ash particles on tube for the blended coal become larger and more spherical than those of the bituminous coal. However, the mass of the deposited ash for the blended coal does not greatly increase and no slagging problems occur during the 8 days of boiler operation under the present blending conditions. Therefore, appropriate blending of UBC with bituminous coal enables UBC to be used with a low ash melting point without any ash deposition problems in a practical boiler.

As mentioned above, the ecological and highly efficient combustion technology which enables Indonesian UBC to be utilized in the practical coal combustion boiler has been developed in this study. Finally, I hope that this technology contributes to the effective utilization of unused coal resources such as low-rank coals.

Acknowledgments

I would like to express my sincere gratitude to my advisor, Prof. I. Naruse of Department of Mechanical Science and Engineering, Nagoya University, for his generous support and encouragement throughout the course of this research. The three years, as a student in doctoral course under his supervision, have been fruitful and pleasant owing to his generous and kind consideration.

Also I would like to thank Prof. N. Yoshikawa of Department of the Micro–nano System Engineering, Nagoya University, and Prof. H. Yamashita and Prof. Y. Sakai and associate Prof. R. Yoshiie of Department of Mechanical Science and Engineering, Nagoya University, for participating in my thesis committee, giving discussion regarding to this work.

I would like to thank assistant Prof. Y. Ueki of EcoTopia Science Institute, Nagoya University, for giving discussion and collecting information for the present study.

I wish to thank Prof. Y. Ninomiya of Department of Applied Chemistry, Chubu University, for teaching me the method of chemical equilibrium calculations.

During my research at Transport Phenomena Laboratory, Nagoya University, I like to thank assistant Prof. E. Asakura and Mr. K. Nishio and Mr. M. Shimamura and all students, for providing me a comfortable environment and conducting my experimental study.

I also would like to thank Dr. T. Miyake and Dr. Y. Higashi of Mechanical Engineering Research Laboratory, KOBE STEEL, LTD., for giving chance to learn at doctoral course of Nagoya University.

I am obliged to my colleagues in KOBE STEEL, LTD. Mr. T. Tada advised me about the experimental design. Dr. H. Pak helped me in conducting combustion experiment and analysis. Mr. Y. Takubo helped me in performing parametric computations. Mr. M. Tokugawa and Mr. Y. Hasegawa helped me in conducting the ash deposition experiment. Mr. Y. Kusumoto and Mr. R.

Kokenawa and Mr. M. Shiraishi and Mr. T. Kitamura helped me in conducting the measurement in the practical coal combustion boiler. I also wish to express my gratitude to many colleagues who were not able to describe here.

This study was partly supported by Japan Coal Energy Center (JCOAL), which provided our UBC samples.

Lastly, my families are always mental mainstay for me. I cannot guess how grateful I am to their support and consideration.

July 2011

Katsuya AKIYAMA

論文目録
(Thesis list)

氏名 秋山 勝哉 (AKIYAMA Katsuya)

(発表した論文)

論文題目	公表の方法及び時期	著者
I. 学会誌等		
1. Ash Deposition Behavior of Upgraded Brown Coal and Bituminous Coal.	Energy Fuels, 24 (8), pp.4138–4143 (2010)	Akiyama K, Pak H, Tada T, Ueki Y, Yoshiie R, Naruse I.
2. Ash deposition behavior of Upgraded Brown Coal in pulverized coal combustion boiler.	Fuel Processing Technology, 92, pp.1355–1361 (2011)	Akiyama K, Pak H, Tada T, Ueki Y, Yoshiie R, Naruse I.
3. Effect of MgO Addition to Upgraded Brown Coal on Ash–Deposition Behavior During Combustion.	Fuel (in press)	Akiyama K, Pak H, Ueki Y, Yoshiie R, Naruse I.
II. 国際会議		
1. Comparison of Combustion Characteristics of Upgraded Brown Coal (UBC) and Bituminous Coal.	Proc. of AFRC–JFRC 2007 Joint International Symposium, Hawaii, Oct.22–24, (2007)	Akiyama K, Tada T.
2. Combustion characteristics of upgraded brown coal (UBC).	Proc. of 6th International Symposium on Coal Combustion, Wuhan, China, pp.527–532 (2007)	Akiyama K, Tada T.

3. Characteristics of Ash Deposition Behavior of Upgraded Brown Coal (UBC) and Bituminous Coal.	Proc. of the 6th Mediterranean Combustion Symposium, Ajaccio, Corsica, France, June.7–11, (2009)	Akiyama K, Pak H, Tada T, Yoshiie R, Naruse I.
4. Combustion Characteristics of Upgraded Brown Coal (UBC) and Bituminous Coal.	Poster Presentation of the 33rd International Symposium on Combustion, Beijing, China, Aug.1–6, (2010)	Akiyama K, Pak H, Tada T, Ueki Y, Yoshiie R, Naruse I.
5. Ash deposition behavior of Upgraded Brown Coal (UBC) in pulverized coal combustion boiler.	Proc. of AFRC International Pacific Rim Combustion Symposium, Hawaii, Sep.26–29, (2010)	Akiyama K, Pak H, Tada T, Ueki Y, Yoshiie R, Naruse I.
6. Co-combustion Behavior of Coal and Carbonized Sludge for Pulverized Coal Combustion Boiler.	Proc. of AFRC International Pacific Rim Combustion Symposium, Hawaii, Sep.26–29, (2010)	Pak H, Akiyama K, Tada T.
7. Effect of MgO Additive on Reducing of Ash Deposition for Upgraded Brown Coal (UBC).	Proc. of the 27th Annual International Pittsburgh Coal Conference, Istanbul, Turkey, Oct.11–14, (2010)	Akiyama K, Pak H, Ueki Y, Yoshiie R, Naruse I.
8. Slagging Behavior of Upgraded Brown Coal and Bituminous coal in 145 MW Practical Coal Combustion Boiler.	Proc. of 7th International Symposium on Coal Combustion, Harbin, China, Jul.17–20, (2011)	Akiyama K, Pak H, Takubo Y, Tada T, Ueki Y, Yoshiie R, Naruse I.

III. その他		
1. 微粉炭ボイラ利用に向けた改質褐炭 (UBC) の燃焼特性評価	工業加熱, Vol.45, No.6, pp.33-37 (2008)	秋山勝哉, 朴海洋, 多田俊哉
2. 微粉炭ボイラ利用に向けた汚泥炭化燃料の燃焼特性評価	日本エネルギー学会 石炭科学会議発表論文集, Vol.45, pp.48-49 (2008)	朴海洋, 秋山勝哉, 多田俊哉
3. 改質褐炭 (UBC) と瀝青炭の灰付着性の評価	化学工学会秋季大会 研究発表講演要旨集, Vol.41, V123, (2009)	秋山勝哉, 朴海洋, 植木保昭, 義家亮, 成瀬一郎
4. 改質褐炭 (UBC) と瀝青炭の灰付着性の評価	R&D 神戸製鋼技報, Vol.20, No.1, pp.67-70 (2010)	秋山勝哉, 朴海洋, 多田俊哉
5. 石炭火力発電所におけるボイラ内灰付着およびクリンカの発生抑制技術	R&D 神戸製鋼技報, Vol.20, No.1, pp.50-54 (2010)	菅原弘次, 近藤晶夫, 秋山勝哉, 朴海洋
6. 改質褐炭の基礎燃焼挙動	日本エネルギー学会 石炭科学会議発表論文集, Vol.47, pp.58-59 (2010)	嶋村倫生, 植木保昭, 義家亮, 成瀬一郎, 秋山勝哉